

# A companion guide to the Hodgkin-Huxley papers

Angus M Brown



The Journal of  
**Physiology**

A companion guide to the Hodgkin-Huxley papers

A companion guide to the Hodgkin-Huxley papers

Angus M Brown

School of Life Sciences, University of Nottingham

Nottingham, NG7 2UH, UK

&

Department of Neurology, University of Washington

Seattle, WA 98195, USA

---

## TABLE OF CONTENTS

---

PREFACE.....	6
1. INTRODUCTION..... 8	
Luigi Galvani .....	11
Julius Bernstein .....	11
Kenneth Cole .....	12
Alan Hodgkin .....	15
Hodgkin meets Cole .....	18
Extracellular versus intracellular recordings .....	19
2. THE EFFECT OF SODIUM IONS ON THE ELECTRICAL ACTIVITY OF THE GIANT AXON OF THE SQUID ..... 24	
Ohm's Law.....	25
The Nernst equation .....	25
Effect of low $[Na]_o$ on the action potential .....	26
Action potential properties .....	27
$Na^+$ free seawater abolishes the action potential .....	29
Effect of variable $[Na]_o$ on the action potential .....	30
Effect of altering $[K]_o$ on membrane potential.....	33
GHK voltage equation .....	35
A diversion - astrocytes are $K^+$ electrodes.....	36
Dissection of the GHK voltage equation .....	36
3. MEASUREMENT OF CURRENT-VOLTAGE RELATIONS IN THE MEMBRANE OF THE GIANT AXON OF <i>LOLIGO</i> ..... 40	
The voltage clamp .....	41
Membrane capacitance.....	44
The early and late membrane current amplitudes .....	44
Temperature dependence .....	46
4. CURRENTS CARRIED BY SODIUM AND POTASSIUM IONS THROUGH THE MEMBRANE OF THE GIANT AXON OF <i>LOLIGO</i> ..... 47	

---

Isolation of $I_{Na}$ from the membrane current .....	48
The isolation process.....	49
$Na^+$ conductance .....	51
The independence principle.....	55
<hr/>	
5. THE COMPONENTS OF MEMBRANE CONDUCTANCE IN THE GIANT AXON OF <i>LOLIGO</i> .....	59
Tail currents .....	60
Continuity of sodium conductance .....	63
Independence principle revisited.....	64
$K^+$ current .....	66
Leak current .....	68
<hr/>	
6. THE DUAL EFFECT OF MEMBRANE POTENTIAL ON SODIUM CONDUCTANCE IN THE GIANT AXON OF <i>LOLIGO</i> .....	74
Time constant of inactivation.....	75
Inactivation curve.....	76
<hr/>	
INTERLUDE .....	79
<hr/>	
7. A QUANTITATIVE DESCRIPTION OF MEMBRANE CURRENT AND ITS APPLICATION TO CONDUCTION AND EXCITATION IN NERVE .....	82
The computation process.....	83
From experimental data to model .....	84
The model .....	86
Probability theory applied to the gating particles.....	88
Calculation of rate constants .....	89
The complete model .....	95
Action potential reconstruction .....	96
Propagated action potential .....	98
Ion conductances .....	98
Refractory period .....	101
Anode break excitation .....	104
<hr/>	
8. THE POTASSIUM PERMEABILITY OF A GIANT NERVE FIBRE.....	108

---

The late outward current and K <sup>+</sup> .....	109
The tracer method .....	112
Electrical measurements.....	113
The flux ratio under varying [K] <sub>o</sub> .....	114
The flux ratio under varying driving forces .....	115
Evidence of interaction .....	116
<b>9. CONCLUSION.....</b>	<b>119</b>
Currents that control firing frequency .....	120
Application of the Hodgkin-Huxley model to mammalian neurones .....	122
Predictions of ion channel selectivity.....	123
Ion channel structure .....	124
Application of the Hodgkin Huxley model to ion channels .....	126
J Walter Woodbury and the Nobel Prize nomination .....	128
Autobiographical Chapters.....	129
Specialist texts.....	131
Resources .....	131
Conclusion.....	132
<b>REFERENCES.....</b>	<b>133</b>

---

# PREFACE

This guide is intended for students who are approaching the work of Hodgkin and Huxley for the first time. It has been written as a companion piece for use in conjunction with the Hodgkin and Huxley papers. The core canon of this work are the five seminal papers published in 1952 (Hodgkin & Huxley, 1952a, b, c, d; Hodgkin *et al.*, 1952), and although I have bookended these with two additional papers, which complete the narrative, the constant presence in these seven papers is Alan Hodgkin. These additional papers were co-authored with Bernard Katz (Hodgkin & Katz, 1949a) and Richard Keynes (Hodgkin & Keynes, 1955), where the former acts as a logical introduction to the work, and the latter provides a suitable conclusion, predicting the presence of ion channels, the elementary units that underlie electrical activity. I have included an introduction (Chapter 1) that places the Hodgkin and Huxley work in the appropriate historical context, commencing with the discovery of bioelectricity by Galvani in 1791 and concluding with the recording of the first intracellular action potential in 1939. I have dedicated a chapter to each of the seven papers (Chapters 2 to 8), describing in detail aspects of the paper to aid student understanding. Where I have considered detail lacking in the original papers, I have added relevant sections, most notably in relation to the Goldman-Hodgkin-Katz voltage equation (Chapter 2) and the leak current (Chapter 5). For the most part I have ignored the methods, as these tend to be antiquated and refer to obsolete equipment and techniques. Although of relevance to the accuracy of the data, I have also ignored detailed reference to junction potentials, polarisation of electrodes, series resistance and compensation as their inclusion would only serve only to confuse the modern reader. I have however, made an exception in describing the voltage clamp technique (Chapter 3), as this was a key technological innovation, which allowed measurement and isolation of the trans-membrane currents. In the conclusion (Chapter 9) I demonstrate how the Hodgkin-Huxley model, which was derived from macroscopic currents to produce a deterministic model, can be adapted to create probabilistic models that accurately describe the microscopic ion fluxes through individual channels.

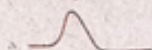
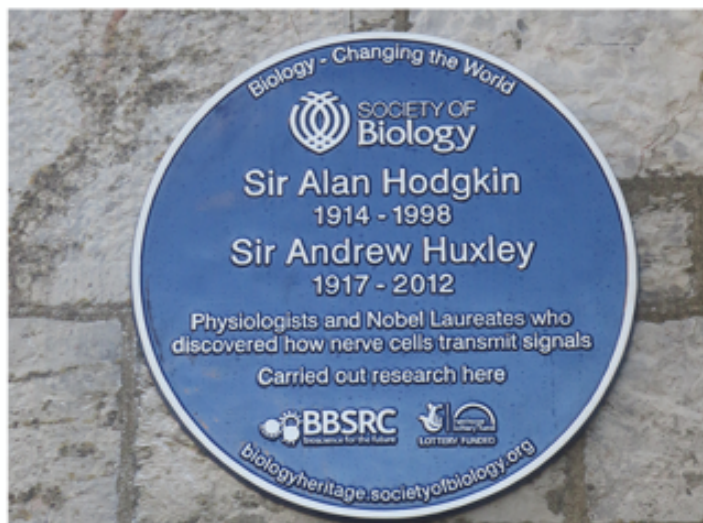
A significant impediment to students' understanding of the Hodgkin and Huxley papers is that the conventions they used for reporting voltage and current were different to those in use today. I have updated all seven papers to reflect the modern convention and these papers are freely available on *The Journal of Physiology* website under the heading *Classics Updated*. The process by which the papers were updated has been described in detail (Brown, 2019a, b), and throughout this guide I refer only to the updated papers, not the original papers. For the most part the textbooks I refer to have adopted the updated conventions, but the exception is Cronin's book (Cronin, 1987), where I have modified the relevant equations referred to in the derivation of the independence principle (Chapter 4). When referring to figures in the updated papers I use italics (e.g., *Figure 3*, *Table 1*), but where the figure is present in this guide, I use normal text (e.g., Fig 3.2A). Regarding terminology I use *V* to refer to an experimental measure of membrane potential and *E<sub>x</sub>* is a calculated reversal potential. I do not use the term 'ion channels', which were unknown to Hodgkin and Huxley, as this strikes me as premature, depriving the reader of the rewards earned by the gradual progress towards the revelations in Chapter 8. Before embarking on a detailed analysis of Hodgkin and Huxley's work students must have a solid foundation in the basics relating to membrane potential, passive properties and the Nernst equation. These topics are covered in sufficient detail in all elementary neuroscience textbooks, of which the following can be confidently recommended (Hille, 2001; Nicholls *et al.*, 2012; Purves *et al.*, 2012; Kandel *et al.*, 2013a).

# 1. INTRODUCTION

The esteem in which the scientific community holds Hodgkin and Huxley is evident from the commemorative plaques in Cambridge and Plymouth, and the decision of The Physiological Society in 2012 to re-name their London headquarters ‘Hodgkin Huxley House’ on the 60<sup>th</sup> anniversary of the publication of their five seminal papers (Fig 1.1). The reasons for this continued celebration of their achievements (Brown, 2022) warrant attention since the incremental nature of scientific discovery consigns all but the truly great to oblivion. The narrative of the Hodgkin and Huxley work spans 1938 to 1952 and includes ingredients that guarantee a captivating tale; memorable characters, youthful optimism tempered with ruthlessness, hardship, competition, and ingenuity played out against the deprivations of a devastating world war. What Hodgkin and Huxley achieved was to provide the first mathematical description of biological phenomena, summarised in an empirical model of impressive predictive power that successfully reproduced the action potential. Although the model derived from experiments carried out on the squid giant axon, its impact was universal since it was broadly applicable to all excitable cells. My goal is to make the work of Hodgkin and Huxley accessible to modern undergraduate students, since there is much that students can learn from studying this work. The first part of this process involved updating the five seminal Hodgkin and Huxley papers alongside the two additional related papers, to reflect the modern convention of reporting voltage and current, and this is complete (see Preface). The second part of the process is to provide a detailed analysis of the updated papers, with the expectation that students will benefit from the clarity of thought applied by Hodgkin and Huxley. In the course of their work Hodgkin and Huxley had to contend with time constraints, limited resources, and the unpredictable performance of bespoke electrical equipment, all of which precipitated a distillation of seemingly disparate ideas to a cogent narrative that could be expressed in a few key concepts that they tested experimentally. Limitations imposed by their rudimentary equipment forced the application of indirect methods when they could not measure a desired parameter directly, a recurring theme in these papers. The compromises involved in using indirect methods often required complex mathematical solutions to analyse data. The achievements of Hodgkin and Huxley highlight the benefits of adopting a multi-disciplinary approach to scientific problem solving. The success of their endeavour was facilitated by (i) a pragmatic and flexible experimental approach to what was feasible and what was not, (ii) the ability to design electrical equipment based on an understanding of electrical circuitry, (iii) a practical knowledge of calculus using differentiation in the derivation of the model and integration in the reconstruction of the action potential, and (iv) dogged determination and superhuman focus required to complete the computations.

**A**

In this building E.D. Adrian first recorded impulses from single nerve fibres, and A.L. Hodgkin & A.F. Huxley determined their mechanism and principles of conduction, transforming our understanding of how the nervous system processes information.

**B****C**

**Figure 1.1** - Commemorative plaques celebrating Hodgkin and Huxley's work at (A) the Physiology Building at the University of Cambridge, and (B) the Marine Biological Association in Plymouth. (C) The Physiological Society headquarters are located in 'Hodgkin Huxley House', 30 Farringdon Lane, London, EC1R 3AW.

## Luigi Galvani

To fully understand what Hodgkin and Huxley achieved their work must be viewed in an appropriate historical context. The advent of modern electrophysiology may be dated to 1791, the year of Mozart's death and the birth of Michael Faraday, the founder of electrochemistry (Faraday, 1834). It was in this year that Galvani demonstrated the phenomenon of bioelectricity, where electrical stimulus of the crural nerve in the form of a spark from a Leiden jar, an ancestral capacitor that stored charge, caused a twitch in the leg muscle of a frog (Piccolino, 1998). To isolate the local response from any central input Galvani decapitated the frog. The importance of this observation was that dead animals were capable of movement, a sinister observation in an era when the fear of live burial was very real. The repeated movement of the muscle in response to electrical stimulus clearly showed the response was an intrinsic property of the tissue, devoid of any central nervous system input. Galvani's research rapidly reached a wide audience with the result that others sought to emulate his experiments. Whereas Galvani proposed electricity was generated within the muscle of the frog, Volta, who had been inspired by his work, provided evidence that the muscle was simply responding to external electrical input and was incapable of any endogenous ability to create electricity. Volta's investigations led to the invention of the battery, whose structure comprised alternating plates of dissimilar metals separated by paper soaked in a salt solution. Volta referred to the battery as an 'artificial animal organ' in reference to the stack like assembly of the electric organ of the eel (Piccolino & Galvani, 1997). Galvani did demonstrate that muscle twitches could be produced by touching the surface of the muscle with the cut end of the sciatic nerve, and that the cut end of a sciatic nerve, when in contact with the sciatic nerve of another leg muscle, could produce muscle twitches (McComas, 2011) i.e., muscle contraction could be evoked in the absence of any external stimulus. However public opinion was in Volta's favour, his fame and fortune a direct contrast with Galvani who died discredited and destitute. The phenomenon of bioelectricity directly inspired the classic gothic novel *Frankenstein*, published in 1818, in which the teenage Mary Shelley envisaged the ability of electricity to resurrect the dead.

## Julius Bernstein

The subsequent advances in the field of bioelectricity followed a slow incremental trajectory facilitated by technical innovation (Piccolino, 1998; McComas, 2011). What was of fundamental importance was the application of the laws of physics and chemistry to biology in the 19<sup>th</sup> century to create physiology, which may be considered the science of the mechanism of living organisms. For example, the behaviour of gases defined by Boyle and Charles and summarised in the Ideal Gas Law had direct relevance to gaseous exchange in the respiratory system (Boron & Boulpaep, 2009), and Poiseuille's demonstration of the behaviour of fluids at rest and in motion was applicable to the circulation and the role of the heart as a pump (Boron & Boulpaep, 2009). Indeed it was the concept of physiology as the mechanical engineering of living things that attracted Huxley to the field (Angel, 1996). The contribution of electricity, that most mysterious of forces, to biology reached its zenith when Bernstein considered the work of Nernst applicable to cell membranes. Walther Nernst was a physical chemist who showed if two copper electrodes were placed in separate vessels, interconnected via a tube, containing solutions with differing salt concentrations, the salt passed from the high to the low concentration until an equilibrium was reached, which was accompanied by a flow of electrical current between the electrodes. This was called Nernst's

cell. It was quantified and expressed in an equation that showed the electrical potential was temperature dependent and was determined by the logarithm of the ratio of the ion concentrations (Woodbury, 1982; Hille, 2001). In this atmosphere of discovery, integration of the natural science disciplines inspired the work of Bernstein, which is considered the foundation of 20<sup>th</sup> century electrophysiology. Bernstein was aware of the work of his contemporaries, particularly Pfeffer, who proposed that cells possessed a semi-permeable membrane across which select ions could move, but to which other ions were impermeable (De Palma & Pareti, 2011). Assimilating the cellular semi-permeable membrane with Nernst's electrical cell was the foundation of Bernstein's 'membrane theory', which was published in 1902. Despite being widely cited it is unlikely that the paper has been widely read as it was published in German (Bernstein, 1902) and received its first English translation as late as the 1970s (Bernstein, 1971, 1979). Although this paper was the foundation of the membrane theory that explicitly proposed the selective permeability of cell membranes to K<sup>+</sup> as the basis of the intracellular negative membrane potential compared with an external ground, there was little in the paper explicitly about the role of K<sup>+</sup>. Indeed, the main focus of the paper was on the effect of temperature on the potential difference. In neuronal cells we know that there is a large excess of intracellular K<sup>+</sup> compared to the fluid bathing the cells, with the opposite being the case for Na<sup>+</sup> (Hille, 2001). Bernstein proposed that while at rest the membrane was selectively permeable to K<sup>+</sup>, but during activity the permeability to K<sup>+</sup> was lost. He did not consider that any other ions played a role during activity, and thus proposed that during activity the potential difference across the membrane would reach 0 mV (Seyfarth, 2006; De Palma & Pareti, 2011). In fact the intracellular presence of a high concentration of organic anions means that there exists an inequality in the total trans-membrane concentrations of permeable ions (Kandel *et al.*, 2013a) with elementary calculations suggesting the membrane potential would approach, but not reach 0 mV.

### Kenneth Cole

At the start of the 20<sup>th</sup> century the pervading dogma regarding excitable cells was that the membrane at rest was selectively permeable to K<sup>+</sup>, the resting membrane potential governed by the ratio of the intra- and extracellular concentrations of K<sup>+</sup>, resulting in a negative membrane potential compared to the outside of the cell. During excitation the selective permeability of the membrane to K<sup>+</sup> was lost and the potential difference across the membrane reached 0 mV. An important consequence of this relationship, which was intensively studied, was that the selective permeability to K<sup>+</sup> would ensure a high membrane resistance at rest, which would decrease markedly on loss of selective permeability during excitation (Cole, 1979). It was against this backdrop that researchers started exploring the mechanisms underlying electrical excitability in nerves, facilitated by technical advances in instrumentation. The first of these groups was Erlanger, Gasser and others in St Louis, USA, in the early 1920s. They used the newly developed cathode ray oscilloscope (Erlanger *et al.*, 1924), to display the stimulus evoked compound action potential (CAP) from frog peroneal nerves, which resolved into multiple peaks (Gasser & Erlanger, 1927), each peak reflecting a discrete conduction velocity that was contributed by sub-populations of axons of a similar diameter (Gasser & Grundfest, 1939). In this manner Erlanger and Gasser correlated conduction velocity i.e., latency of the CAP peak from stimulus, to axon diameter (Erlanger & Gasser, 1937). The axon possesses three main properties that dictate the response to injection of current: (i) axoplasmic resistance ( $r_i$ ), (ii) membrane resistance ( $r_m$ ), and (iii) membrane capacitance ( $c_m$ ). What is crucial to realise is that these properties of resistance

and capacitance conform to the rules of electrical circuits, which means their values can be quantified, and that these properties can be modelled using equivalent electrical circuits, a practice introduced by Cole (Cole & Curtis, 1938) (Fig 1.2). Pairings of these properties combine to produce the length constant ( $\lambda = \sqrt{r_m r_i}$ ) which defines the distance the current travels along the axon, time constant ( $\tau = r_m C_m$ ) which defines the rate at which the membrane responds to the stimulus, and input resistance ( $r_{\text{input}} = 0.5\sqrt{r_m r_i}$ ) which defines the magnitude of the membrane response to current injection (Kandel *et al.*, 2013a). These properties govern the spatiotemporal changes in the membrane potential along an axon, which can be modelled by the cable equation (Fain, 1999; Koch, 1999; Hille, 2001; Byrne & Roberts, 2009; Sterratt *et al.*, 2011).

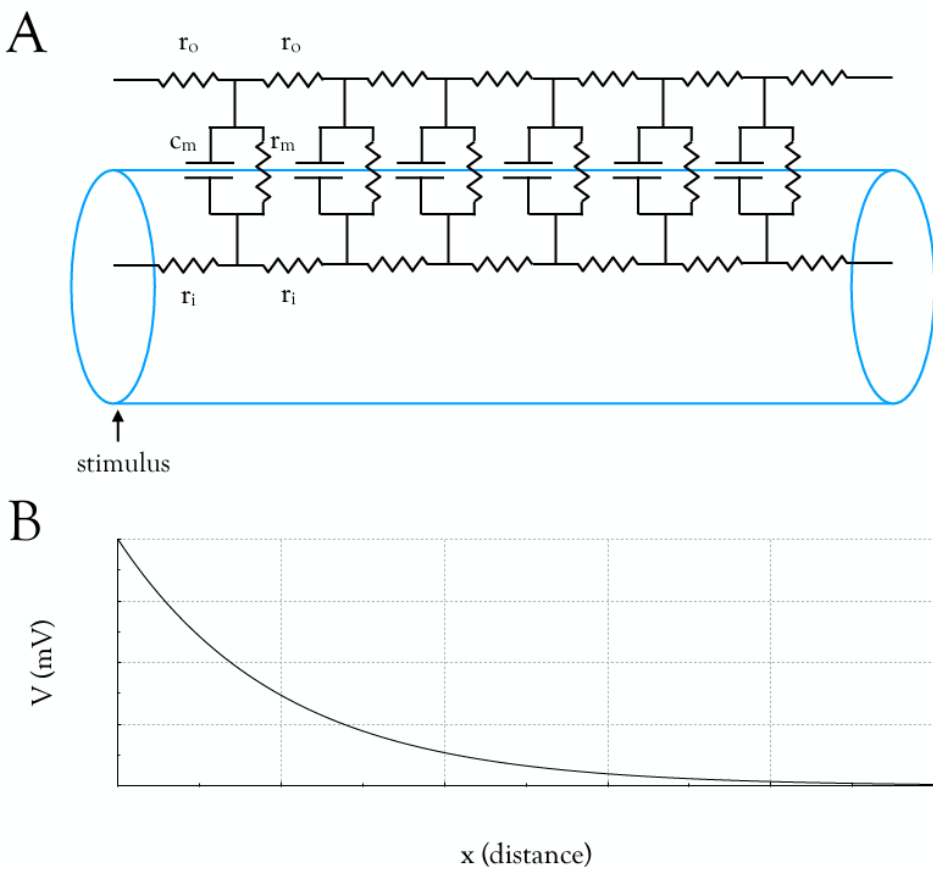


**Figure 1.2 - The electrical properties of an axon.** A. The axon (blue outline) represented by an equivalent circuit. The pathways for current spread along the axon are dictated by the values of  $r_i$  relative to those of  $r_m$  and  $c_m$ . In large axons, such as the squid, the value of  $r_i$  is proportionally smaller than  $r_m$ , promoting longitudinal current travel along the axon with minimal shunting across the membrane. B. The passive voltage spread along an axon in response to a brief shock (arrow) decreases with distance.

Kenneth Cole was a physicist by training who applied his knowledge of physics to explore biological phenomena. He was initially based in Cornell during his Ph.D. but visited the Cleveland Clinic where he worked with Fricke on measuring the electrical properties of

red blood cells. The following summer he spent time at Woods Hole, Massachusetts, which he would visit regularly over the next 40 years, where he switched focus to measure the electrical properties of amphibian eggs. After completing his Ph.D., he worked at Yale continuing research on the electrical characteristics of egg membrane. He then spent a year in Leipzig working on the Nernst-Planck theory, which defined the potential difference generated by diffusion of two different concentrations of ions in solution, invaluable training in the theory underlying his future work on the excitability of axon membranes. Cole returned to a post in Columbia University in New York, where in 1935 he used his electronics expertise to design a bridge system that measured membrane resistance (impedance) in small cells, allowing him to demonstrate a decrease in membrane resistance in the seawater alga *Nitella* during excitation, which was in agreement with Bernstein's membrane theory. In the summer of 1936 JZ Young, an English anatomist, met Cole at Woods Hole and suggested he adopt the squid giant axon as a model in his studies on the electrical properties of membranes, since it was many times larger than the axons used so far for such studies (Young, 1936), i.e., the squid axon is up to 600  $\mu\text{m}$  in diameter (Fig 1.3A), whereas the frog axon is only about 20  $\mu\text{m}$ . It was not simply that the squid axons were larger and thus easier to dissect and handle, but that their large lumen made them amenable to experiential techniques such as intracellular recording (Fig 1.3B) that were not viable in the smaller frog axons. This was a momentous event, described in the 1970s by Alan Hodgkin as the most important innovation in axonology of the last 40 years (Keynes, 2005).

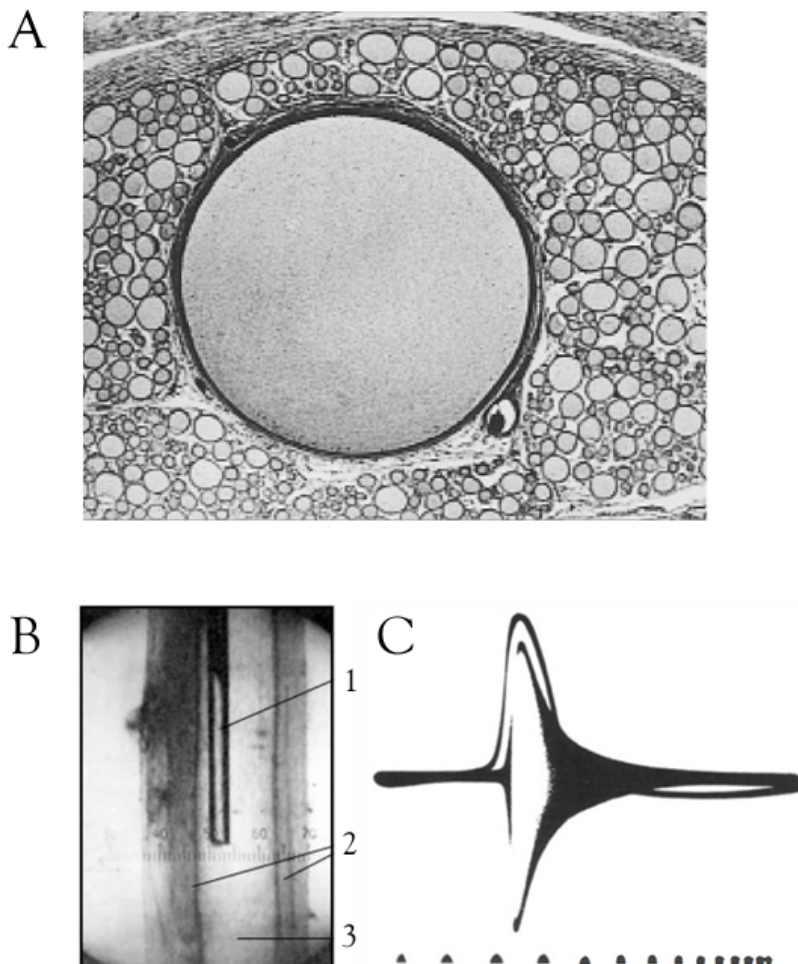


**Figure 1.3 - The squid giant axon.** A. The relative size of a giant axon from *Loligo* is apparent when compared to neighbouring axons. B. The squid axon penetrated by a microelectrode, where (1) indicates the intracellular metal microelectrode, (2) indicates the walls of the axon viewed in cross section, and (3) indicates the axoplasm (Hodgkin & Huxley, 1939). C. The increased impedance (shaded area) associated with excitation reflected in the voltage trace (line) in squid axon (Cole & Curtis, 1949).

### Alan Hodgkin

In England Alan Hodgkin came to Cambridge as an undergraduate in 1932 and was guided by Rushton who encouraged him to study nerve conduction. Hodgkin used extracellular recording techniques to explore the passive response, or local electrical circuits, in isolated frog nerve. Hodgkin was convinced that there was an increased membrane conductance during excitation, and although he did not have suitable equipment to directly measure this, he set out to investigate the phenomenon. The ingenious part of the experimental protocol was that Hodgkin used a cold block, induced by placing a silver rod in ice and then transferred it to the surface of the nerve, to freeze a localised portion of the nerve. This blocked the action potential, which would otherwise obscure the smaller local

electrical circuits. He found that a stimulus distal to this affected portion of the nerve ( $S_1$ ) was not transmitted through the cold region. Addition of a second pair of stimulating electrodes ( $S_2$ ) and careful synchronisation of the stimuli showed there was an additive effect of  $S_1$  and  $S_2$  (Fig 1.4A). i.e., the threshold for the active response was lowered in the region of the nerve proximal to the block as a result of the first stimulus. Measurements of the electrical response of the membrane showed there was an increase in the response immediately proximal to the block, which decreased exponentially (Fig 1.4C), as expected from the passive spread of current. This phenomenon could be explained as the local electrical circuits spreading through the blocked region and exciting the nerve beyond. We now know that the depolarisation of the membrane resulting from this passive spread brings the membrane closer to threshold, thus a smaller second stimulus is required to evoke an action potential. This local electrical circuit explained how action potentials propagated along an axon. The action potential acted as a stimulus, which was conducted by the passive properties of the axon to activate neighbouring areas of the axon. These currents flowed along the axon, out of the membrane, and were conducted via the extracellular fluid ( $r_o$  in Fig 1.2A) back into the region of excitation through the membrane, thereby completing the circuit (Fig 1.4B). Thus, Hodgkin's effect was not an increase in membrane conductance, but rather the passive spread of current along the axon. In the excitement of subsequent discoveries of the active response i.e., action potentials, it is sometimes forgotten how important these local circuits are in bringing the membrane potential to threshold. This phenomenon will be described in detail later in the appropriate context, but emphasises an extremely important point, which is that the physiological stimulus for an action potential is membrane depolarisation. The results were published as a pair of papers in *The Journal of Physiology* with Hodgkin as sole author, an extremely impressive feat for a 23 year old (Hodgkin, 1937a, b). Hodgkin was awarded a grant and spent the period from September 1937 to July 1938 in the United States, which is where the trans-Atlantic strands of our story converge.

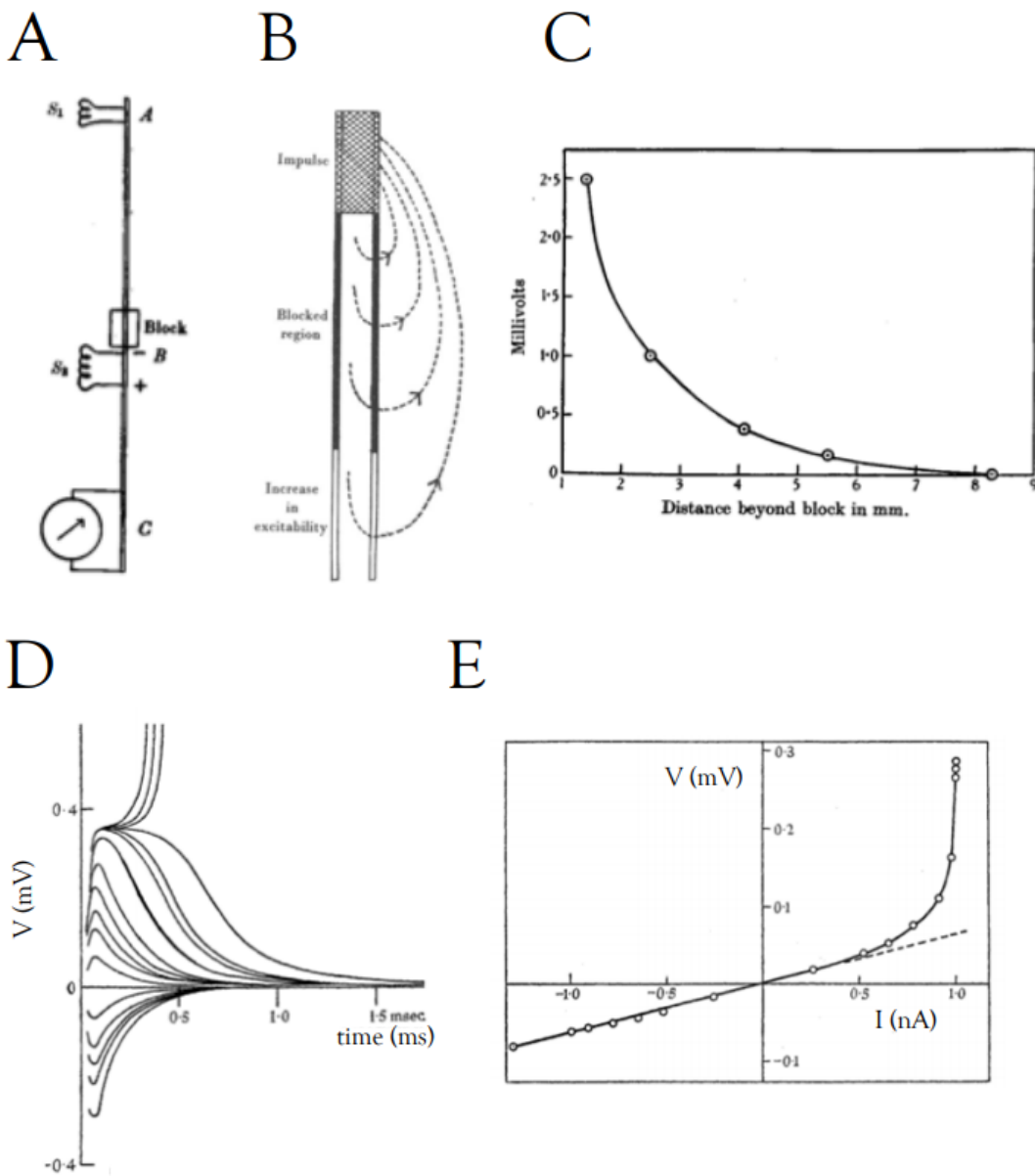


**Figure 1.4 - The local circuits in frog nerve.** A. The location of the stimulus and recording relative to the region of cold block. The nerve was stimulated at one end ( $S_1$ ) and the response recorded at the other end (C). The cold block was applied in the middle of the nerve, with the second stimulus ( $S_2$ ) appropriately located to demonstrate excitation spread beyond the block. B. The flow of local electrical circuits illustrated how current spread beyond the region of block. C. Excitation beyond the block decreased in an exponential manner as expected of passive current spread along a cable (Hodgkin, 1937a). D & E. The response of the membrane potential to stimuli of identical amplitude but opposite polarity produced symmetrical deviations in membrane potential for small stimuli. Large depolarising stimulus evoked all or nothing action potentials (Hodgkin, 1938).

## Hodgkin meets Cole

Hodgkin visited Gasser at the Rockefeller Institute in New York in 1937 and commenced experiments investigating sub-threshold potentials in individual axons teased apart from crab nerve. He found that a small stimulus would produce an electrical change in the nerve membrane. If a sufficiently large stimulus was applied the nerve would fire an action potential. At membrane potentials just below threshold there was clear instability in the membrane response, but if threshold was reached an all or nothing action potential was evoked (Hodgkin, 1938). Imposing sub-threshold stimuli of either polarity caused current to flow along the axon ( $r_i$ ) but also across the membrane on account of its resistance ( $r_m$ ) and capacitance ( $c_m$ ). This stimulus charged up the membrane capacitance and produced a voltage deflection resulting from current flow through the capacitive and resistive properties of the membrane, called an electrotonic potential (Aidley, 1996). On cessation of stimulus the membrane capacitance discharged allowing the membrane to relax back towards rest (Fig 1.4D). For small stimuli the response i.e., change in membrane potential, was defined by Ohm's law. For stimuli above threshold an all or nothing action potential was evoked. However, in the absence of an action potential local circuits would dissipate with distance along the axon, evidence that the passive response is not a suitable means of long-distance transmission of electrical signals (Fig 1.4C). In the spring of 1938 Hodgkin visited Erlanger in St Louis, who was unconvinced by Bernstein's membrane theory or the role of local circuits in the propagation of excitation and challenged Hodgkin to devise a convincing experiment to support his ideas (Huxley, 2000). Hodgkin duly obliged, ingenious experimental design allowed him to complete these experiments on his return to New York. He realised that the basis of the local circuit theory was the return of current through the membrane via the extracellular fluid (Fig 1.4B), thus if the resistance of the extracellular fluid was altered then the conduction velocity would change accordingly. To increase the resistance, he arranged the isolated crab axon in a bath of seawater, but he could raise the axon, so it was immersed in oil with only a very thin layer of seawater being retained between the axon and the oil, thereby increasing extracellular resistance. Under these conditions the conduction velocity was decreased compared to the axon bathed in seawater. An equivalent experiment in which extracellular resistance was decreased by increasing the salt content of the seawater would have potentially damaging osmotic effects on the nerve, so Hodgkin devised an arrangement where the nerve was placed on a grid of platinum strips, which caused an increase in conduction velocity, strong evidence of the existence of local circuits carried by electric current (Hodgkin, 1939).

Hodgkin then travelled up to Woods Hole where he met Cole and Curtis (Cole is unsure whether he met Hodgkin on a visit he made to Cambridge in 1936, Cole, 1979). They had taken Young's advice and proceeded with experiments on squid axons. Cole had devised a means of reproducing the experiments carried out on *Nitella*, which demonstrated a decreased impedance associated with excitation, on squid (*Loligo*) axon to determine the response of the membrane impedance to excitation and it was at this point that Hodgkin visited. Hodgkin had not measured membrane conductance directly and was very interested to see whether excitation was linked to changes in membrane conductance. Cole demonstrated decreased impedance (increased conductance) in the axon membrane in response to excitation (Fig 1.3C), but there was no effect on capacitance, which indicated that the membrane did not lose its structural integrity during excitation. According to Cole, Hodgkin literally jumped with delight when he saw the famous image on the cathode ray display (Fig 1.3C), a wonderful snapshot of the unbridled enthusiasm of youth (Cole, 1979).

At this point Hodgkin spoke with Curtis about recording intracellular action potentials from squid axons, but Cole's opinion was 'why bother with an upside down action potential?' (Cole, 1979).

## Extracellular versus intracellular recordings

This is a suitable point to discuss the differences between extra- and intracellular recording as it highlights the tenet that scientific advances are made through technological advances. Externally recorded action potentials tend to be small in amplitude. The electrical signal recorded is an aggregate of all the potentials present in the vicinity of the electrode, and the complex theory of volume conduction must be applied in order to fully understand the nature of the recording (Patton, 1982). In this manner the extracellular technique can be considered easier to implement but more difficult to interpret than intracellular recording (Dempster, 1993). The most important distinction is that the membrane potential cannot be directly measured, and thus any estimates of the membrane potential are crude approximations. Given Bernsteins's hypothesis that the resting membrane potential was the result of differences in the trans-membrane K<sup>+</sup> concentrations, measuring the potential difference across the membrane could very well provide information regarding the mechanism that underlies the action potential, i.e., the change in membrane potential during an action potential is likely facilitated by ion movements across the membrane. The giant axon(s) of the squid was identified by JZ Young (Young, 1938), although in a bizarre case of coincidence the husband of one of Cole's previous landladies had published a description of the axon in 1912, many years prior to Young's discovery (McComas, 2011). There are in fact ten giant axons on each side of the mantle, making twenty in total per squid, where each giant axon innervates a distinct area of mantle. Young demonstrated a few very important electrical properties of the axons. Firstly, that there was a threshold of stimulus required to produce an action potential, but supra-threshold stimuli elicited no additional response. Secondly, that variable axon diameter resulted in simultaneous action potential arrivals enabling coordinated contraction of the mantle. These results complemented those of Erlanger and Gasser who demonstrated that conduction velocity of an axon was determined by its diameter in frog nerves (Erlanger & Gasser, 1937).

## The first action potential

Hodgkin returned to Cambridge in late July 1938 and invited an undergraduate student, Andrew Huxley, to join him in experiments to determine the magnitude of the action potential. These experiments were carried out using extracellular recording techniques on crab axons and showed that the action potential was larger than the resting potential i.e., the action potential overshot 0 mV. Although the extracellular technique only provided an approximation of the action potential amplitude the results were intriguing, as any errors in recording would apply to both potentials. This result stimulated Hodgkin and Huxley to try to record intracellular action potentials from squid. These experiments would take place in Plymouth, the only laboratory with access to fresh squid. Huxley, who had received a classical education, was well versed in physics, maths and chemistry with a practical knowledge of mechanics and an interest in excitable nerves (Huxley, 2004). Hodgkin could not have chosen a more suitable partner. Huxley initially tested the viscosity of the squid axoplasm by vertically hanging an axon to see how far a bead of mercury placed

on the surface of the cut axon would fall. To their surprise the mercury did not fall, evidence of the viscous jellylike composition of axoplasm. However, Huxley realised that this was an ideal orientation in which to penetrate the axoplasm with an intracellular electrode made from chlorided silver wire, and thus non-polarisable, a path for its penetration being created by insertion then withdrawal of a fine needle (Fig 1.3B). Hodgkin and Huxley were thus able to record the first intracellular action potential. The recording was of sufficient resolution to identify the following components. The resting membrane potential of the axon was about -45 mV, the action potential was very rapid and exceeded 0 mV, peaking at about 40 mV, followed by a rapid repolarisation towards, and then past, the resting membrane potential to about -60 mV, before slowly returning to its initial resting value of -45 mV (Fig 1.5A). With war imminent they sent a brief paper to *Nature* in which they described their findings but offered no suggestions as to a mechanism (Hodgkin & Huxley, 1939). War was declared two weeks later in September 1939 and their work on the squid axon was suspended for 8 years.

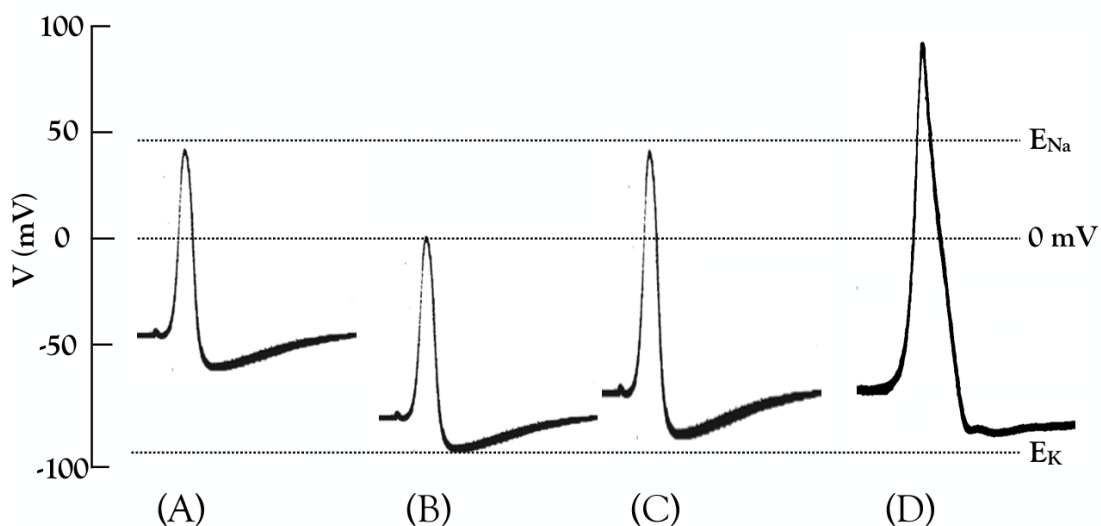


**Figure 1.5 - The intracellularly recorded action potential.** A. The action potential recorded by Hodgkin and Huxley in 1939 from squid giant axon, displayed a resting potential of -45 mV and peaked at about 40 mV (Hodgkin & Huxley, 1939). The approximate values for  $E_{Na}$  and  $E_K$  have been superimposed, based on experimental values of  $[Na]_o$  and  $[K]_o$  and measurements of  $[Na]_i$  and  $[K]_i$  from squid (Steinbach & Spiegelman, 1943). B. Assuming the deviation of AHP from  $E_K$  was due to junction potentials, an appropriate correction where the AHP peak approached  $E_K$  resulted in loss of the overshoot. C. Improvement and refinement of technique resulted in the resting membrane potential approaching  $E_K$ , whilst the peak of the action potential was unchanged. D. The action potential recorded by Curtis and Cole had a resting membrane potential of close to -60 mV, peak AHP approached  $E_K$ , but the action potential peaked at about 100 mV, far in excess of  $E_{Na}$  (Curtis & Cole, 1942).

This recording was an important technological advance as it demonstrated the first membrane potential recording from inside an axon and made possible experiments inconceivable with the existing extracellular techniques. It was also important in that the negative resting membrane potential was consistent with Bernstein's membrane theory, but the positive peak of the action potential was inconsistent with Bernstein's breakdown of selective permeability to  $K^+$  during excitation. As the war came to an end Hodgkin and

## A companion guide to the Hodgkin-Huxley papers

Huxley reconvened in early 1945 and published a fuller account of the intracellular recording, suggesting four possible mechanisms underlying the action potential, none of which mentioned the reversal potential for  $\text{Na}^+$ ,  $E_{\text{Na}}$  (Hodgkin & Huxley, 1945). Why Hodgkin and Huxley made no claims that the reason the membrane potential approached  $E_{\text{Na}}$  was that the membrane must have become selective permeable to  $\text{Na}^+$ , known as the  $\text{Na}^+$  theory, has been a source of debate ever since, and has in retrospect been called ‘stupid’ by Huxley (Huxley, 2002). The reasons for this likely included an extremely important point that is forgotten in the world of modern electronics and off the shelf amplifiers. Hodgkin and Huxley designed and built their own amplifiers with no commercial versions available for comparison. They also fabricated their own electrodes of complex design. In addition, the complications of junction potentials, which are potentials that occur at the interface of two salt solutions as would be present with the hollow glass capillary electrodes filled with seawater that they employed in their recordings, and the polarisation of later electrodes, which contained silver wires running the length of the electrode, meant that they could not be certain that their recordings were a true reflection of the membrane potential. This uncertainty was compounded by a paper published during the war in which Cole reported two confounding pieces of information (Curtis & Cole, 1942). The first was that the peak amplitude of action potentials they recorded sometimes exceeded the calculated  $E_{\text{Na}}$  (Fig 1.5D), and the second was that the action potential was not affected by switching the seawater bathing the axon with dextrose solution i.e., the axon continued to conduct in the absence of  $\text{Na}^+$  bathing the axon. The first point was indeed recorded experimentally, but the large action potential amplitude was later discovered to be due to an artefact of the electronics identified as overcompensation for electrical capacity of the electrode (Angel, 1996). However Cole and Curtis took great care to minimise junction potentials and thus their measurement of resting membrane potential was more accurate than Hodgkin and Huxley’s (McComas, 2011), which can be appreciated by comparing Figs 1.5A and D. If the Cole recordings were accurate and the  $\text{Na}^+$  theory was valid, then the  $[\text{Na}]_i$  in the axoplasm of squid used by Cole and Curtis would have to be very low, an unlikely proposition in light of recently published measurements of squid axoplasm  $[\text{Na}]_i$  (Steinbach & Spiegelman, 1943). It appears that the second point was never actually shown experimentally and was a result of confusion between Curtis, who wrote the paper and had now moved from Chicago, and Cole who read a draft of the paper believing that such an experiment had been carried out (McComas, 2011). However, the uncertainty surrounding the magnitude of an action potential is clear when comparing the traces in Fig 1.5. The first trace illustrates Hodgkin and Huxley’s action potential (Hodgkin & Huxley, 1939). The calculated  $E_{\text{Na}}$  and  $E_{\text{K}}$  have been superimposed using experimental measures of  $[\text{Na}]_i$  and  $[\text{K}]_i$  from squid axoplasm (Steinbach & Spiegelman, 1943). We shall ignore chloride in our discussion. The resting membrane potential was consistent with a membrane predominantly, but not exclusively, permeable to  $\text{K}^+$  since the membrane potential was not equal to  $E_{\text{K}}$ . However, the after-hyperpolarisation (AHP) was more negative than the resting membrane potential, suggesting that at this point the  $\text{K}^+$  permeability of the membrane transiently increased compared to rest. The membrane potential at the peak of the action potential approached  $E_{\text{Na}}$  indicative of a transient increase in permeability to  $\text{Na}^+$  relative to  $\text{K}^+$  (Fig 1.5A). If we shift the action potential profile vertically down the voltage axis so that the peak AHP meets  $E_{\text{K}}$  we find that the action potential overshoot all but disappears (Fig 1.5B), consistent with Bernstein’s prediction relating to permeability changes during excitation. Given the uncertainty about junction potentials and polarisation of electrodes this may have dissuaded Hodgkin and Huxley from making any claims about  $E_{\text{Na}}$ . We know that Hodgkin and Huxley’s technique improved during subsequent recordings, the resting membrane potential they recorded

becoming progressively more hyperpolarised, with the action potential peak maintained at just below  $E_{Na}$ . Adjusting the action potential record for this improvement by stretching the original record on the voltage axis so the resting membrane potential approaches -70 mV, but maintaining the action potential peak at 40 mV, results in a more accurate reflection of the membrane potential during an action potential in squid axon (Fig 1.5C). It is illuminating to plot the Cole and Curtis 1942 action potential on the same scale, to appreciate the degree by which the action potential peak exceeded  $E_{Na}$  (Fig 1.5D) and acknowledge the reluctance of Hodgkin and Huxley in making any declarations regarding  $E_{Na}$ . However, Bernard Katz had no such reservations in disputing the fidelity of the Cole and Curtis action potential, preferring to believe the magnitude of the Hodgkin and Huxley action potential and the underlying assumptions regarding permeability changes that it suggested, as the template for his experiments. He was convinced that  $Na^+$  influx was involved in the upstroke of the action potential and used extracellular recording techniques on teased single fibres of crab nerve to show that reducing the  $[Na]_o$  caused a reduction in conduction velocity in axons, as one would predict if  $Na^+$  influx was involved in generation of the action potential (Katz, 1947). Thus, the stage was set for the golden era of electrophysiology.

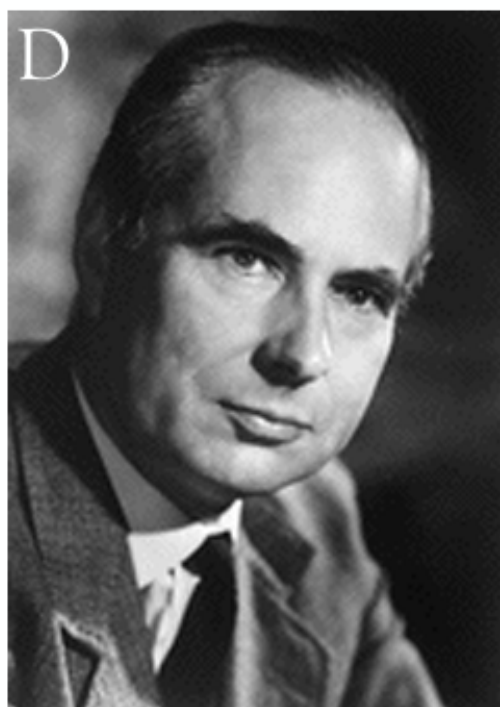
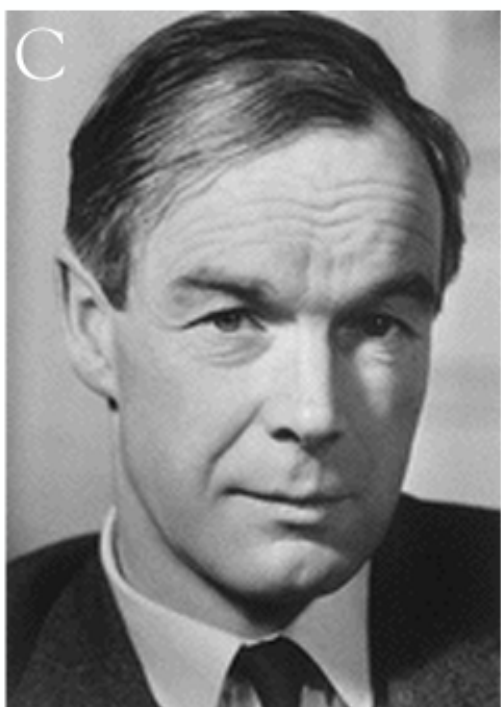


**Figure 1.6** - Kenneth (Kacy) Cole (A) and (B) Bernard Katz. (C) Professor Sir Alan Hodgkin, John Humphrey Plummer Professor of Biophysics at Cambridge University and (D) Professor Sir Andrew Huxley, Jodrell Professor of Physiology, UCL.

## 2. THE EFFECT OF SODIUM IONS ON THE ELECTRICAL ACTIVITY OF THE GIANT AXON OF THE SQUID

## Ohm's Law

There are two relationships that explain the foundation of electrical activity in neurones, Ohm's law and the Nernst equation. Ohm's law expresses a fundamental rule of electricity that  $V = IR$  i.e., voltage = current multiplied by resistance, or the flow of current through a resistor is proportional to the applied voltage. For our purposes it is more convenient to express Ohm's law in terms of conductance ( $g$ ), which is the reciprocal of resistance ( $g = 1/R$ ), and to rearrange the equation such that  $I = gV$  i.e., current = conductance times voltage (Hille, 2001). This equation expresses a very important relationship, which is that no current will flow if there is no driving force i.e., if  $(V - E_x)$  is zero. The separation of the intra- and extracellular spaces by the cell membrane into compartments that contain unequal concentrations of ions creates the negative resting membrane potential that underlies the trans-membrane current flow associated with the electrical activity that defines brain function. A large proportion of the energy substrate that the brain receives is devoted exclusively to maintaining these trans-membrane ion gradients (Attwell & Laughlin, 2001).

## The Nernst equation

The Nernst equation predicts the reversal potential, which is the membrane potential at which no net current flows across a semi-permeable membrane that results from the uneven distribution of ions. The Nernst equation is:

$$E_x = \frac{RT}{zF} \ln \frac{[X^+]_o}{[X^+]_i} \quad (\text{Eq. 2.1})$$

where  $E_x$  is the reversal potential for monovalent cation  $X^+$ ,  $R$  is the gas constant ( $8.315 \text{ V C mol}^{-1} \text{ K}^{-1}$ ),  $T$  is the temperature in Kelvin ( $20^\circ\text{C} = 293 \text{ K}$ ),  $z$  is the unit-less valency of the cation,  $F$  is the Faraday constant ( $96,485 \text{ C mol}^{-1}$ ), and  $[X^+]_{o/i}$  are the extracellular and intracellular concentrations of monovalent cation  $X^+$  (Hille, 2001).  $E_x$  varies linearly with temperature and logarithmically with the ratio of the ion concentrations. A series of four papers has recently been published, which if read sequentially provide the requisite information on the topic of the Nernst equation (Cardozo, 2016; Crowther, 2017; Sawyer *et al.*, 2017; Brown, 2018). Briefly, the key relationships to understand are, (i) for monovalent cations such as  $\text{Na}^+$  and  $\text{K}^+$ , the value of  $RT/zF$  can be reduced to a constant at a fixed temperature. It is convenient to express the logarithmic ratio to the base 10 rather than as the natural logarithm, which requires a conversion factor of 2.303, since  $e^{2.303} = 10$  equates to  $\ln 10 = 2.303$ .

$$\frac{RT}{zF} = \frac{8.315 \text{ V C mol}^{-1} \text{ K}^{-1} \times 293 \text{ K}}{1 \times 96,485 \text{ C mol}^{-1}} = 0.0252 \text{ V}$$

which becomes 58 mV at  $20^\circ\text{C}$ , the temperature at which experiments in this paper were carried out, when taking into account the logarithmic conversion factor. As such the Nernst equation can be expressed as

$$E_x = 58 \log_{10} \frac{[X^+]_o}{[X^+]_i} \quad (\text{Eq. 2.2})$$

for the purposes of this paper. (ii) When the membrane potential ( $V_m$ ) is not equal to  $E_x$ , cation  $X^+$  will cross the membrane in the direction that drives the membrane potential towards  $E_x$ , the greater the separation the greater the flow of ions, and (iii) if the intracellular ion concentration remains constant, and the external concentration increases by a factor of 10, then the value of  $E_x$  will increase by 58 mV, since  $\log_{10}(10/1) = 1$ . If we use

$K^+$  as an example, where  $[K]_i$  is fixed at 345 mM, then graphically representing the Nernst equation in the form  $y = mx$ , where  $y$  is  $E_K$  and  $x$  is  $[K]_o$  plotted on a  $\log_{10}$  scale, results in the slope of the relationship ( $m$ ) between  $E_K$  and  $\log_{10}[K]_o$  of 58 mV. Where  $[K]_o = [K]_i$  the value of  $E_K$  is 0 mV since  $\log_{10} (1/1) = 0$  (Fig 2.1).

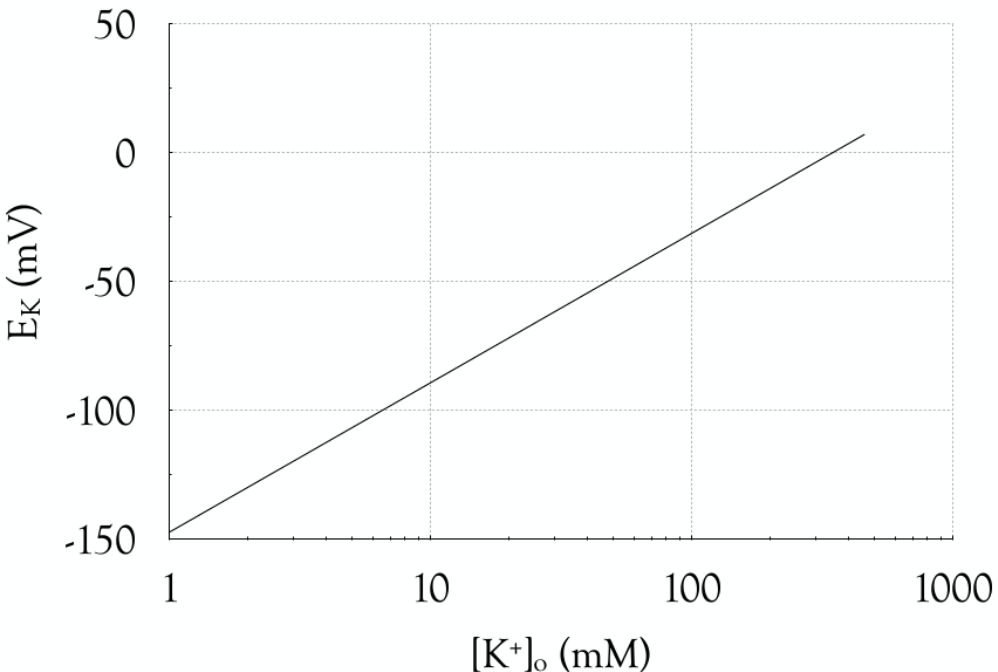


**Figure 2.1** - The Nernst equation applied to  $K^+$ , where the intracellular  $[K]_i$  is constant at 345 mM and the  $[K]_o$  varies along the x-axis. With  $[K]_o$  plotted on a  $\log_{10}$  scale the slope of  $E_K$  versus  $[K]_o$  is 58 mV at 20 °C according to Eq. 2.2.

### Effect of low $[Na]_o$ on the action potential

Hodgkin had access to preprints of Katz's paper that demonstrated decreasing  $[Na]_o$  reduced axon conduction velocity (Katz, 1947). This convinced Hodgkin of the validity of the  $Na^+$  theory, which he set out to rigorously test (Hodgkin, 1992). Hodgkin commenced a series of experiments in Cambridge in January 1947 using extracellular recording techniques on crab axons that demonstrated the action potential fell in reduced  $[Na]_o$  seawater in a manner consistent with the  $Na^+$  theory. These experiments were halted as the post-war austerity lack of fuel resulted in ambient room temperatures of about 6°C, too cold for the delicate dissections. It is of great irony that this was a more appropriate temperature in which to conduct the experiments than the room temperature (20°C to 25°C) reported in the paper. It is also of extreme interest that Hodgkin, in a throwaway sentence in his autobiography (p.271, Hodgkin, 1992) revealed an unreported aspect of their work that was not publicised until 2002, namely that Huxley was already computing reconstructed action potentials on the Brunsviga calculator (see Chapter 7) before any voltage clamp experiments had been carried out (Huxley, 2002). Katz joined Hodgkin in Plymouth in mid-June 1947 to

investigate the effects of  $[Na]_o$  on the action potential of squid giant axon using intracellular electrodes. Huxley, who was busy preparing for his wedding, did not attend these sessions and was excluded from the author list although his contribution to discussions on the work was acknowledged. These experiments recorded only the voltage response i.e., membrane potential, and are thus easier to interpret than the later papers. In this paper Hodgkin and Katz optimised design of the intracellular electrodes and settled on an electrode that incorporated a silver wire that extended the length of the glass capillary, which contained seawater as the conducting medium (*Figure 2*). This design minimised both polarisation of the electrode and junction potentials when recording from axons bathed in seawater.

## Action potential properties

The experiments were based on a very simple premise; altering the concentration of  $Na^+$  or  $K^+$  in the seawater bathing the axon should reveal to which component of the action potential profile these ions contributed. Hodgkin and Katz used seawater to bathe the axon, but when the seawater was diluted with isotonic dextrose solutions all ions were diluted, not just the ion of interest. Indeed because of these dilutions the baseline  $[Na]_o$  varied around 450 mM (it was 465, 450 or 445 mM in *Table 7*) and  $K^+$  varied around 10 mM (it was 13 mM in *Figure 13*). This also changed the junction potential between the bathing solution and the electrode. The average value of the resting membrane potential was -48 mV with the action potential amplitude of 88 mV, thus the overshoot, defined as the potential by which the action potential exceeded 0 mV was 40 mV (Fig 2.2A). The amplitude of the after-hyperpolarisation (AHP), defined as the extent of the post-action potential membrane hyperpolarisation beyond the resting membrane potential, was 14 mV (*Table 1*). These values are interesting in light of previous discussions as they show that the resting potential value of -48 mV was 40 mV more depolarised than  $E_K$ , and indeed about 10 mV more depolarised than the resting membrane potential recorded a year later (Hodgkin *et al.*, 1952), indicative of improvement of technique and accuracy of measurement achieved through practice. It was also 15 mV more depolarised than the resting potential recorded by Cole and Curtis (Curtis & Cole, 1942). These results were, however, inconsistent with Bernstein's membrane hypothesis. The amplitude of the action potential was smaller than that recorded later (Hodgkin *et al.*, 1952) due to the depolarised membrane potential, but the peak approached  $E_{Na}$  (46 mV) as expected. Since Hodgkin and Katz did not have an accurate cooling system, they conducted the experiments at 20°C to 22°C, significantly warmer than the sea temperature in which the squid lived. In retrospect the axon was probably deteriorating under such conditions and at these higher temperatures the more rapid inactivation of the  $Na^+$  permeability pathway (see Chapter 6), resulted in smaller action potentials at higher temperatures. This phenomenon was reported in a little known paper also published by Hodgkin and Katz in 1949 in which they described the effect of temperature on action potential profile (Hodgkin & Katz, 1949b). The most obvious explanation for the existence of the AHP was that the membrane, in the immediate aftermath of an action potential, became predominantly permeable to  $K^+$ . What Hodgkin and Katz didn't explicitly state was that the presence of an AHP indicated that at rest the axon could not be exclusively permeable to  $K^+$ , since if that were the case the resting membrane potential would equal  $E_K$  and there would be no AHP (but see *Figure 12*).

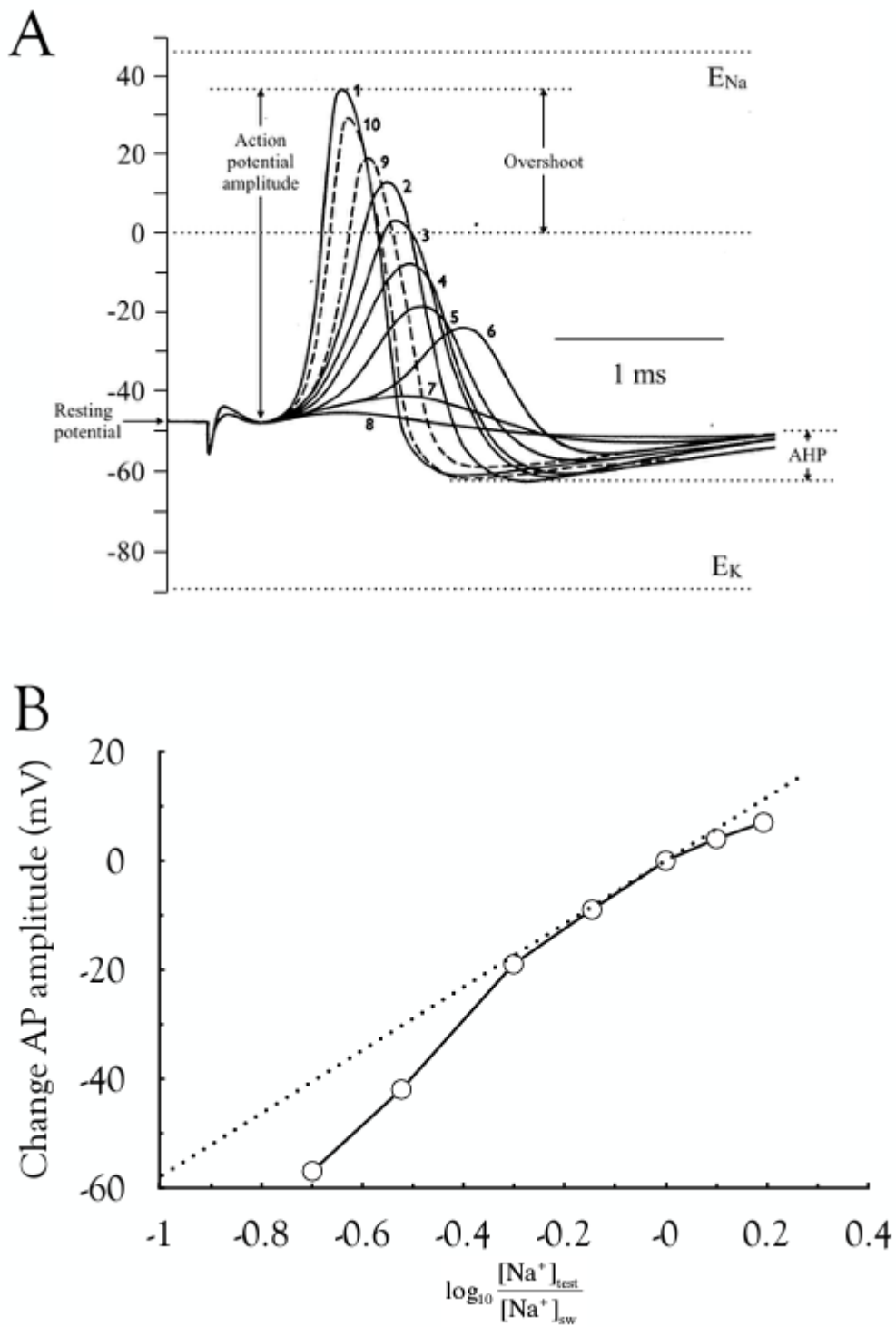


**Figure 2.2 - Reduced  $[Na]_o$  caused action potential attenuation. (A)** Replacing the seawater bathing the axon with isotonic dextrose caused a gradual attenuation of the action potential as the seawater was dispersed. **(B)** A plot of the change in action potential amplitude compared to the logarithm of the ratio of  $[Na]$  in seawater compared to test  $[Na]$  seawater revealed that the action potential peak followed  $[Na]_o$ . The dotted line depicts the Nernstian relationship.

## Na<sup>+</sup> free seawater abolishes the action potential

The effect of substituting seawater with isotonic dextrose is illustrated in Fig 2.2A. Under these conditions it was not only Na<sup>+</sup> that was removed, but all the ions, presenting a confusing picture. There is considerable information present in these traces, which can be summarised as follows. The most obvious effect was that the amplitude and the rate of rise of the action potential decreased as the salts dissipated on replacement of seawater with isotonic dextrose. However, the AHP also decreased, as did the rate of repolarisation. The resting membrane potential hyperpolarised, but this may have been due to junction potentials, so the resting membrane potential was judged the same for all records. With exchange of Na<sup>+</sup> for dextrose, the value of  $E_{Na}$  would become less depolarised i.e., decrease from a value of 46 mV towards 0 mV, due to [Na]<sub>o</sub> decreasing while [Na]<sub>i</sub> was unchanged, and would eventually fall below 0 mV causing loss of overshoot. An estimate of the value of [Na]<sub>o</sub> could be made by inserting the value of peak action potential amplitude as  $E_{Na}$  and calculating the corresponding value of [Na]<sub>o</sub>, which when compared to the [Na] in seawater of 450 mM, would give the degree of dilution of seawater for each action potential. Perhaps it would be more instructive to realise that based on the first figure in the next paper (Hodgkin *et al.*, 1952) a depolarisation of 15 mV above rest i.e., to about -50 mV was required to generate an action potential, thus if  $E_{Na}$  fell below -50 mV no action potential would be produced. Calculations based on Eq. 2.1 suggest this would be in the order of 10 mM [Na]<sub>o</sub>, which could potentially correspond with trace 8 in Fig 2.2, but a reasonable estimate of the point where the action potential failed was when [Na]<sub>o</sub> decreased below 20% of that in seawater. The attenuation in action potential amplitude can be understood as a consequence of the fall in  $E_{Na}$  resulting from the decreasing [Na]<sub>o</sub> (Fig 2.2B). The decrease in the rate of rise can also be explained. With lower [Na]<sub>o</sub> there was less of a Na<sup>+</sup> concentration gradient of across the membrane, so although the permeability of the membrane to Na<sup>+</sup> had not changed the driving force ( $V - E_{Na}$ ) had been reduced. The relationship is known as the Hodgkin cycle (Hodgkin, 1951). A supra-threshold depolarisation causes the opening of Na<sup>+</sup> permeability pathways with the resulting influx of Na<sup>+</sup> causing a further depolarisation, which in turn leads to opening of more Na<sup>+</sup> permeability pathways, etc. If this process went unchecked the membrane potential would depolarise in an exponential manner until it reached  $E_{Na}$ . As illustrated in Fig 2.3 the Na<sup>+</sup> permeability and membrane potential interact in a regenerative manner resulting in a positive feedback cycle (Hodgkin, 1951).

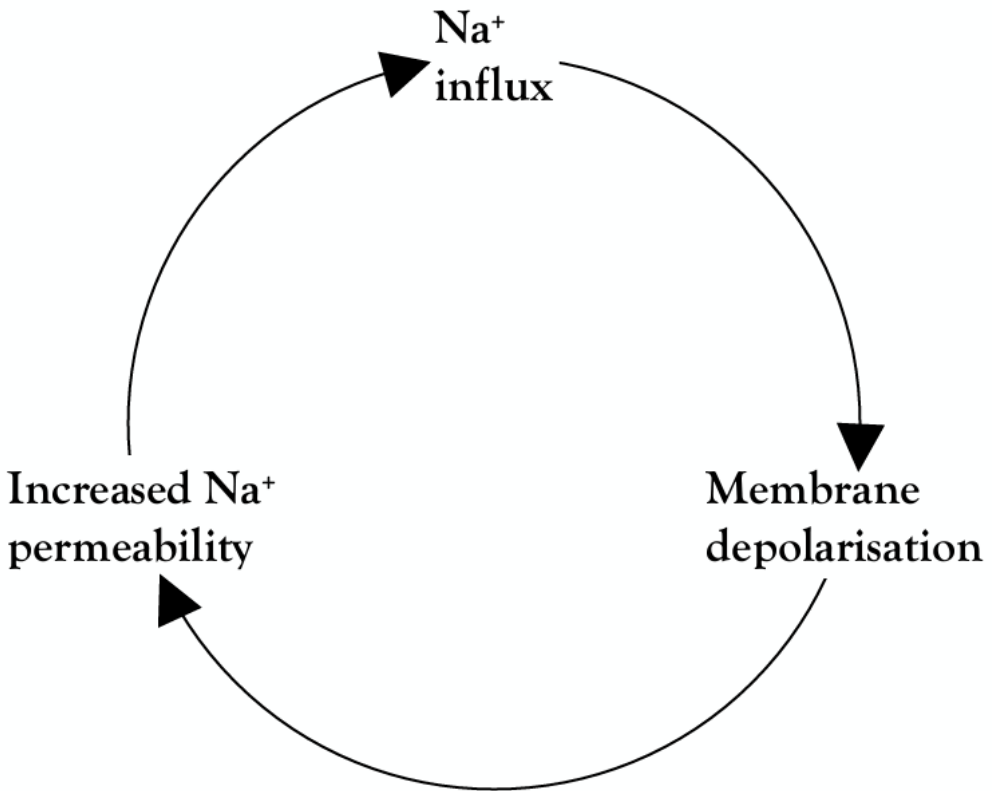


**Figure 2.3** - The Hodgkin cycle illustrates the positive feedback mechanism whereby membrane depolarisation increases Na<sup>+</sup> permeability allowing Na<sup>+</sup> influx, which causes more depolarisation.

The resting membrane potential hyperpolarised on switching to dextrose as expected, since  $E_K$  would hyperpolarise as [K]<sub>o</sub> decreased, causing the AHP to increase in amplitude. The rate of repolarisation also decreased, which is a balance between the increased concentration gradient for K<sup>+</sup> to leave the axon as [K]<sub>o</sub> was decreased, and the reduced driving force ( $V - E_K$ ) as the membrane potential at which the action potential peaked decreased.

### Effect of variable [Na]<sub>o</sub> on the action potential

Whilst Fig 2.2 illustrates the effects of a general reduction of [Na]<sub>o</sub> on the action potential no quantification was possible since the [Na]<sub>o</sub> for any of the traces illustrated was not known. In Figures 4 to 8 known concentrations of [Na]<sub>o</sub> were included in the seawater bathing the axon, which allowed quantification of the effects, which could then be compared with predictions based on the Nernst equation. However, this matter was complicated by the fact that [Na]<sub>i</sub> was unknown for the axon recorded. Hodgkin and Katz overcame this obstacle by applying their knowledge of the laws of logarithms to create an algebraic expression that allowed them to exclude this unknown parameter. The reductions of [Na]<sub>o</sub> in seawater to 33%, 50% or 71% of control (450 mM) resulted in a common effect of

reduced action potential amplitude and reduced rate of rise, the effect being dependent upon the degree of  $[Na]_o$  reduction. The action potential peak closely followed the  $[Na]_o$  (Fig 2.2B). This reduction in action potential amplitude was not the result of changes in the resting membrane potential, which only hyperpolarised by a few mV, whereas the decrease in action potential amplitude was an order of magnitude greater (*Table 4*). Hodgkin and Katz predicted that the change in action potential amplitude when  $[Na]_o$  was decreased could be accurately quantified by the Nernst equation. Their reasoning was as follows. If the action potential resulted from increased  $Na^+$  permeability, then the peak of the action potential would approximate with  $E_{Na}$ , with the result that reducing the  $[Na]_o$  would result in a predictable reduction in action potential amplitude. Thus, the difference between the action potential peak in normal seawater and test seawater containing reduced  $[Na]_o$  would be predicted by the difference between the  $E_{Na}$  calculated in seawater and the  $E'_{Na}$  calculated in reduced  $Na^+$  seawater. The  $E_{Na}$  where the axon was bathed in seawater was:

$$E_{Na} = 58 \log_{10} \frac{[Na^+]_{seawater}}{[Na^+]_i} \quad (\text{Eq. 2.3})$$

The reversal potential ( $E'_{Na}$ ) when  $[Na]_{seawater}$  was reduced to  $[Na]_{test}$  was calculated as

$$E'_{Na} = 58 \log_{10} \frac{[Na^+]_{test}}{[Na^+]_i} \quad (\text{Eq. 2.4})$$

Thus the difference between the two values was

$$E_{Na} - E'_{Na} = 58 \log_{10} \frac{[Na^+]_{seawater}}{[Na^+]_i} - 58 \log_{10} \frac{[Na^+]_{test}}{[Na^+]_i}$$

By using the 2nd law of logarithms, where  $\log a/b = \log a - \log b$

$$\begin{aligned} E_{Na} - E'_{Na} &= 58 \log_{10} \frac{\frac{[Na]_{seawater}}{[Na]_i}}{\frac{[Na]_{test}}{[Na]_i}}, \\ E_{Na} - E'_{Na} &= 58 \log_{10} \frac{[Na]_{seawater}}{[Na]_{test}} \end{aligned} \quad (\text{Eq. 2.5})$$

In this manner both the action potential amplitude and the overshoot could be compared to predicted values (*Figures 6 and 7, Table 4*). The values were consistent except at lower values of  $[Na]_o$ . The effects of varying  $[Na]_o$  on the action potential properties were quantified and were as expected if the rise of the action potential was due to  $Na^+$  influx. However, in substituting the seawater there was no compensation made for  $K^+$ , so there were small effects on resting membrane potential, and minor effects on the AHP. Increasing the  $[Na]_o$  had significant effects on the action potential. In this classic experiment (*Figure 8*), which is beautifully simple and entirely convincing, the action potential became larger in amplitude as a result of elevating  $[Na]_o$  and it is unlikely that any increase in the action potential amplitude would result from abnormal solutions (Hodgkin, 1992). It must be borne in mind that in these experiments there was almost certainly a constant steady depolarisation of the membrane potential by up to 2 mV per hour, thus it would be difficult experimentally to induce an action potential to increase in amplitude. Increasing the  $[Na]_o$  would cause  $E_{Na}$  to increase, and if the action potential was caused by  $Na^+$  influx then the action potential amplitude would increase.

The rate of change of the membrane potential during the action potential was covered in *Figures 9 to 11*. It is important to appreciate what the rate of change was

showing. Based on the Hodgkin cycle, the increase in rate of membrane depolarisation would continually increase if unchecked, a rare example of a physiological positive feedback cycle. However, there were several factors that would act to limit this. These include the decreased driving force ( $V - E_{Na}$ ) as the membrane potential approached  $E_{Na}$ , the limited availability of permeability pathways, the inactivation of the  $Na^+$  permeability pathways (Chapter 6) and the activation of the  $K^+$  permeability pathways, which would oppose the membrane depolarisation. A rate of membrane change of zero, did not mean the membrane potential was zero, but that the *rate of change* was zero, and there were two clear points where this would occur, at the peak of the action potential and at the peak of the AHP (Fig 2.4). At the onset of the action potential the regenerative relationship between  $Na^+$  permeability and membrane potential would occur (Fig 2.3). The decrease in the rate of change of membrane potential that occurred about halfway up the action potential was due to the factors mentioned above. It is clear that the rate of membrane depolarisation during an action potential provided a clear indication of the rate of  $Na^+$  influx and that when  $[Na]_o$  was altered the rate of change followed accordingly.

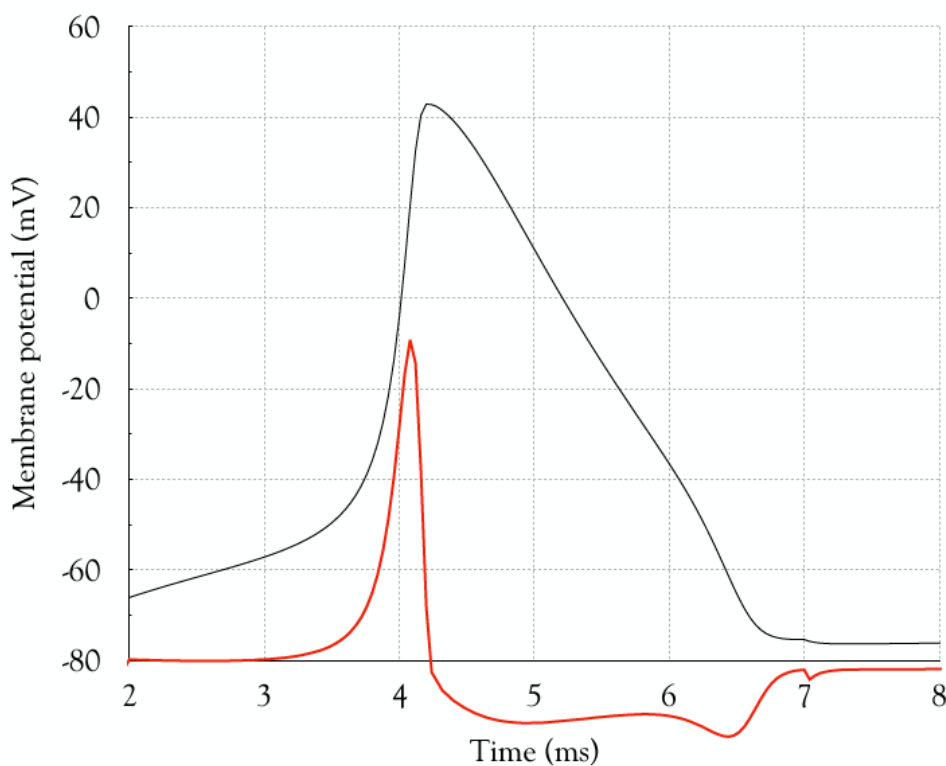


**Figure 2.4** - The rate of change of membrane potential ( $dV/dt$  - red trace) superimposed on an action potential (black trace). The figure is derived from a model of the Hodgkin Huxley squid axon (Brown, 2000) and shows a zero rate of change at the peak of the action potential and at the peak of the AHP.  $dV/dt$  (red trace) is plotted on an arbitrary y axis.

## Effect of altering $[K]_o$ on membrane potential

The results concerning the effect of changing  $[Na]_o$  on the action potential provided convincing evidence that the upstroke of the action potential was due to an influx of  $Na^+$ . Hodgkin and Katz then sought to determine if the repolarisation of the action potential was caused by a  $K^+$  efflux, and they used a similar experimental strategy i.e., alter  $[K]_o$  to see the effect on putative  $K^+$ -dependent components of the action potential. It is important to realise that since the resting membrane potential was sensitive to  $[K]_o$ ,  $[K]_o$  could not be altered to the same extent as  $[Na]_o$  i.e., removing  $K^+$  completely for any length of time would inevitably damage the axon nullifying the results. Since the resting membrane potential and the AHP were close to the computed value for  $E_K$  it was likely that the magnitude of the changes would not be as great as those for the  $Na^+$ , since  $E_{Na}$  was more than 100 mV distant from the resting membrane potential. If we suppose that at rest the membrane is permeable to  $K^+$ , then the resting potential is governed by the ratio of  $[K]_o$  to  $[K]_i$ , and since  $[K]_i > [K]_o$  the resting membrane potential must be negative, about -65 mV. A test of the role of  $K^+$  in the repolarising phase would be to increase  $[K]_o$  by an order of magnitude, thereby depolarising the value of  $E_K$  by 58 mV, and depolarising the resting membrane potential, thus during the repolarising phase of the action potential the AHP would fall to this depolarised level. However, such experiments could not be reasonably carried out since depolarising the membrane potential by such a large amount would inactivate the  $Na^+$  permeability pathways (Chapter 6) responsible for generating the action potential. Given these constraints Hodgkin and Katz were limited in the scope of their experiments, but they did vary  $[K]_o$  from its resting value of 10 mM to 20 mM and 0 mM. Under these conditions the following generalisations applied. When they decreased  $[K]_o$  the membrane potential hyperpolarised, since with decreased  $[K]_o$  the value of  $E_K$  hyperpolarised. In addition, the action potential amplitude increased due to the hyperpolarising effect on resting membrane potential. This would have no effect on  $E_{Na}$  and hence the action potential approached  $E_{Na}$  as previously described. With lower  $[K]_o$  the AHP was larger, and the rate of repolarisation increased (Fig 2.5A), equivalent to the effect of reducing  $[Na]_o$  decreasing the rate of depolarisation.

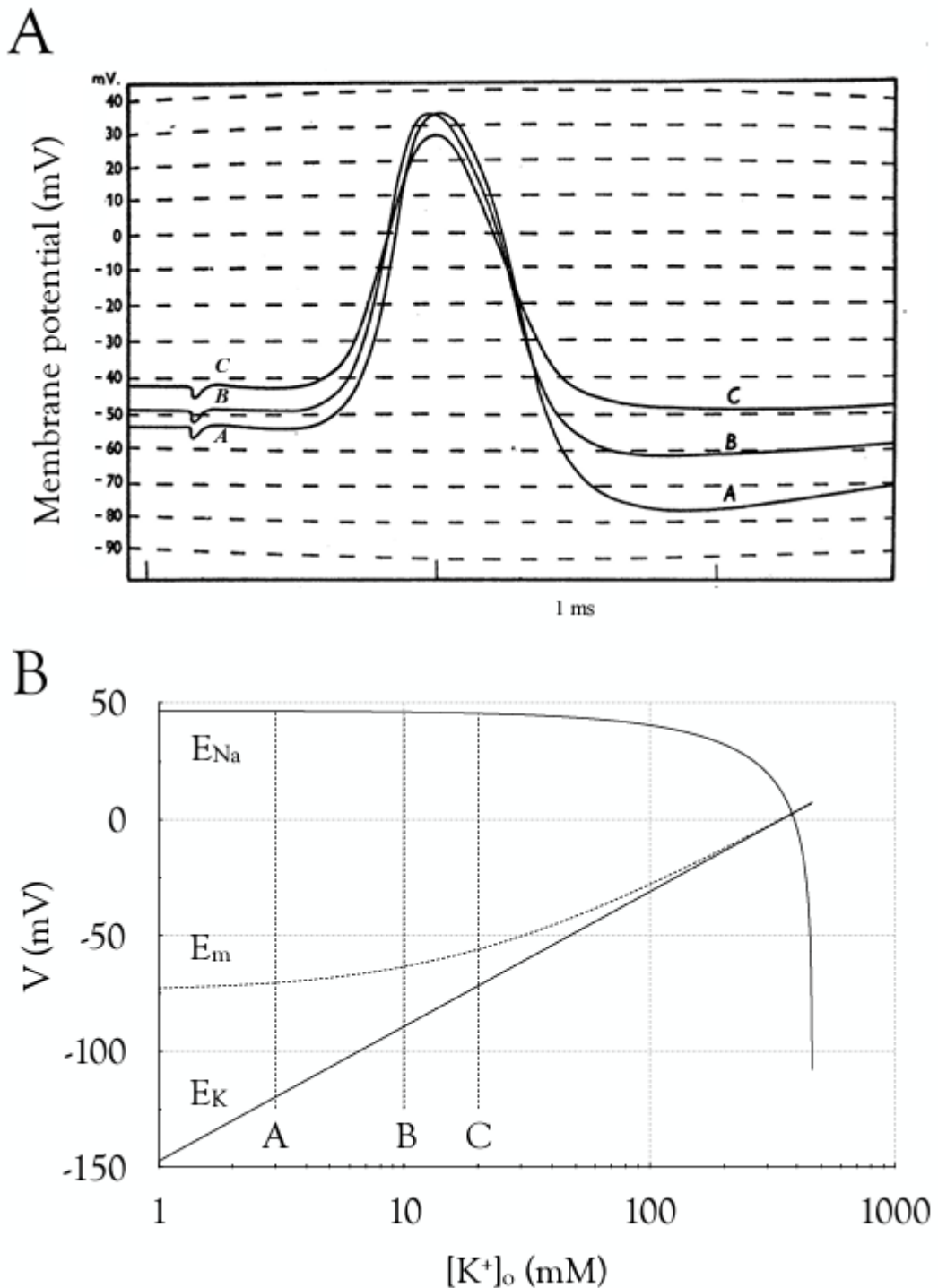


**Figure 2.5 - Effect of  $[K]_o$  on action potential profile.** (A) Three action potentials recorded under various  $[K]_o$ , (A) 0 mM  $[K]_o$ , (B) 10 mM  $[K]_o$  and (C) 20 mM  $[K]_o$ . (B) The values of  $E_{Na}$ ,  $E_K$  and  $E_m$  calculated for  $[K]_o$  over the range 1 to 1000 mM. The vertical lines indicate  $[K]_o$  for equivalent conditions under which traces (A – C) in A were recorded. The intercept of these lines with  $E_{Na}$ ,  $E_K$  and  $E_m$  approximate to the value of the action potential peak, AHP peak and resting membrane potential, respectively. The similarity is qualitatively if not quantitatively accurate.

If we assume a simplified situation, in which the membrane is only permeable to  $\text{Na}^+$  and  $\text{K}^+$ , then the membrane potential at any time will lie between  $E_{\text{Na}}$  and  $E_{\text{K}}$ . In addition, we assume that as a result of activity the intracellular and extracellular concentrations of  $\text{Na}^+$  and  $\text{K}^+$  do not change. The fact that the AHP is more hyperpolarised than the resting membrane potential and approaches  $E_{\text{K}}$  allows us to make several assumptions that can be mathematically modelled (see below). The first of these is that since the AHP is more hyperpolarised than the membrane potential at rest, the membrane cannot be selectively permeable to  $\text{K}^+$  at rest as proposed by Bernstein since it must have a finite permeability to  $\text{Na}^+$ . Secondly, as the AHP approaches  $E_{\text{K}}$ , at this point the membrane is more permeable to  $\text{K}^+$  than at rest. Thirdly, at the peak of the action potential the membrane is more permeable to  $\text{Na}^+$  than it is at rest, and it is far more permeable to  $\text{Na}^+$  than to  $\text{K}^+$  at this point. It may be reasonably assumed that the membrane potential gravitates towards the reversal potential for the particular ion to which the membrane at that instant is predominantly permeable.

## GHK voltage equation

Hodgkin and Katz carried out the unusual step of plotting previously published data from another research group as their *Figure 13* (Curtis & Cole, 1942). This now classic relationship showed the membrane potential response to varying  $[K]_o$  (N.B. the alterations in  $[K]_o$  were compensated for by equimolar changes in  $[Na]_o$  such that  $[Na]_o + [K]_o = 463 \text{ mM}$ ). The most important aspect of this non-linear relationship between membrane potential and  $\log_{10}[K]_o$  was that it could not be adequately described by the Nernst equation but was described by the Goldman-Hodgkin-Katz (GHK) voltage equation. This equation was derived in the *Appendix*. What Hodgkin and Katz did was to adapt the relationship first described by Goldman, which stated that (1) the membrane was homogeneous, (2) the concentration of ions at the edge of the membrane were the same as those in bulk solution, (3) the electric field was constant across the membrane, and (4) ions in the membrane moved under the influence of diffusion and the electric field as they would act in free solution (Goldman, 1943). This last point is in essence what the Nernst equation states, where it is diffusion i.e., the trans-membrane difference in ion concentrations, and the electric field ( $V - E_x$ ) caused by this uneven ion distribution across the membrane, that determines the direction and magnitude of trans-membrane ion movements.

A comparison of the action potentials recorded under various  $[K]_o$  with the computed values of  $E_{\text{Na}}$ ,  $E_{\text{K}}$  and resting membrane potential ( $E_m$ ) at equivalent values of  $[K]_o$  is extremely enlightening (Fig 2.5B) and demonstrates the applicability of the GHK voltage equation. The first step is to plot  $E_{\text{K}}$  and  $E_{\text{Na}}$  versus  $[K]_o$  on a  $\log_{10}$  scale where  $[K]_o + [Na]_o = 460 \text{ mM}$ , such that at e.g.,  $[K]_o$  of 200 mM,  $[Na]_o$  equals 260 mM. We use the values  $[Na]_i = 72 \text{ mM}$ ,  $[K]_i = 345 \text{ mM}$  (Steinbach & Spiegelman, 1943), with the baseline values of  $[K]_o = 10 \text{ mM}$  and  $[Na]_o = 450 \text{ mM}$  in this graph. As expected, the  $E_{\text{K}}$  (calculated as  $58 \log_{10}([K]_o/345)$ ) is a straight line with a slope of 58 mV, whereas the  $E_{\text{Na}}$  (calculated as  $58 \log_{10}((460 - [K]_o)/72)$ ) commences as an almost flat line at low values of  $[K]_o$  that hyperpolarises dramatically when  $[K]_o$  increases (and  $[Na]_o$  decreases). The membrane potential is calculated according to Eq. 2.6 with a  $P_{\text{Na}}$  value of 0.04. It is noteworthy that the membrane potential calculated from the GHK voltage equation must always lie between  $E_{\text{K}}$  and  $E_{\text{Na}}$  and where  $E_{\text{Na}}$  falls below the value of  $E_{\text{K}}$  ( $> 390 \text{ mM } [K]_o$ ) the membrane potential must be smaller than  $E_{\text{K}}$ . This is not apparent from most of the textbook illustrations of this relationship, where it appears that membrane potential is always greater than  $E_{\text{K}}$  irrespective of the  $[K]_o$  (Hodgkin & Horowitz, 1959; Woodbury, 1982; Aidley, 1996; Nicholls *et al.*, 2012; Purves *et al.*, 2012). At the range

of  $[K]_o$  used (0 to 20 mM) the  $E_{Na}$  does not alter, but the  $E_K$  and  $E_m$  do. For the baseline condition of  $[K]_o = 10$  mM the  $E_m$  is about -50 mV and the AHP reaches about -60 mV, a difference of about 10 mV (compare the intercept of the vertical line at  $[K]_o = 10$  mM with  $E_m$  and  $E_K$ ). When the  $[K]_o$  is reduced to low values (assume a value of 3 mM) the intercept illustrates an unchanged  $E_{Na}$  but the  $E_K$  is now about 15 mM more hyperpolarised than  $E_m$  with 10 mM  $[K]_o$ . An appreciation of the relationships illustrated in this graph is the foundation for understanding how the action potential profile responds to changes in  $[K]_o$  (Powell & Brown, 2021). These considerations likely encouraged Hodgkin and Katz in the modelling that they employed at the end of the paper. Note that Fig 2.5B is a qualitatively, but not quantitatively, accurate representation of the effect of  $[K]_o$  on the action potential profile, the disparity between the measured and predicted due to inaccuracies of the experimental method.

### A diversion - astrocytes are $K^+$ electrodes

Although not explicitly stated by Hodgkin and Katz there are certain assumptions that can be derived from the GHK voltage equation. Over fifteen years after Hodgkin and Katz published this work Stephen Kuffler investigated the response of the membrane potential of glial cells (astrocytes) in the optic nerve of the mudpuppy *Necturus* to changes in  $[K]_o$  using sharp micro-electrodes (Kuffler *et al.*, 1966; Orkand *et al.*, 1966). Kuffler found that these cells were exclusively permeable to  $K^+$  and could thus be considered  $K^+$  electrodes, in which the  $E_K$  transformed from a concept to a value that could be measured, since in these cells membrane potential equalled  $E_K$ . As we shall soon discover neurones release  $K^+$  as a result of excitation, leading to an accumulation of  $[K]_o$ . The consequence of this for the glial cells and for axon membranes is different as illustrated graphically (Fig 2.5B), where  $E_m$  represents the axon membrane potential and  $E_K$  represents the astrocyte membrane potential e.g., a glial cell membrane will depolarise by more than a neuronal membrane when exposed to the same increase in  $[K]_o$ . In this manner glial cells (in particular astrocytes) are more sensitive to changes in  $[K]_o$  than neuronal membranes, which may underlie their ability to respond to increased neuronal firing by releasing lactate to fuel neuronal activity (Sotelo-Hitschfeld *et al.*, 2015).

### Dissection of the GHK voltage equation

Awareness of the Nernst equation may lead one to expect that if a membrane is exclusively permeable to  $K^+$  and displays a slope of 58 mV, then a slight permeability to  $Na^+$  may cause the membrane potential to behave as illustrated in Fig 2.6A, where it is parallel but slightly depolarised relative to  $E_K$  for all values of  $[K]_o$ . This is not the case, but in order to explain why we must examine the GHK voltage equation in detail. Let's assume the simplified case where the membrane is only permeable to  $K^+$  and  $Na^+$ .

$$E_m = 58 \log_{10} \frac{P_K [K]_o + P_{Na} [Na]_o}{P_K [K]_i + P_{Na} [Na]_i} \quad (\text{Eq. 2.6})$$

where  $E_m$  is the membrane potential,  $P_K$  is the permeability to  $K^+$ , usually given a value of 1,  $P_{Na}$  is the permeability to  $Na^+$  relative to  $P_K$ . To dissect the underlying relationships leading to the distinctive shape of the GHK voltage equation we begin by plotting the individual contribution of  $K^+$  and  $Na^+$  to the total external divalent ion concentration (i.e., the numerator of the equation), where the percentage  $K^+$  contribution is calculated as  $([K]_o / ([K]_o + [Na]_o) \times 100\%$

$+ [Na]_o)) \times 100$ . It is apparent that  $K^+$  only dominates the numerator at concentrations greater than 225 mM (Fig 2.6B). The effect of  $K^+$  on the equation at higher values of  $[K]_o$  can be appreciated by calculating the contribution of  $[K]_o$  to the numerator taking into account the permeability to Na ( $P_{Na}$ ), calculated as  $([K]_o + (P_{Na} \times [Na]_o))$ , hence the contribution of  $K^+$  is  $([K]_o/\text{numerator}) \times 100$ , and equivalent calculations apply for  $Na^+$ . This relationship shows that for a  $P_{Na}$  value of 0.04,  $[K]_o$  dominates the numerator at concentrations greater than about 20 mM (but this will change according to  $P_{Na}$ : Fig 2.6C). It should be noted that since the denominator is  $(345 + (P_{Na} \times 72))$ , it is greater than the numerator except at large values of  $[K]_o$  and hence the value of the membrane potential is negative except at higher values of  $[K]_o$ . By calculating the membrane potential for a range of  $P_{Na}$  values from 0.005 to 0.1 the deviation from  $E_K$  can be visualised. At low values of  $P_{Na}$  the membrane potential is close to  $E_K$  but deviates the most at low values of  $[K]_o$  since here the contribution of  $K^+$  to the numerator is smallest. This effect is amplified for higher values of  $P_{Na}$ , but even under these conditions the value for the membrane potential approaches  $E_K$  at higher values of  $[K]_o$  since here the value of  $P_{Na} \times [Na]_o$  is relatively small (Fig 2.6D). Where  $P_{Na}$  is high there is a small increase in  $E_m$  to physiological elevations (up to 12 mM) in  $[K]_o$ .

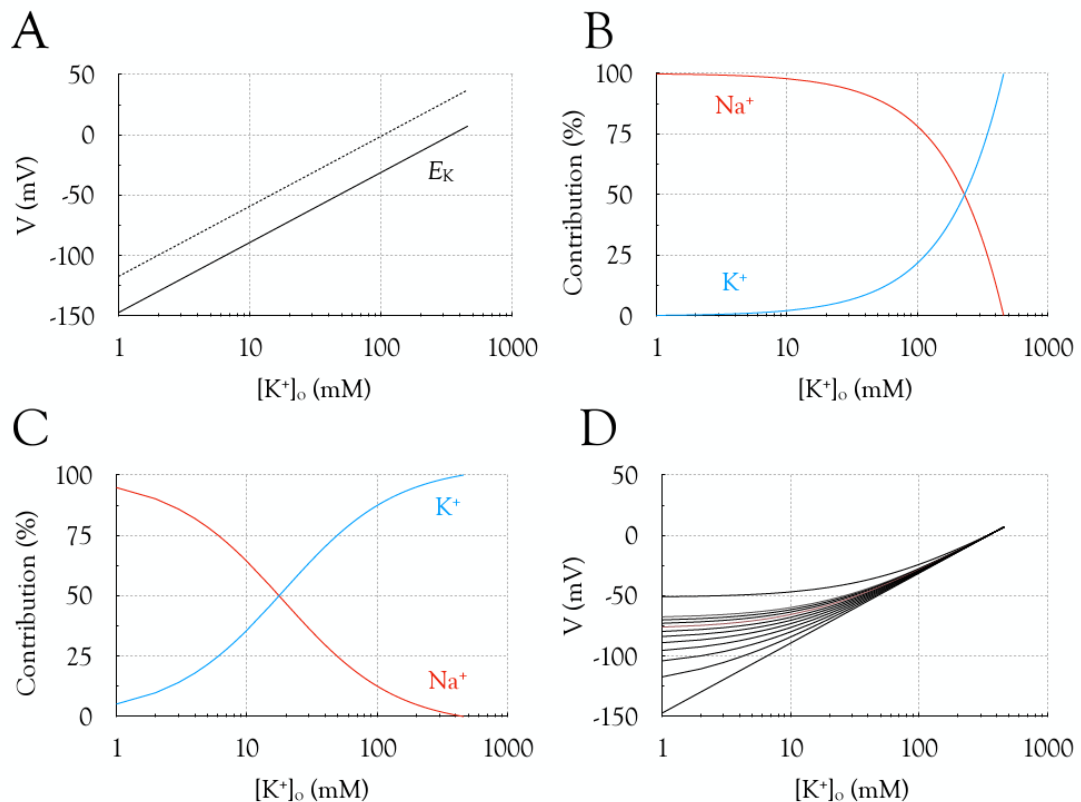


**Figure 2.6 - The GHK voltage equation.** (A)  $E_K$  versus  $[K]_o$  (continuous black line) with an upper parallel relationship (dotted line) indicating a presumed value of membrane potential with a small degree of  $Na^+$  permeability. (B) The percentage contribution of  $[K]_o$  and  $[Na]_o$  to the numerator of Eq. 2.5. (C) The percentage contribution of  $[K]_o$  and  $[Na]_o$  to the numerator for a  $P_{Na}$  of 0.04. (D) Values of membrane potential versus  $[K]_o$  for  $E_K$  (lowest trace), for  $P_{Na}$  values ranging from 0.005 to 0.05 in 0.005 steps, and the uppermost trace reflects  $P_{Na} = 0.1$ .

The limitations of carrying out experiments in which the seawater was simply diluted with dextrose solution were compensated by addition of appropriate ions such that the effect of reduction of  $\text{Na}^+$  and  $\text{K}^+$  could be studied in isolation (*Table 7*). Under these conditions the change in membrane potential in response to altering  $[\text{K}]_o$  were close to those predicted by the GHK voltage equation and of the correct polarity. A similar correlation was found for the AHP. The effects of reducing  $[\text{Na}]_o$  on the action potential amplitude were in agreement, with the exception that at low  $[\text{Na}]_o$  the observed decrease in action potential amplitude was greater than predicted. In addition to comparison of the absolute values of membrane potential, the relative permeability of the membrane to  $\text{Na}^+$  and  $\text{Cl}^-$  relative to  $\text{K}^+$  could be estimated for the membrane potential at rest, at the peak of the action potential, and at the peak of the AHP. At rest the membrane potential was predominantly permeable to  $\text{K}^+$  with relative permeability of 0.04 for  $\text{Na}^+$  and 0.45 for  $\text{Cl}^-$ . Using these values for a range of different salt concentrations, the change in membrane potential for control seawater was compared to the theoretical predictions. The match was accurate for most of the solutions (*Table 7*). Similarly at the peak of the action potential the observed and predicted membrane potentials matched for most of the salt concentrations, as was the case at the peak of the AHP where  $P_{\text{Na}}$  was negligible. These data indicate that at rest the membrane was predominantly permeable to  $\text{K}^+$ , but at the action potential peak this changed so that the membrane became transiently, predominantly permeable to  $\text{Na}^+$ , but during the AHP the membrane was predominantly permeable to  $\text{K}^+$  (Fig 2.7).

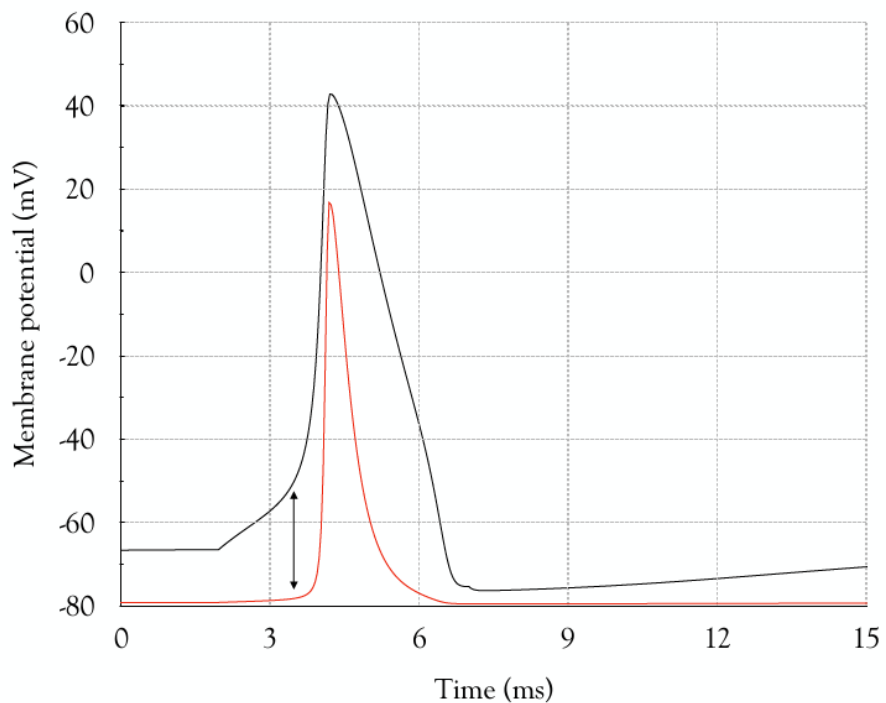


**Figure 2.7** - The changes in  $P_{\text{Na}}$  (relative to  $P_K$  of 1) during the action potential (black line) calculated according to Eq. 2.6 using Microsoft Solver to solve for  $P_{\text{Na}}$  for all values of membrane potential. Note how in the depolarisation of the membrane potential towards threshold (vertical arrow) the value of  $P_{\text{Na}}$  is close to zero, emphasising the point made by Hodgkin that it is local electrical circuits that bring the membrane potential to threshold.  $P_{\text{Na}}$  (red line) is plotted on an arbitrary y-axis.

An interesting postscript to this paper was that the 15-month delay between submission and publication in *The Journal of Physiology* so frustrated Hodgkin that he submitted his next paper to the *Journal of Cellular and Comparative Physiology* (Hodgkin & Nastuk, 1950). *The Journal of Physiology* editors were duly warned, and the seminal papers were all published within six months of submission.

### 3. MEASUREMENT OF CURRENT-VOLTAGE RELATIONS IN THE MEMBRANE OF THE GIANT AXON OF *LOLIGO*

## The voltage clamp

This paper concerns the basics of the voltage clamp technique, first of all verifying that insertion of the new microelectrode configuration did not damage the axon, confirmed by recording action potentials of normal amplitude. The membrane current evoked at a wide range of membrane potentials in normal seawater was reported. This was the most important result presented in the paper, but I discuss this in detail in more suitable context in Chapter 4, hence the brevity of this chapter. The first seven figures in this paper were methodological and described in detail the voltage clamp system. A key aspect that must be understood in appreciating some of the figures is this: because of the way in which the voltage clamp was designed, the membrane current could be measured via the amplifier as well as being recorded from the axon, since the current injected by the amplifier during a clamp matches the current that moves across the membrane. Obtaining the current density in this manner was referred to by Hodgkin and Huxley as the indirect method. The major advance in this (and subsequent papers) was the use of the voltage clamp technique. This was not the first paper to report on the voltage clamp technique, that honour goes to Cole (Cole, 1949), but the analysis applied to the voltage clamp records elevated Hodgkin and Huxley beyond their contemporaries (Angel, 1996). A very important aspect of Cole's recordings, of which Hodgkin was aware, having visited Cole and Marmont in Chicago in spring of 1948, was that there appeared to be no threshold i.e., the curves were smooth continuous traces (Fig 3.1). The development then decrease of the early inward current, which Hodgkin was convinced was carried by  $\text{Na}^+$ , illustrated the ability of the amplifier to clamp the membrane at a particular voltage and to cancel out the regenerative  $\text{Na}^+$  influx and depolarisation cycle via the negative feedback passing of opposing current (Hodgkin, 1992).

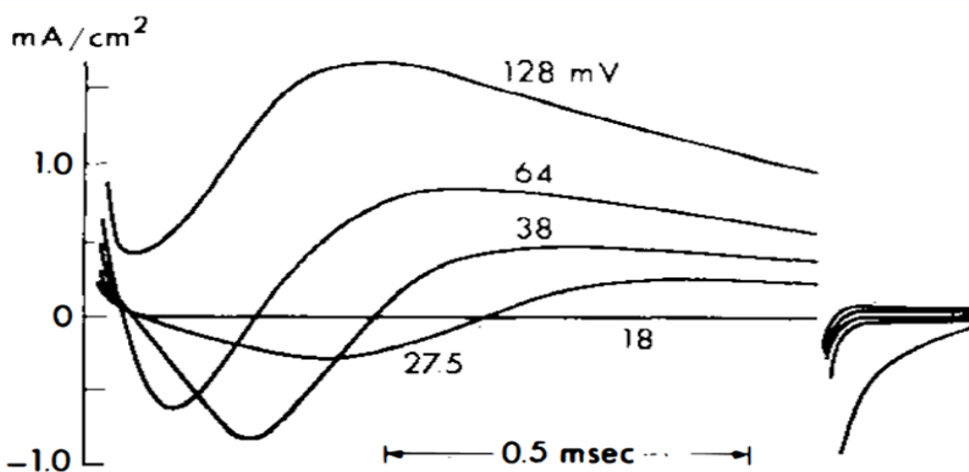


**Figure 3.1** - The first published voltage clamp recordings showed the currents evoked by depolarisation from rest. The numbers indicated the depolarisation in mV from rest (Cole, 1949). An early inward current developed smoothly then declined to reveal a later outward current. At greater levels of depolarisation, the inward current was replaced with an early outward current followed by the later attenuating outward current caused by electrode polarisation.

As mentioned in the Preface the convention by which current and voltage are reported in this guide is different from that used by Hodgkin and Huxley. The modern convention states that inward movement of positive ions is depicted as downward current deflection with the resulting voltage change depicted as an upward deflection. In this manner a downward current deflection indicates the entry of positive ions into the axon, whereas an upward current deflection indicates positive ions are leaving the axon (Brown, 2019a).

It is a common misconception that Hodgkin and Huxley invented the voltage clamp amplifier. They did not. It was invented by George Marmont (Marmont, 1949), who worked with Cole. On a visit to Cole in 1948, Cole not only showed Hodgkin the currents he had recorded by applying depolarising voltage steps, which comprised smoothly developing inward current followed by a late outward current (Cole, 1949), but also provided details of the voltage clamp design. On his return to the UK Hodgkin supervised the building of a voltage clamp amplifier with the important modification that he introduced two separate wires into the axon, one to record the voltage and the other to pass current. Cole only used one wire to measure voltage and pass current (Fig 3.1) thus his electrode polarised, causing distortion of the larger outward currents (Angel, 1996).

Based on preliminary data (Hodgkin *et al.*, 1949) Hodgkin believed that the early inward current did not subsequently decrease, and assumed that the smooth rise of the current recorded by Cole (Fig 3.1) was due to an artefact of his equipment. It was only later, as a result of refinement of the technique, when Hodgkin himself recorded early inward currents of a similar profile to those of Cole, that he accepted the accuracy of the data. The voltage clamp technique and the manner in which it was implemented demands close attention, as there are important conceptual considerations involved. Hodgkin and Huxley inserted an electrode over 1 cm in length into the axon. The very low resistance metal electrodes short-circuited the longitudinal travel of the current along the axon, such that under voltage clamp conditions the entire length of axon membrane was clamped to the same voltage. When stepping to a different voltage the transition was considered instantaneous and was marked by an extremely brief capacitive transient. Since the potential over the area of membrane was iso-potential there was no further capacitive current, and the voltage did not vary with time or distance. The current recorded under these circumstances varied with time only, not distance. It is worthwhile considering how artificial this situation was relative to the 'real life' regenerative propagation of an action potential along the axon at constant velocity, where the membrane potential varied with both time and distance.

In this manner there was no contribution to the current recorded under voltage clamp conditions from either the axial current flow along the axon or from the capacitive current. Thus the voltage clamp avoided the cable complications of axial current flow. The total membrane current ( $I$ ) in an axon was:

$$I = C_M \frac{dV}{dt} + I_i + \frac{d}{4Ra} \frac{\partial V}{\partial x^2} \quad (\text{Eq. 3.1})$$

Voltage clamping removed the first and third expressions on the right-hand side of the equation leaving only  $I_i$ , the sum of the voltage dependent ionic currents and the leak current. This greatly simplified the reconstruction of the space clamped action potential.

In this paper a coil was introduced to cool the seawater perfusing the axon to temperatures consistent with the ambient sea temperature in which the squid lived (3°C to

11°C). In stimulating the axon from rest brief shocks of increasing magnitude initially evoked sub-threshold responses, but when the depolarisation exceeded 12 to 15 mV an action potential was always evoked. These action potentials were of the appropriate profile and magnitude to convince Hodgkin and Huxley that insertion of the intracellular microelectrode did not damage the axon, and that the subsequent results obtained with voltage clamp were indeed an accurate reflection of the currents across the membrane. It is important to compare this threshold to evoke an action potential with the appearance of the inward current shown in *Figure 10*. Note that once an action potential was evoked it had the same basic profile i.e., the rates of depolarisation and repolarisation were the same, irrespective of the stimulus intensity, although the latency to action potential firing was correlated with the magnitude of the stimulus. The peak of the action potential was independent of the magnitude of the stimulus. These experiments were carried out at 23°C (*Figure 8*) and 6°C (*Figure 9*) and showed the same basic pattern, with the exception that the action potentials recorded at 23°C were faster. Injection of hyperpolarising current produced hyperpolarisation of the axon membrane that was stimulus strength dependent. In the terminology of Hodgkin and Huxley we can say that these hyperpolarising potentials were due to the leak current (Fig 3.2: see Chapter 5). Clearly something other than a leak current was activated 12 to 15 mV depolarised from rest, which was in the opposite direction to that expected from the polarity of current injection i.e., one would expect the current to develop linearly in an outward direction.

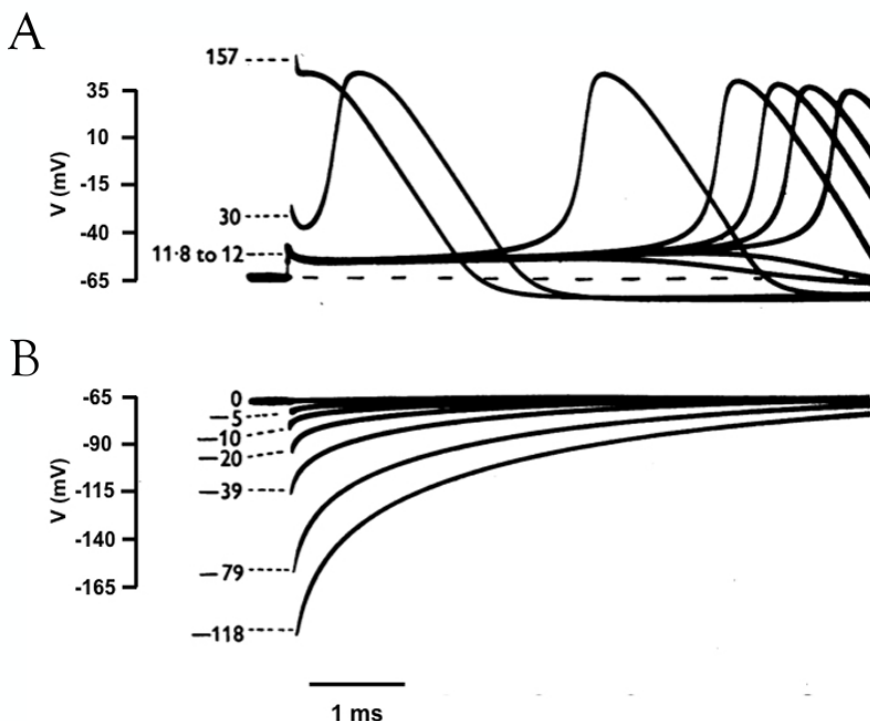


**Figure 3.2 - Response of the membrane potential to brief shocks.** A. Action potentials evoked by brief shocks measured in  $nC\ cm^{-2}$  at 6°C. Sub-threshold shocks did not evoke an action potential, but once evoked all action potentials had the same profile irrespective of stimulus magnitude. B. Hyperpolarising shocks evoked transient membrane hyperpolarisations, the amplitudes of which were linearly related to the magnitude of the stimulus.

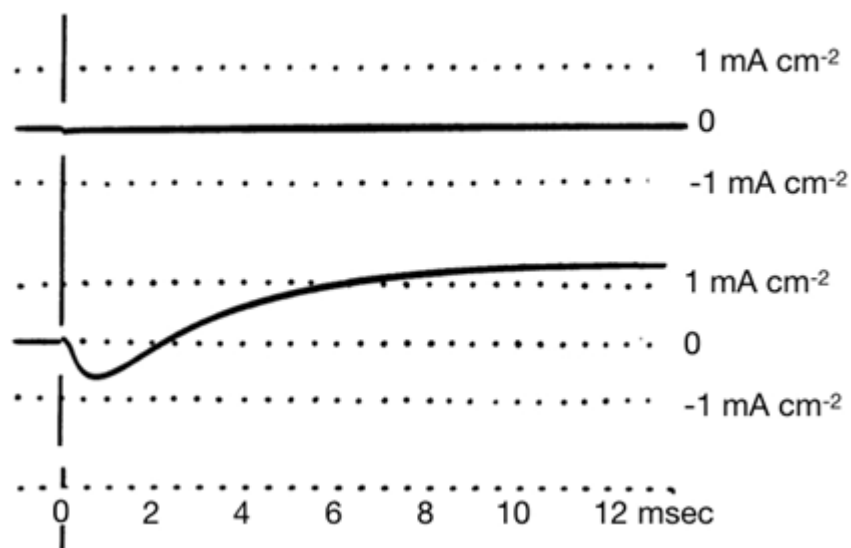
## Membrane capacitance

The capacitance of the membrane could be estimated based on the charge imposed on the membrane. Since the membrane current evoked by a stimulus could be measured, the charge imposed on the membrane ( $Q = I \times \text{time}$ ) could be calculated. The voltage deflection that resulted from this shock was then used to calculate the membrane capacitance, since  $C = Q/V$ . The data in *Table 1* showed a mean membrane capacitance of  $0.9 \mu\text{F cm}^{-2}$ . The manner in which the membrane capacitance was estimated is illustrated in *Figure 16*. The capacitive transients evoked by brief shocks showed symmetrical responses to shocks of equal magnitude but opposite polarity. The maximum current amplitude evoked was about  $4.5 \text{ mA}$ , which then returned to baseline along an exponential decay within  $60 \mu\text{s}$ . The integral of the current over this period was estimated as  $500 \mu\text{A cm}^{-2}$ . This is equivalent to a charge of  $35 \text{ nCoulomb cm}^{-2}$  according to the relationship  $1 \text{ Amp} = 1 \text{ Coulomb sec}^{-1}$ . This particular shock elicited a depolarisation of  $40 \text{ mV}$  amplitude, from which the membrane capacitance of  $0.9 \mu\text{F cm}^{-2}$  was calculated according to  $C = Q/V$ .

## The early and late membrane current amplitudes

The amplitude of the membrane current  $0.29 \text{ ms}$  after application of the stimulus was plotted against the voltage displacement and revealed a classic profile. Hyperpolarising from rest evoked a linear inward current from  $-150 \text{ mV}$  to  $-65 \text{ mV}$ , the result of the leak current. Depolarising by  $10 \text{ mV}$  from rest produced an outward linear current, consistent with the extracellular recordings reported by Hodgkin (Hodgkin, 1938) and illustrated in Fig 1.4D and E. These obeyed Ohm's law and were in the direction of current flow expected from such voltage changes since a depolarisation would evoke an outward movement of positive charge from the voltage clamp in order to control the membrane potential. However, at  $10$  to  $15 \text{ mV}$  depolarisation an inward current developed (Fig 3.3B). It is important to realise that this was the same level of depolarisation required to trigger an action potential and may be termed threshold, suggesting that this inward current was responsible for the action potential (this was investigated in later experiments). As the membrane potential was further depolarised the inward current increased in amplitude until at about  $15 \text{ mV}$  it peaked and then decreased, crossing the voltage-axis at about  $40 \text{ mV}$ . The three points where the curve crossed the voltage-axis (i.e., where current was  $0 \text{ nA}$ ) are important. It crossed first at rest ( $-65 \text{ mV}$ ) then at  $-50 \text{ mV}$  (the action potential threshold) and at  $40 \text{ mV}$  ( $E_{\text{Na}}$ ). The U shape of the curve will be explained in Chapter 5. The region of negative slope conductance at threshold was important in that it was in the opposite direction to that expected by the direction of current flow across the membrane and produced the membrane instability that determined threshold (Chapter 5).

A



B

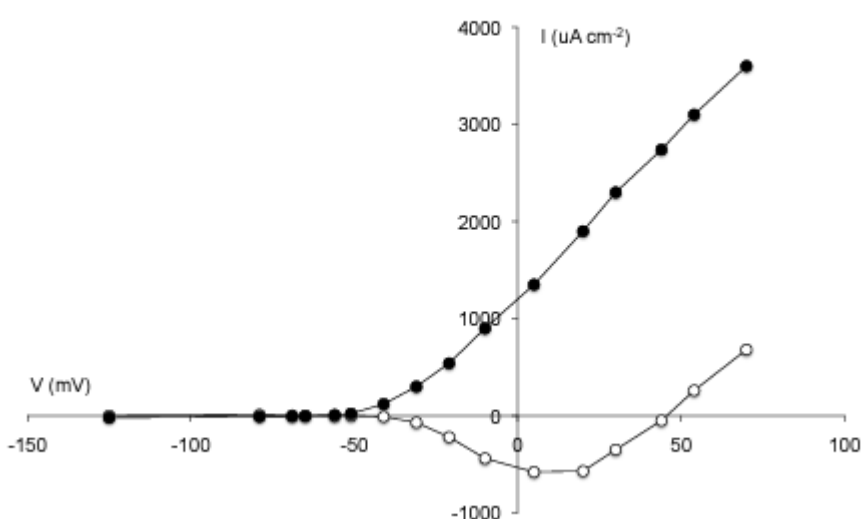


**Figure 3.3 - Early inward and late outward currents.** A. Upper trace - current evoked by a 65 mV hyperpolarisation from rest and (lower trace) a 65 mV depolarisation evoked a radically different current. The hyperpolarisation evoked a small steady inward current that was maintained for the duration of the stimulus. The depolarisation evoked a smoothly developing inward current that fell to become a sustained steady outward current. Compare with the profile of equivalent currents recorded by Cole in Fig 3.1. (B) Plots of the early inward (-○-) and late outward currents (-●-) at a range of voltages showed the classic U shape of the inward current, and the steady increase of the late outward current.

An important conceptual point, which became apparent on examining the current records, was that after an initial increase in amplitude at small depolarisations the early inward current started to decrease at larger depolarisations. It is not a difficult concept to appreciate that if the inward current was carried by  $\text{Na}^+$  then this inward current should reverse direction at membrane potentials more depolarised than  $E_{\text{Na}}$  to become outward. This would occur based on consideration of the Nernst equation since where the voltage clamp command potential was more depolarised than  $E_{\text{Na}}$ , the  $\text{Na}^+$  ions would cross the membrane in the direction that drove the membrane potential towards  $E_{\text{Na}}$  i.e., an outward movement of positively charged  $\text{Na}^+$  ions would hyperpolarise the membrane potential towards  $E_{\text{Na}}$ . The records in *Figure 14* showed this to be the case where the inward current disappeared at 52 mV and became outward at more depolarised potentials, whilst appearing as a distinct early current separate from the sustained later current. Therefore it was likely the early current was carried by  $\text{Na}^+$  ions, which was consistent with the early inward current being responsible for the action potential and the fall in action potential amplitude that occurred when  $[\text{Na}]_o$  was reduced (Hodgkin *et al.*, 1949). This phenomenon will be explored in detail in the next chapter.

## Temperature dependence

The introduction of the cooling coil to reduce the temperature of the seawater perfusing the axon to one more appropriate to the ambient conditions in which the squid lived required reconciling with the experiments reported in the previous chapter, which were carried out at 20°C to 22°C. Thus, a comparison of the currents recorded at a variety of voltages was carried out in two separate axons, one recorded at 22°C and the other at 6°C. The axons were considered suitable for comparison as they gave action potentials of amplitude 103 mV and 105 mV when recorded at 22°C and had resting membrane potentials of -55 mV. It must be borne in mind that 22°C was hyperthermic for a squid axon, which almost certainly deteriorated at this temperature. It is no surprise that increased temperature increased the rate at which the currents developed. This was quantified by superimposing the currents recorded at the two temperatures using the concept of  $Q_{10}$ , which gave a value to the rate at which the current changed with temperature. The equation to calculate  $Q_{10}$  was

$$Q_{10} = \frac{R_2}{R_1} \left[ \frac{10^\circ\text{C}}{T_2 - T_1} \right] \quad (\text{Eq. 3.2})$$

where  $R_1$  and  $R_2$  were the reaction rates at temperatures  $T_2$  (22°C) and  $T_1$  (6°C), respectively. The rate of change of the current was about 6-fold for an increase in temperature from 6°C to 22°C, and resulted in a  $Q_{10}$  of about 3. It was noticeable that the effect of increased temperature was far greater on the rates of the current development rather than the amplitude achieved.

# 4. CURRENTS CARRIED BY SODIUM AND POTASSIUM IONS THROUGH THE MEMBRANE OF THE GIANT AXON OF *LOLIGO*

In this paper Hodgkin and Huxley focussed almost exclusively on the  $\text{Na}^+$  current. Having shown that the membrane current evoked by depolarising pulses was non-linear, displaying an initial transient inward component (the early current) followed by a sustained outward current (the late current), they set out to resolve the current into its component parts.

### Isolation of $I_{\text{Na}}$ from the membrane current

Since action potential threshold and onset of the inward current were both about 10 to 15 mV more depolarised than rest, the early current reversed direction at  $E_{\text{Na}}$ , and the action potential was reduced in low  $[\text{Na}]_o$  seawater, it was likely that the early component was carried by  $\text{Na}^+$  ions. To test this Hodgkin and Huxley depolarised the membrane over a range of potentials from -107 mV to +47 mV in normal seawater and then in artificial seawater in which the  $\text{Na}^+$  was replaced with choline to measure the effect of removal of  $[\text{Na}]_o$  on the profile of the current (choline was impermeant at the  $\text{Na}^+$  permeability pathways but did not affect the resting membrane potential). At all potentials tested the inward current was lost in choline seawater, but the shape of the late outward current remained unchanged although its amplitude decreased. However, when  $\text{Na}^+$  was completely replaced by choline the resistance of the artificial seawater increased, distorting the recorded currents, invalidating like-for-like comparisons of the currents in normal seawater and choline seawater i.e., Hodgkin and Huxley could not simply subtract the choline seawater current from the normal seawater to isolate the early current, since under these conditions the late outward components were not comparable. In order to resolve this issue Hodgkin and Huxley had to complete additional experiments to which they applied a complex and elegant mathematical solution in order to separate the currents. Experiments were carried out in low  $\text{Na}^+$  seawater containing 10% or 30% of the normal  $\text{Na}^+$  concentration of 450 mM, where there was no effect on the resistance of the seawater. In a similar manner to that in which Hodgkin and Katz used the Nernst equation to compare calculated and measured changes in  $E_{\text{Na}}$  (Eq. 2.5), so Hodgkin and Huxley estimated the change in  $E_{\text{Na}}$  of the early inward current in 10% and 30% Na seawater and compared these measurements to those predicted by the Nernst equation. They assessed the  $E_{\text{Na}}$  as the voltage at which there was no early inward current or the appearance of an outward current, so they took the voltage as one at which the ionic current appeared horizontal at the beginning of the voltage pulse (*Figure 4*). They used this familiar equation derived by Hodgkin and Katz (Hodgkin & Katz, 1949a) to compare the difference between the experimentally estimated  $E_{\text{Na}}$  and the calculated  $E_{\text{Na}}$ .

$$E_{\text{Na}} - E'_{\text{Na}} = 58 \log_{10} \frac{[\text{Na}]_{\text{seawater}}}{[\text{Na}]_{\text{test}}} \quad (\text{Eq. 4.1})$$

In seawater with 10% or 30%  $\text{Na}^+$  the observed shift in  $E_{\text{Na}}$  matched that predicted by the Nernst equation closely. Hodgkin and Huxley were then ready to separate the membrane current into its constituent parts, the presumed early  $\text{Na}^+$  component and a late outward  $\text{K}^+$  component. It is interesting that at the time Hodgkin considered the most convincing evidence of  $\text{K}^+$  contribution to the late current were the tracer studies in cuttlefish (*Sepia*) axons (see Chapter 8,) which identified  $\text{K}^+$  as the carrier of the outward current, and not their electrophysiological data (p.292, Hodgkin, 1992). In these calculations they had to make several assumptions, which were:

- (i) the time course of the late K<sup>+</sup> current was not affected when axons were bathed in low Na<sup>+</sup> seawater
- (ii) the time course of the Na<sup>+</sup> current was the same in seawater or low Na<sup>+</sup> seawater. In low Na<sup>+</sup> seawater the constant  $k$  (see Eq. 4.15) defined the ratio between  $I_{\text{Na}}$  and  $I'_{\text{Na}}$ , where  $I'_{\text{Na}}$  indicated the Na<sup>+</sup> current recorded in low Na<sup>+</sup> seawater
- (iii) the K<sup>+</sup> current had yet to appear by the time taken for the  $I_{\text{Na}}$  to reach one third of its maximum amplitude.

## The isolation process

The subtraction process involved the following steps.

- (iv) the currents were recorded at a series of depolarisations in low Na<sup>+</sup> seawater (10% or 30%), then in normal seawater, then repeated in low Na<sup>+</sup> seawater. The first and third records were averaged to give a current in low Na<sup>+</sup> seawater
- (v) capacitive currents were subtracted using scaled currents evoked from hyperpolarising pulses of the appropriate magnitude
- (vi) any variation in resting membrane potential resulting from the switch between low Na<sup>+</sup> seawater and normal seawater was taken into account.

Hodgkin and Huxley assumed that the total current recorded in normal seawater could be expressed as the sum of the Na<sup>+</sup> and K<sup>+</sup> currents.

$$I_i = I_{\text{Na}} + I_K \quad (\text{Eq. 4.2})$$

and the current recorded in low Na<sup>+</sup> seawater could be expressed as the sum of the Na<sup>+</sup> and K<sup>+</sup> currents recorded in low Na<sup>+</sup> seawater

$$I'_i = I'_{\text{Na}} + I'_{\text{K}} \quad (\text{Eq. 4.3})$$

where  $I_{\text{Na}}$  and  $I'_{\text{Na}}$  denoted the sodium current and  $I_K$  and  $I'_{\text{K}}$  denote the potassium current. From point (i) above Hodgkin and Huxley assumed  $I_K = I'_{\text{K}}$ , and from point (ii) that the ratio between  $I_{\text{Na}}$  and  $I'_{\text{Na}}$  could be described by a constant,  $k$ .

$$I'_{\text{Na}} = kI_{\text{Na}}$$

so

$$I'_i = kI_{\text{Na}} + I_K$$

subtracting we get

$$I_i - I'_i = (I_{\text{Na}} + I_K) - (kI_{\text{Na}} + I_K)$$

$$I_i - I'_i = (I_{\text{Na}} + I_K) - (kI_{\text{Na}} + I_K)$$

$$I_i - I'_i = I_{\text{Na}} - kI_{\text{Na}}$$

$$I_i - I'_i = I_{\text{Na}}(1 - k)$$

$$I_{\text{Na}} = \frac{(I_i - I'_i)}{(1 - k)}$$

In order to calculate the values of  $I'_{Na}$  and  $I'_K$  complex differentiation of Eq. 4.2 and Eq. 4.3 produced the following expressions:

$$I'_{Na} = \frac{k}{1-k} [I_i - I'_i] \quad (\text{Eq. 4.4})$$

$$I'_K = \frac{I'_i - kI_i}{1-k} \quad (\text{Eq. 4.5})$$

A detailed description of this process is available (Cronin, 1987).

These equations allowed Hodgkin and Huxley to separate  $I_{Na}$  and  $I_K$  from the experimentally recorded membrane currents. This procedure was carried out for experiments in 10% and 30%  $\text{Na}^+$  seawater and resulted in isolated  $K^+$  currents that were deemed to be an accurate representation, since the general shape of  $I_K$  was the same at all potentials, based on point (ii) the similar shape of  $I_{Na}$  and  $I'_{Na}$  resulted in complete removal of  $I_{Na}$  leaving only  $I_K$ , and calculation of the  $I_K$  at  $E_{Na}$  matched the  $I_K$  recorded experimentally at this potential, which would be unlikely to occur if point (i) was not true (Fig 4.1).

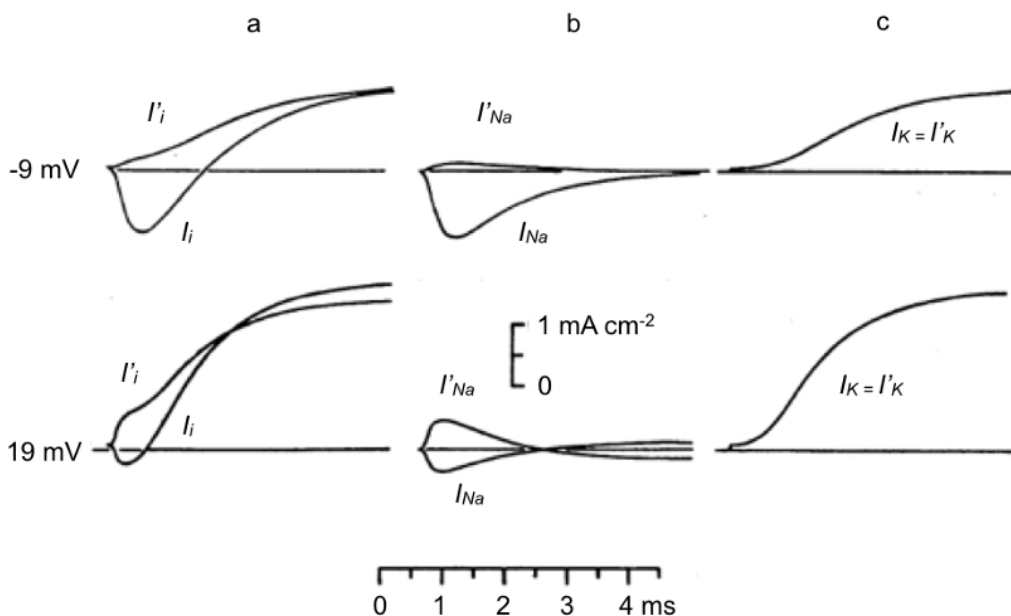


**Figure 4.1** - An illustration of the subtraction process by which the membrane current was separated into  $I_{Na}$  and  $I_K$ . (a)  $I_i$  and  $I'_i$  recorded in normal seawater and 10% seawater, respectively, (b) shows  $I_{Na}$  and  $I'_{Na}$  after the subtraction process, and (c)  $I_K$ . Currents were evoked by depolarisation to -9 mV (upper trace) or 19 mV (lower trace).

These experiments are an example of the indirect methods that Hodgkin and Huxley were forced to resort to throughout the papers. The records in choline seawater also provided good evidence of the separation of the early and late components due to the shape of the current. A current that was evoked by depolarisation to 19 mV in choline seawater displayed

two distinct components, both of which were outward (Fig 4.2). It is difficult to conceive of how  $I_K$  could account for both the early and late components of the trace. It is also important to note that the outward  $\text{Na}^+$  current was smaller than the inward current since there was a higher concentration of  $\text{Na}^+$  outside the axon than inside, which generally resulted in larger inwardly directed currents.

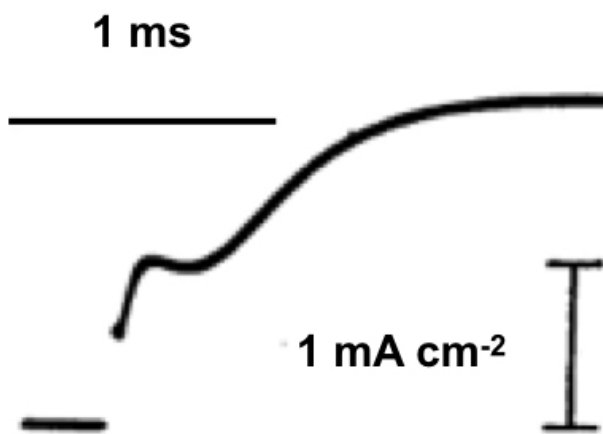


**Figure 4.2** - A current recorded when the membrane was depolarised to 19 mV in choline seawater. The biphasic nature of the outward current was a clear indication that two independent components were present.

This complex solution to a conceptually simple problem demonstrated the advantages of a sound foundation in calculus, which both Hodgkin and Huxley (and Cole) possessed. This point is generally overlooked since the textbook explanation of the separation of the membrane current into  $I_{\text{Na}}$  and  $I_K$  is that the currents in  $\text{Na}^+$  free seawater were simply subtracted from currents recorded in seawater to reveal the early  $\text{Na}^+$  current. It is interesting to note in *Figure 6* that the ohmic leak current can clearly be seen at the onset of each current trace. We shall deal with the leak current in Chapter 5.

### $\text{Na}^+$ conductance

The current that moves through a membrane is determined by two key parameters, the ion concentrations on either side of the membrane and the electrical driving force. Since the driving force for an ion is zero at the reversal potential, the driving force is defined as the difference between the membrane potential and the equilibrium potential ( $V - E_x$ ). The driving force determines the direction of current flow, but the magnitude of the current is determined by a property called permeability, which can be defined as the ease with which the ion crosses the membrane. According to Ohm's law the current that flows across the membrane is a product of the conductance times the driving force  $I = g(V - E_x)$ , which means

conductance can be assumed to define permeability of the ions crossing the membrane. The conductance for  $g_K$  and  $g_{Na}$  can be calculated from the current records as  $g = I/(V - E_x)$ . Such records are shown in *Figure 8*. Note how there is no reversal in polarity of the conductance for  $g_{Na}$  as there is with the current. I have reproduced this conversion using  $\text{Na}^+$  and  $\text{K}^+$  currents acquired from a modelling study (Brown, 2000) to illustrate the process. The colour coded  $\text{Na}^+$  currents with the voltage at which the currents were acquired are noted in the figure legend (Fig 4.3). By sequentially stepping through the currents using the relationship  $g_{Na} = I_{Na}/(V - E_{Na})$ , both the magnitude and the polarity of the conductances can be understood. The reason that the conductances have the same polarity is that at voltages less than  $E_{Na}$  the value of  $(V - E_{Na})$  is negative, as is the  $\text{Na}^+$  current (i.e., inward). However, at voltages greater than  $E_{Na}$  the relationship of  $(V - E_{Na})$  is positive, as is the polarity of the  $\text{Na}^+$  current. The properties and quantification of conductance are discussed in the next chapter.

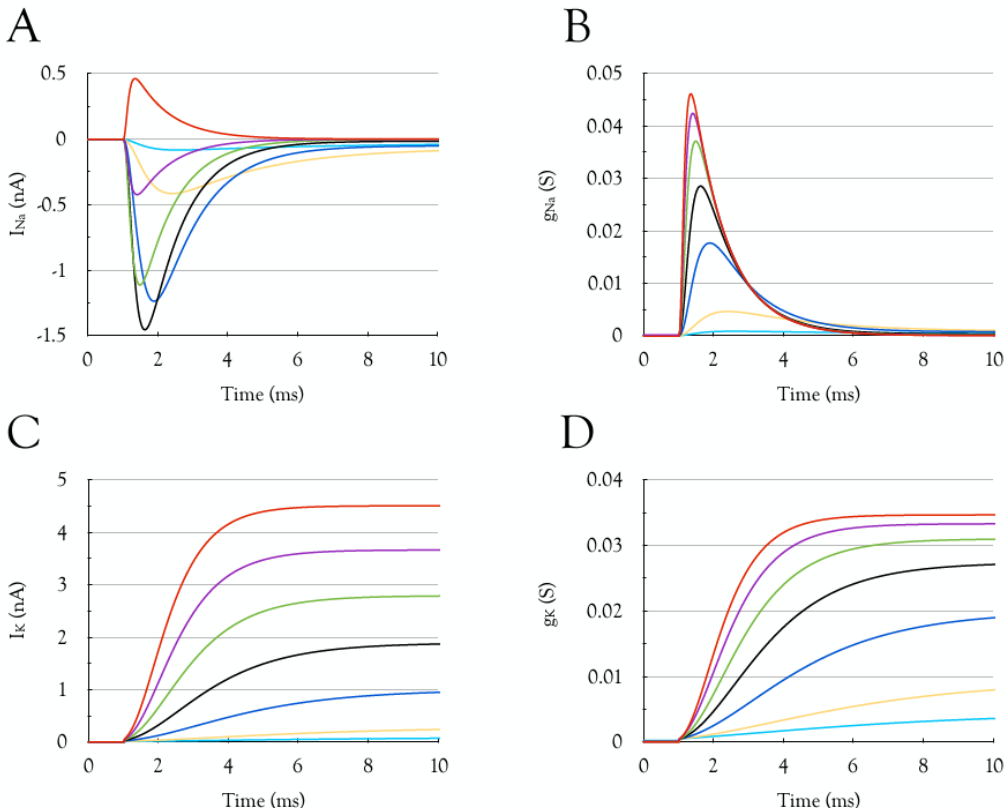


**Figure 4.3 - Membrane currents and conductances.** Simulations of recordings carried out to illustrate how Hodgkin and Huxley derived conductances from recordings of current. (A)  $I_{Na}$  simulated when the voltage was clamped at -50 mV (turquoise), -40 mV (yellow), -20 mV (blue), 0 mV (black), 20 mV (green), 40 mV (purple) and 60 mV (red). The pulse commenced at 1 ms and lasted until 10 ms. (B) The calculated  $g_{Na}$  derived from the data in A with  $E_{Na}$  of 50 mV. Same colour scheme as in A. (C)  $I_K$  simulated in the same manner as  $I_{Na}$ . (D) The calculated  $g_K$  has the same shape as the current but asymptotes at more depolarised voltages.

Similar calculations for the  $\text{K}^+$  current illustrated that the general shape of the traces did not change, but whereas with increasing depolarisation the  $I_K$  continues to increase in an

almost linear manner,  $g_K$  tended to asymptote at larger depolarisations. Stepping through the calculations for each voltage clarifies this procedure (Fig 4.3).

From these conversions of current to conductance the peak conductance for  $g_{Na}$  and  $g_K$  were plotted versus the voltage at which they were evoked (*Figure 9 and 10*). By normalising the peak conductance to that evoked by depolarisation to 35 mV, and plotting the normalised conductance on a  $\log_{10}$  scale, an extremely steep relationship between conductance and voltage was seen for membrane potentials immediately beyond rest (Fig 4.4A). The log plot meant the linear relationship expressed an e-fold increase in conductance for 4 mV for  $Na^+$  and 5 mV for  $K^+$ . The shape of these curves was extremely important, as they resembled the Boltzmann principle (Fig 4.4B) and were consistent with the movement of a charged particle within the membrane (Hille, 2001; Baxter & Byrne, 2009) that opened the permeability pathway upon membrane depolarisation (see Chapter 6). The Boltzmann principle can be described as

$$O_f = \frac{1}{1+e^{[(\frac{w-z_B q_e E}{k_B T})]}} \quad (\text{Eq. 4.6})$$

and defines the fraction of permeability pathways that are open ( $O_f$ ) relative to membrane potential ( $E$ ), where  $w$  defines the energy increase upon moving the permeability pathway from closed to open,  $z_g$  defines the gating charge,  $q_e$  is the elementary charge,  $k_B$  is the Boltzmann's constant and  $T$  is temperature in Kelvin (p.57-59, Hille, 2001).

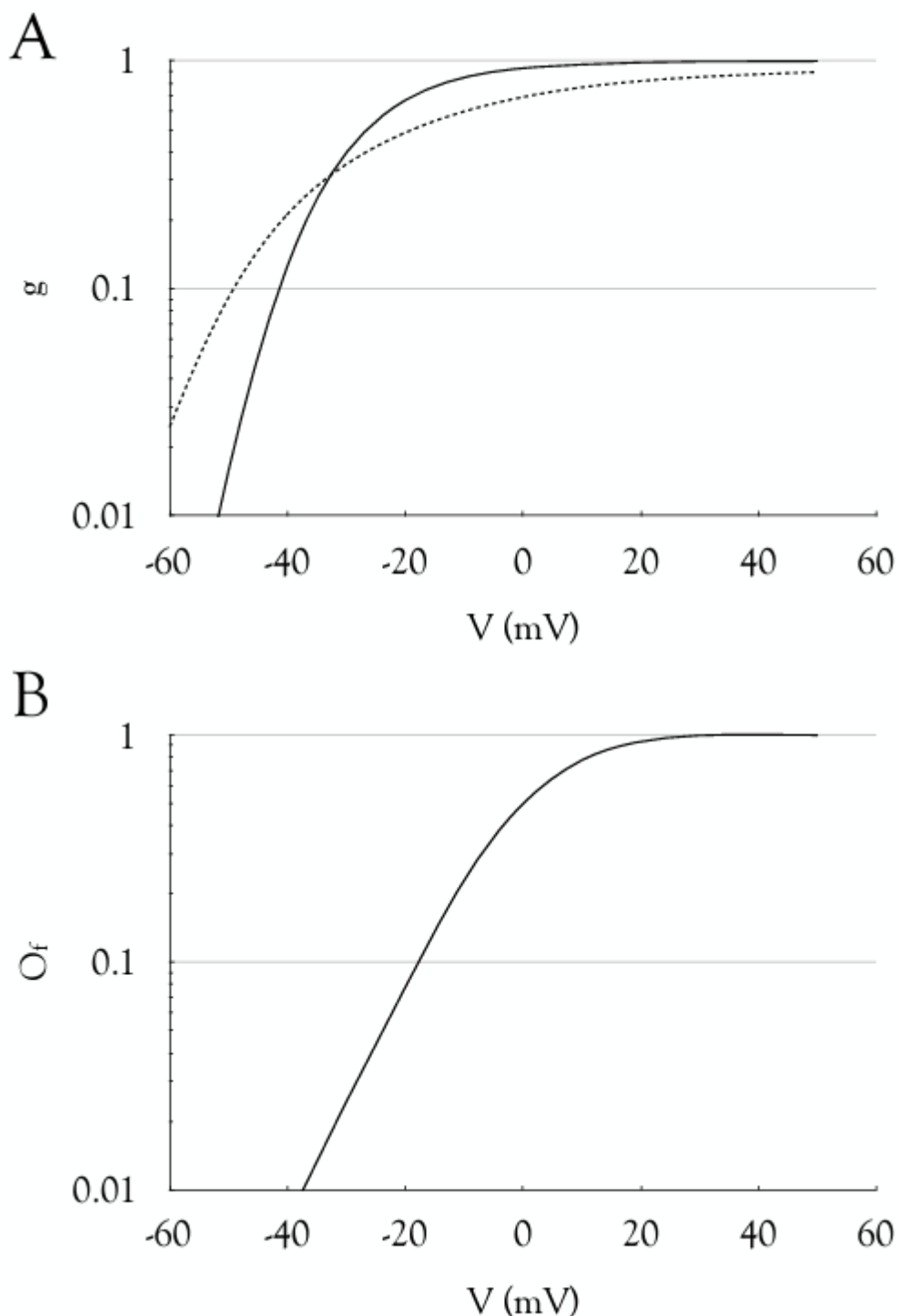


**Figure 4.4** - Relationship between  $g_{Na}$  and  $g_K$  and membrane potential. A. The amplitudes for  $g_{Na}$  (continuous line) and  $g_K$  (dotted line) normalised for the maximum conductance reached during a depolarisation to 35 mV plotted on  $\log_{10}$  scale, revealed very steep voltage dependence. (B) The Boltzmann principle for the voltage dependence of a charged particle present within a membrane according to Eq. 4.6.

It is clear from the conductance traces in *Figure 8* that with increasing depolarisation there was an increased rate of rise of the conductance as illustrated in *Figures 11 and 12*, that increased in an almost linear fashion and did not flatten, unlike the amplitude of the conductance.

## The independence principle

It is likely that based on the similarity of the shape between the Boltzmann principle and the conductance relationship for  $\text{Na}^+$  and  $\text{K}^+$ , versus voltage, Hodgkin and Huxley considered this an indication of a complex mechanism involving charges in the membrane responding to potential difference across the membrane, thereby facilitating increased membrane permeability. They realised that the data presented in Fig 3.3B could be used to investigate the nature of the permeability pathway. Several papers had recently been published, which described the ‘independence principle’ (Teorell, 1949; Ussing, 1949). This was widely accepted at the time and stated that the movement of ions across the membrane was not affected by the presence of other ions, only by trans-membrane ion gradients and the driving force ( $V - E_x$ ). If the independence principle was shown to apply to  $I_{\text{Na}}$ , it would support the view of  $I_{\text{Na}}$  and  $I_K$  as separate permeability pathways that operated independently. A simple way to envisage a system in which the independence principle applies is to imagine the membrane instantly adopts a sieve-like structure upon depolarisation to facilitate increased permeability, with an infinite number of paths for ions to cross the membrane i.e., there are more paths than ions. If the independence principle does not apply, it implies a more complex pathway exists where ions do interfere with the movement of other ions. A suitable example of this is a system where ions moved in single file via a tunnel or a channel through the membrane, (Chapter 8). The model developed by Hodgkin and Huxley was based on the equations of Ussing and Teorell and requires a rather discursive description. However, this topic is revisited in the next Chapter, and Chapter 8, which is devoted exclusively to the topic, so it is worthwhile examining the underlying assumptions, which may be described as follows. If we imagine an axon bathed in seawater, then the rate of influx of an ion is  $M_1 = k_1 c_1$ , where  $M_1$  is the influx of the ion from the seawater into the axon,  $k_1$  is a constant that describes the properties of the membrane and the potential difference across the membrane, and  $c_1$  is the concentration of the ion in seawater. Likewise, the efflux of the ion from the axon  $M_2$  may be described as  $M_2 = k_2 c_2$ , where  $k_2$  has an equivalent meaning to  $k_1$ , and  $c_2$  is the ion concentration inside the axon. According to Eq. 4.7 the effect of changing  $[\text{Na}]_o$  on  $I_{\text{Na}}$  would provide the opportunity to test the independence principle. Under these conditions it is assumed that altering  $[\text{Na}]_o$  would have no effect on the membrane potential i.e.,  $k_1$  and  $[\text{Na}]_i$  would be unaffected. In this manner Eq. 4.7 reduces to  $M_1 \approx c_1$  i.e., there should be a linear relationship between the extracellular concentration of an ion and its influx, whereas the efflux should be unaltered. If we divide the influx by the efflux, we get:

$$\frac{M_1}{M_2} = \frac{k_1 c_1}{k_2 c_2} \quad (\text{Eq. 4.7})$$

When  $M_1 = M_2$  the system is in equilibrium and influx = efflux such that  $k_1 c_1 = k_2 c_2$  and  $k_2/k_1 = c_1/c_2$ . We can now define  $c^{*1}$  as the external concentration of  $c$  where the equilibrium potential is  $E$ . So

$$\frac{k_2}{k_1} = \frac{c^{*1}}{c_2}$$

and from Eq. 2.1 in Chapter 2

$$E = \frac{RT}{F} \ln \frac{c^*_1}{c_2}$$

This can be rearranged as

$$\frac{EF}{RT} = \ln \frac{c^*_1}{c_2}$$

and since  $\ln x = y$  is equivalent to  $e^y = x$  then

$$\frac{c^*_1}{c_2} = e^{\left[ \frac{EF}{RT} \right]} \quad (\text{Eq. 4.8})$$

It follows that

$$\frac{k_2}{k_1} = e^{\left[ \frac{EF}{RT} \right]}$$

Now since

$$\frac{M_1}{M_2} = \frac{k_1 c_1}{k_2 c_2}$$

then

$$\frac{M_2}{M_1} = \frac{k_2 c_2}{k_1 c_1}$$

and

$$\frac{k_2}{k_1} = \frac{M_2 c_1}{M_1 c_2}$$

substituting we get

$$\frac{M_2 c_1}{M_1 c_2} = e^{\left[ \frac{EF}{RT} \right]}$$

which equals

$$\frac{M_2}{M_1} = \frac{c_2}{c_1} e^{\left[ \frac{EF}{RT} \right]} \quad (\text{Eq. 4.9})$$

which is equivalent to the expression derived by Hille to describe the flux ratio criterion (Eq 11.7a, Hille, 2001)

$$\frac{\text{Efflux}}{\text{Influx}} = \frac{[S]_i}{[S]_o} e^{\left[ \frac{EF}{RT} \right]} \quad (\text{Eq. 4.10})$$

This is a suitable point to pause and assess the implications of this equation. If we assume  $[Na]_o = 450$  mM and  $[Na]_i = 72$  mM, then at 20°C  $E_{Na} = 46$  mV and the ratio of efflux to influx is 1, as expected of a system in equilibrium. However, if  $[Na]_o$  is reduced to 225 mM then the ratio of efflux to influx increases to 2. We assume that if the independence principle applies the efflux of  $Na^+$  is unchanged, but the  $Na^+$  influx is reduced by half. However, Hodgkin and Huxley were measuring trans-membrane current not fluxes, which required further rearrangement of the model. We can define  $E^*$  as the reversal potential when  $c_1$  is the external concentration of  $c$ , and  $c_2$  is the internal concentration

$$E^* = \frac{RT}{F} \ln \frac{c_1}{c_2}$$

which, as described above, can be rearranged as

$$\frac{c_1}{c_2} = e^{\left[ \frac{E^* F}{RT} \right]} \quad (\text{Eq. 4.11})$$

Dividing Eq.4.8 by Eq. 4.11

$$\begin{aligned} \frac{\frac{c_{*1}}{c_2} = e^{\left[ \frac{EF}{RT} \right]}}{\frac{c_1}{c_2} = e^{\left[ \frac{E^* F}{RT} \right]}} &= \frac{c_2}{c_1} \times \frac{c_{*1}}{c_2} = e^{\left[ \frac{EF - E^* F}{RT} \right]} \\ \frac{c_{*1}}{c_1} &= e^{\left[ \frac{(E - E^*)F}{RT} \right]} \end{aligned} \quad (\text{Eq. 4.12})$$

It should be appreciated that this is simply Eq. 4.1 rearranged. We can now compare the ratio of the sodium current recorded in seawater ( $I_{Na}$ ) and in low Na seawater ( $I'_{Na}$ )

$$\frac{I'_{Na}}{I_{Na}} = \frac{M'_1 - M'_2}{M_1 - M_2}$$

where  $M'_1$  and  $M'_2$  are the  $\text{Na}^+$  influx and efflux, respectively, in low  $\text{Na}^+$  seawater. Based on Eq. 4.7, if we assume that the independence principle applies, then  $k_1$  and  $k_2$  equal 0 and it follows that

$$\frac{M'_1}{M_1} = \frac{[Na]'_o}{[Na]_o} \quad (\text{Eq. 4.13})$$

and

$$M'_2 = M_2 \quad (\text{Eq. 4.14})$$

Substituting from Eq. 4.13 and 4.14 gives

$$\frac{I'_{Na}}{I_{Na}} = \frac{M_1 \frac{[Na]'_o}{[Na]_o} - M_2}{M_1 - M_2},$$

then

$$\frac{I'_{Na}}{I_{Na}} = \frac{\left[ \frac{[Na]'_o}{[Na]_o} \left( \frac{M_1}{M_2} \right) \right] - M_2}{M_1 - M_2},$$

Substituting from Eq. 4.12 gives

$$I'_{Na} = I_{Na} \times \frac{\left[ \frac{[Na]'_o}{[Na]_o} e^{\left[ \frac{-(E - E_{Na})F}{RT} \right]} \right] - 1}{e^{\left[ \frac{-(E - E_{Na})F}{RT} \right]} - 1}. \quad (\text{Eq. 4.15})$$

From this relationship a comparison of the ratio of  $I_{Na}$  and  $I'_{Na}$  can be made to assess whether the independence principle applied. It should be realised that the second expression of the right-hand side of the equation equates to  $k$  as described in point (ii). When the currents Hodgkin and Huxley recorded were compared to the model there was an approximate, but not an exact, match (Figure 13). Given the degree of experimental error in the recordings Hodgkin and Huxley concluded that the results were a match for the model and made the erroneous claim that the independence principle applied to  $\text{Na}^+$  currents, justifying the treatment of  $I_{Na}$  and  $I_K$  as separate independent currents.

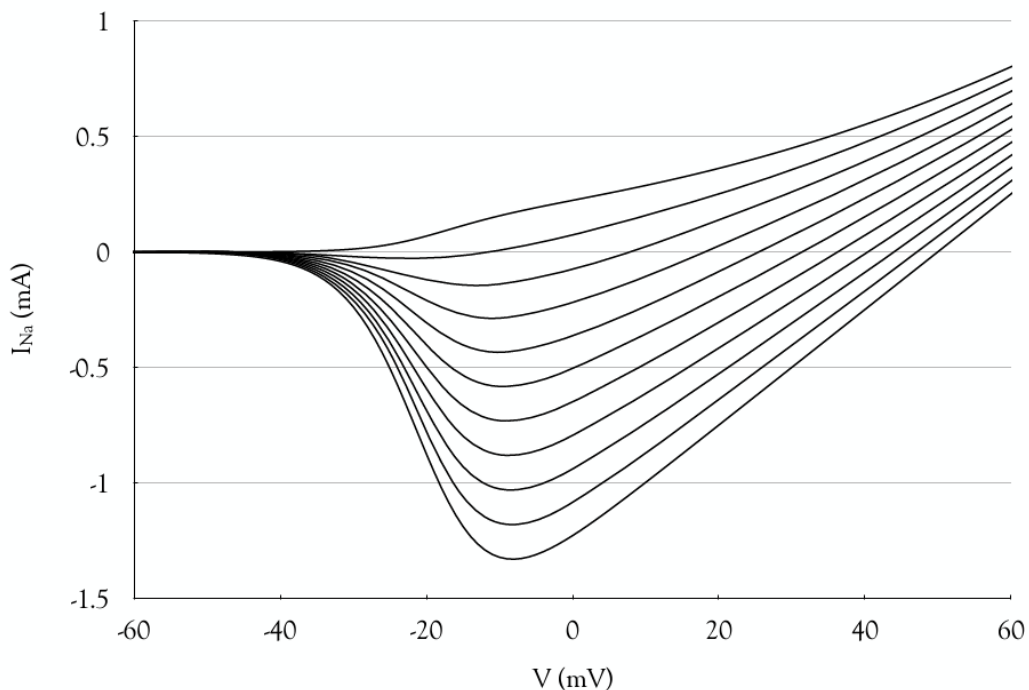


**Figure 4.5** - A simulation of the steady state  $I_{Na}$  calculated for seawater in which the  $[Na]_o$  decreased from 100% to 0% in 10% steps based on Equation 4.15. The largest current is that for normal seawater, and the records indicate in decreasing order the calculated  $I_{Na}$  for 90% Na seawater, 80% Na seawater etc. As  $[Na]_o$  decreases the records cross the voltage-axis at less depolarised potentials in agreement with predictions of  $E_{Na}$ .

In Fig 4.5 I have modelled the steady state  $\text{Na}^+$  current if the  $[Na]_o$  in the seawater was decreased in 10% steps from 100% to 0%, as this provides a clearer picture of the effects of reducing  $[Na]_o$  on  $I_{Na}$  than that presented by Hodgkin and Huxley (Figure 13). One may expect under such circumstances a simple parallel drop in  $I'_{Na}$  would occur, but the magnitude of the steady state relation not only decreases, but the point where it crosses the voltage-axis becomes less depolarised with falling  $[Na]_o$  in agreement with  $E_{Na}$ . Hodgkin and Huxley revisited this theme in the next paper and in the final paper in this series.

# 5. THE COMPONENTS OF MEMBRANE CONDUCTANCE IN THE GIANT AXON OF *LOLIGO*

## Tail currents

In the previous papers the appearance of an early inward  $\text{Na}^+$  current followed by a later outward  $\text{K}^+$  current in response to a membrane potential depolarisation was demonstrated. In addition, the permeability of the membrane was assumed to equal the conductance, and the current flow across the membrane was described as  $I_x = g_x(V - E_x)$ . In this paper aspects of conductance were examined in more detail using ingenious double pulse protocols, where the conditioning pulse opened the permeability pathway, and the test pulse stepped to a wide range of potentials spanning  $E_x$ . In axons that were depolarised by about 40 mV for a period of time exceeding 5 ms the inward current developed and then decayed back towards baseline, indicative of a reversible mechanism associated with sodium permeability. In axons in which the depolarisation was curtailed after a period of 1 ms or so, at which point a significant portion of the early inward current was still present, repolarisation towards rest resulted in an instantaneous increase in the amplitude of the current, which then followed an exponential time course as it decayed towards zero; this was called the tail current. The appearance of the tail current can be readily explained if we understand the implications of the Nernst equation by taking into account the change in driving force that occurs during the repolarising voltage step. Upon depolarisation the permeability pathway opens and  $\text{Na}^+$  ions flow down the electrochemical gradient from outside to inside. If a repolarising voltage step is imposed while there is significant current present, i.e., the permeability pathway is still open, there is a large increase in driving force, since the membrane potential is now more distant from  $E_{\text{Na}}$  than during the depolarising pulse i.e., the value of  $(V - E_{\text{Na}})$  is greater during the repolarising voltage step than during the depolarising step.

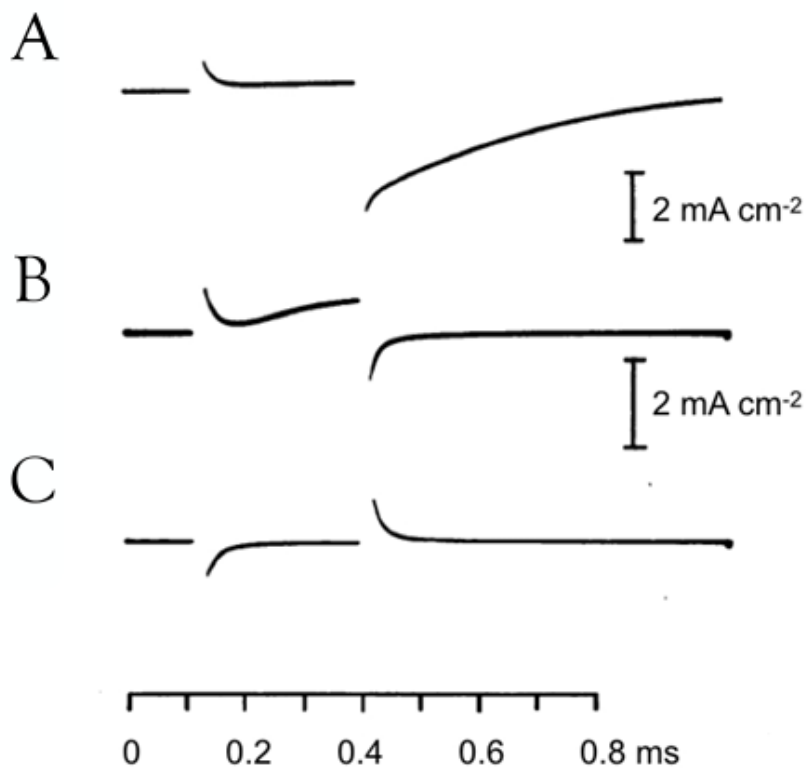


**Figure 5.1** - The tail current. A. When the conditioning pulse was stepped to  $E_{Na}$  in axons perfused with seawater, there was no early inward current, but a large tail current was evoked following repolarisation to rest. B. In choline seawater the tail current disappeared with only capacitive transients present, upon repolarisation, C, verified by the similar profile of transients evoked by a hyperpolarisation of equivalent magnitude.

Altering the duration of the depolarising conditioning pulse had predictable effects on the amplitude of the tail current from the perspective of conductance. It is reasonable to argue that the duration of pulse that produces the maximal amplitude of the current will also produce the largest tail current. This was found to be the case, since increasing the duration of the depolarising pulse from small values also increased the amplitude of the steady state and tail currents. However, for more extended pulse durations during which time the steady state current began to decrease in amplitude, the tail current also decreased. Under these conditions the driving force was fixed but the conductance of the channel varied as a function of time. In order to test which ion carried the tail current experiments were carried out in normal seawater and in choline seawater, which contained no  $Na^+$ . Depolarising pulses to  $E_{Na}$  evoked no inward current in normal seawater as expected, but a large tail current was evoked upon repolarisation to resting membrane potential after 0.28 ms. However, in choline seawater a small outward current was produced upon depolarisation but no tail current followed repolarisation to rest. The small deflection in the current trace upon repolarising was capacitive in nature as a hyperpolarising pulse of equal magnitude but opposite polarity produced a deflection of equal but opposite polarity (Fig 5.1).

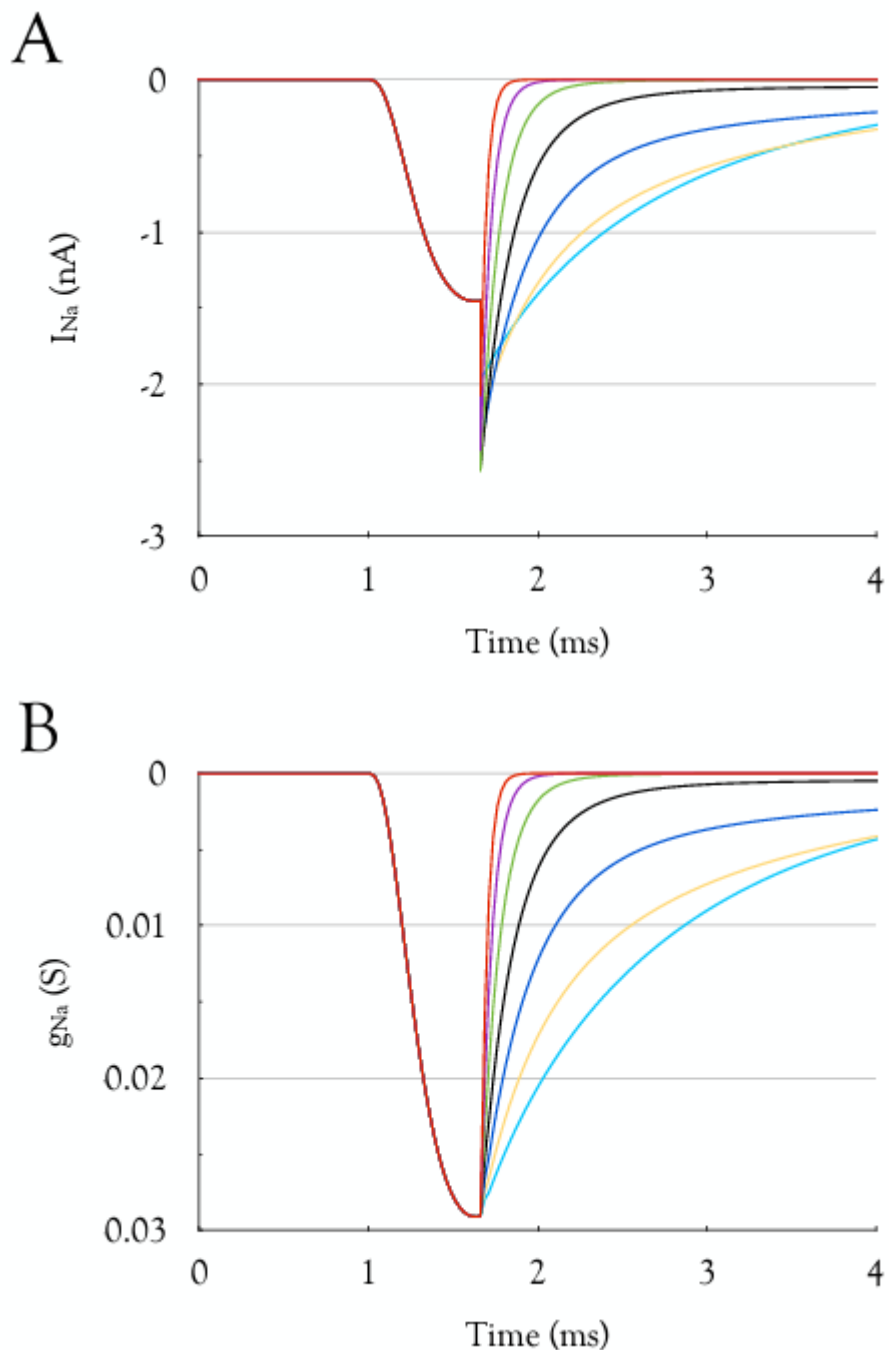


**Figure 5.2 -  $\text{Na}^+$  conductance.** A. Simulation of  $I_{Na}$  evoked by conditional depolarisation to 20 mV for 0.6 ms in order to open the permeability pathway. Repolarisation to a variety of potentials (red -80 mV; purple -70 mV; green -60 mV; black -50 mV; blue -40 mV; yellow -30 mV; turquoise -20 mV) results in tail currents whose magnitude is dependent upon the driving force ( $V - E_{Na}$ ). B. Converting the current traces in A to conductance according to  $g_{Na} = I_{Na} / (V - E_{Na})$  produces conductance traces which converge on the same point i.e., there is continuity of conductance.

## Continuity of sodium conductance

As a test of whether conductance was a true measure of membrane permeability, the conductance was calculated based on the current response to short duration depolarisations where there was discontinuity in the amplitude of the  $I_{Na}$ , resulting from the appearance of the tail current on stepping to hyperpolarised potentials. Converting the current to a conductance according to  $g_{Na} = I_{Na} / (V - E_{Na})$  resulted in continuity of the traces (Fig 5.2B). This was also the case for  $\text{Na}^+$  currents of very small duration before the current had a chance to decrease in amplitude i.e., data collected from pulses of varying durations were consistent with this hypothesis. This data indicated that the membrane permeability behaved in an ohmic manner since  $g_{Na}$  could be predicted from  $I_{Na}$  based on the driving force ( $V - E_{Na}$ ). This was demonstrated by depolarising the membrane for a period of time (1.53 ms) to levels at which a sufficiently large steady state current was evoked. The membrane potential was then stepped to a wide range of potentials, from about -100 mV to  $> E_{Na}$ . This procedure evoked tail currents whose amplitude was dependent upon the magnitude of the repolarising potential. Plotting the amplitude of the tail current at the instant of repolarisation versus the repolarising potential produced a straight line, whose slope was an indication of the conductance of the permeability pathway (Fig 5.3C). This allowed measurement of the current through the open permeability pathways at a variety of different driving forces without the influence of time dependent effects. This linear relationship was indicative that the conductance was a function of the driving force but was unaffected by membrane potential. Conceptually this was an important point and suggested that since the membrane potential did not affect conductance it must control the opening of the permeability pathways to account for the voltage dependence of the current. In this manner membrane potential controls opening of the individual permeability pathways but does not affect the ions flowing through the pathways once open. As we shall see in the last chapter, we can state that gating, but not conductance, is voltage dependent. The current crossed the voltage-axis close to the  $E_{Na}$  at 20 mV, the difference probably due to experimental error. This instantaneous IV relation was in direct contrast to the steady state current amplitude plotted against the depolarising potential, which displayed the classic U shape (Fig 5.3C).

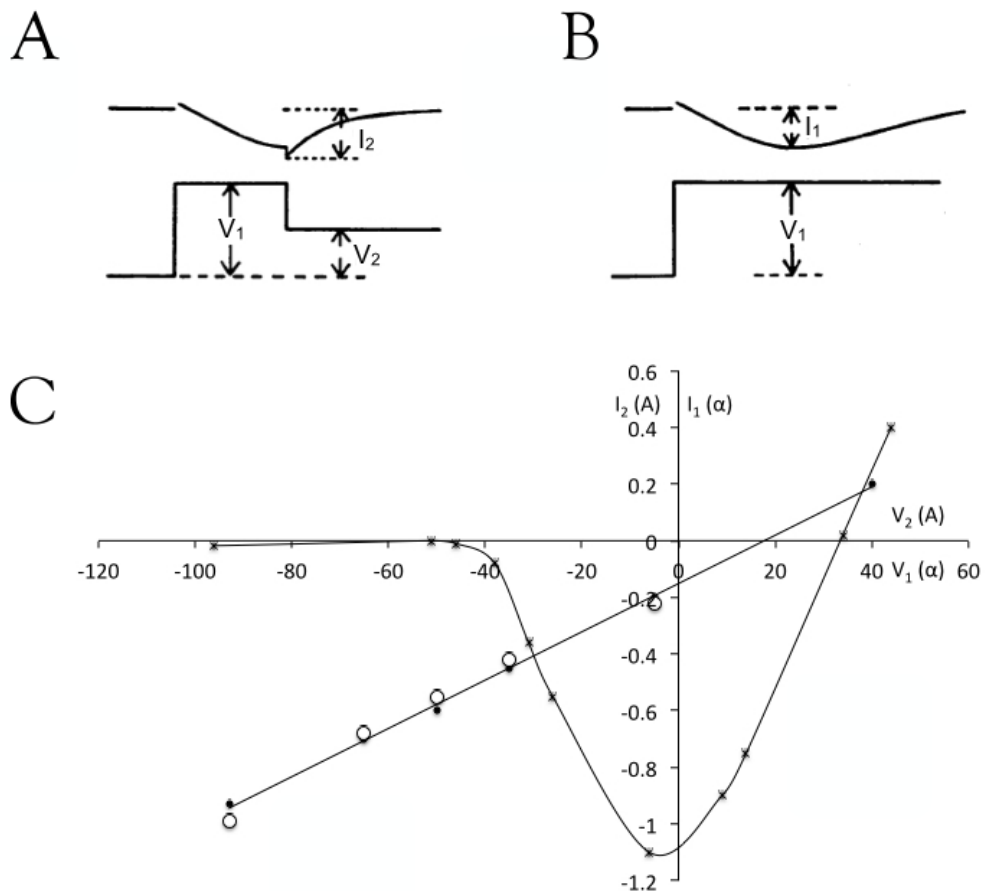


**Figure 5.3** - The instantaneous IV relationship. A. A conditioning pulse to  $-36$  mV was followed by repolarisation to a range of test voltages from  $-110$  to  $40$  mV. The schematic illustrates how the magnitude of the tail currents was measured. B. The steady state current was measured during longer pulses, which allowed to current to peak then decrease in magnitude. C. Plot of the tail current (-○-) and steady state currents (-x-) versus voltage, indicating the U shape of the steady state and linear relationship of the instantaneous IV, which crossed the voltage-axis close to  $E_{Na}$ .

### Independence principle revisited

It is interesting to note that this feature was not integral to the Hodgkin Huxley equations and could be regarded as a stand-alone topic distinct from the model, although it led to the assumption that  $I_{Na}$  and  $I_K$  were independent currents. Despite the crudity and uncertainty associated with their recordings Hodgkin and Huxley attempted to investigate the independence principle for both the steady state and instantaneous currents. The decision to investigate the independence principle applied to  $I_{Na}$  was based on the membrane potential sensitivity to  $K^+$ , whereby altering  $[K]_o$  would alter the membrane potential, which would alter  $K^+$  conductance, hopelessly confusing the electrophysiological recordings (this aspect is addressed in Chapter 8). Thus, the movement of  $Na^+$  recorded as trans-membrane current was measured in response to alterations in  $[Na]_o$ . If ions moved freely, this was termed independence, but if they were influenced by the presence of other ions their movement was not independent. Based on limitations of their electrophysiological

techniques Hodgkin and Huxley had to develop a model with which to fit their recordings of the membrane currents, rather than measure actual flux of ions. To calculate this they modified the equations of Ussing and Toerell, realising that they could test the independence principle by quantifying how altering  $[Na]_o$  affected the steady state  $I_{Na}$ . They measured  $I_{Na}$  in normal seawater at a variety of depolarisations and plotted the steady state peak  $I_{Na}$  versus voltage, which displayed the classic U-shaped response, and activated at about -40 mV, then crossed the voltage-axis at  $E_{Na}$  to become outward. They then repeated the experiment in low  $[Na]_o$  (10% and 30%) to see if the measured  $I_{Na}$  matched the model. It should be appreciated that reducing  $[Na]_o$  would not simply result in a parallel decrease in the steady state U shaped relationship, since  $E_{Na}$  would also vary according to  $[Na]_o$ . Hodgkin and Huxley found that the experimental results and the model converged closely, but not exactly, thus scaling factors were introduced for each  $[Na]_o$  to force a match. Hodgkin and Huxley proposed several reasons for the mismatch including that the membrane hyperpolarised in choline seawater and the continuous rundown of the current over the duration of the experiment. Based on these assumptions Hodgkin and Huxley erroneously claimed that the independence principle applied to  $Na^+$  currents. This data was described in detail in Chapter 4.

Hodgkin and Huxley then sought to determine the behaviour of this instantaneous IV relationship when seawater  $[Na]_o$  was reduced. Their results highlighted an extremely important point, which was that given the limited time constraints when carrying out their experiments, some were not carried out optimally, the deficiency only becoming apparent after analysis when there was no possibility of repeating the experiments. The major flaw in these experiments was that they left insufficient time between switching from seawater to choline seawater before commencing the double pulse paradigm, with the result that the initial inward current was still present, whereas in later pulses it had disappeared. Hodgkin and Huxley also reflected that the delay between switching to choline seawater and commencing the voltage steps led to a deterioration of the nerve, reducing the amplitude of the currents by up to 30%. Under such conditions the results can only be viewed as an approximation and their claims of independence must be viewed as tentative at best. However in 1955 Hodgkin and Keynes (see Chapter 8) showed that this was incorrect and that ion movement was influenced by the presence of other ions – this anticipated the concept of the ion channels, where ions move sequentially through channels (Hille, 1972). The basic result was the development of a curvature of the instantaneous IV relationship as  $[Na]_o$  decreased. Hodgkin and Huxley then applied their model of the independence principle to see if it matched the data (note the subtle change in expression of the model in the *Figure 7* legend compared to Eq. 4.15). Rather than illustrate the Hodgkin and Huxley data I have carried out a simulation where the instantaneous IV relationship is modelled as a linear function of repolarising voltage i.e.,  $I_{Na} = g_{Na}(V - E_{Na})$ . Eq. 4.15 was applied for all reductions in  $Na^+$  from 100% to 0% in 10% steps. As the  $[Na]_o$  decreased the relationship becomes less linear and crosses the voltage-axis relative to the  $E_{Na}$  based on the  $[Na]_o$  for that particular simulation. It is interesting that the lower the  $[Na]_o$  concentration the more pronounced the curvature, i.e., the relationship transforms to a non-Ohmic description, and is more suitably described by the GHK current equation (Hodgkin & Katz, 1949a). In this context such curves are described as rectifying, where the permeability pathway passes current more easily in one direction more than the other (Fig 5.4).

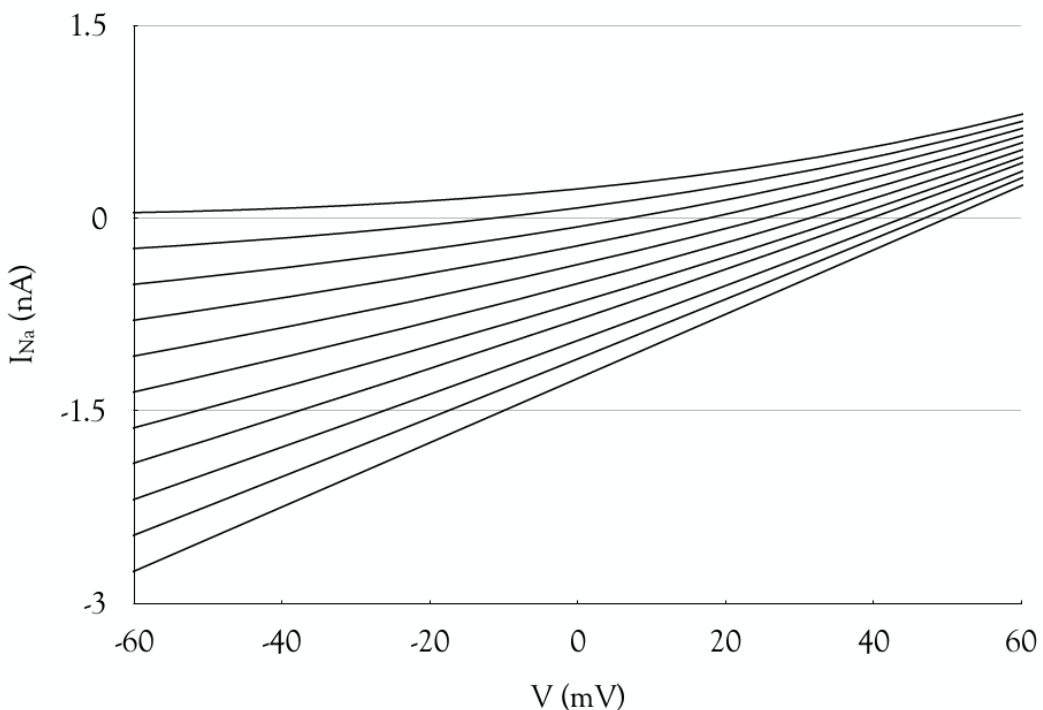


**Figure 5.4** - The instantaneous IV relationship versus membrane potential for simulations in which the  $[Na]$  in the seawater was decreased in 10% steps from 100% to 0%. The lowest trace shows the linear instantaneous IV recorded in 100%  $Na^+$  seawater. As the percentage of  $Na^+$  decreases the relationship became curved and the traces crossed the voltage-axis (i.e.,  $E_{Na}$ ) at less depolarised reversal potentials as expected when  $[Na]_o$  was decreased but  $[Na]_i$  was unchanged.

The time constant of the relaxation of the tail current towards baseline following a conditioning step to -36 mV followed by a test pulse to voltages varying from -122 mV to -8 mV, showed that there was a linear relationship, with the greater the repolarising potential the greater the value of the time constant (*Table 1, Figure 8*). The next experiments investigated the  $Na^+$  conductance and demonstrated that there was consistency between estimates of  $g_{Na}$  calculated as described in the previous chapter where subtraction of the currents, followed by correcting for the capacitive transients, matched well with estimates of  $g_{Na}$  from tail currents (*Figure 10*).

## K<sup>+</sup> current

There was considerable evidence, discussed in the previous chapter, to assume that the late outward current was carried by K<sup>+</sup> ions. This was investigated in the same manner in which the early inward current was associated with  $Na^+$ , but with a few major concessions. The  $E_{Na}$  was far from rest so Hodgkin and Huxley could employ a large range of membrane potentials distant from  $E_{Na}$ , but also where  $V$  was more positive than  $E_{Na}$ , where  $I_{Na}$  should reverse direction. In addition, they used low  $[Na]_o$  seawater where the  $E_{Na}$  should be closer to rest, but again the inward current should reverse at the calculated  $E_{Na}$ . They compared the measured change in  $E_{Na}$  in seawater and low  $[Na]_o$  seawater with theoretical predictions.

With  $K^+$  the situation was less straightforward as the resting membrane potential was closer to  $E_K$  thus Hodgkin and Huxley could not change  $[K]_o$  by the degree to which they changed  $[Na]_o$ , as this would significantly alter the resting membrane potential and potentially damage the axon. They could however use choline to block any  $Na^+$  contribution to the currents, and under these conditions  $E_K$  could be estimated at about -80 mV, thus depolarising to 19 mV would fully activate  $I_K$  with subsequent repolarising potentials varying from -9 mV to -93 mV used to investigate the transition between outward and inward tail current as predicted by the Nernst equation. The current during repolarisation was outward for  $V$  more depolarised than -78 mV and inward for more hyperpolarised potentials, but since the amplitudes of the currents were small where  $E_K$  was close to the membrane potential, the accuracy of these estimates was compromised.

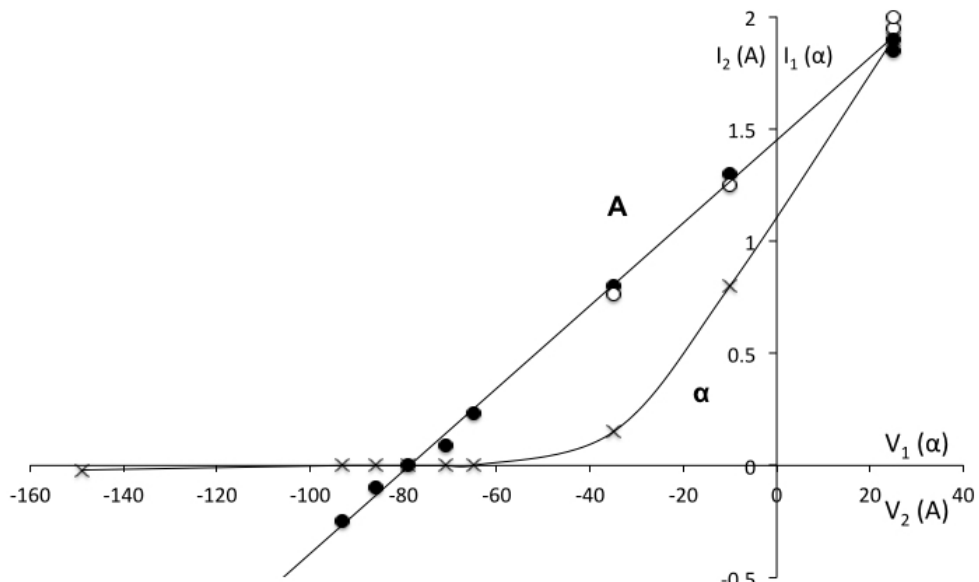


**Figure 5.5** - The instantaneous IV of the late outward (presumably  $K^+$ ) current (-●-) displayed similar properties to the instantaneous IV for  $I_{Na}$  in that it was linear, but crossed the voltage-axis near  $E_K$ . The steady state outward current (-x-) was calculated as described previously.

The instantaneous IV relationship for  $K^+$  was calculated in a manner similar to that for  $I_{Na}$ , evoking tail currents by stepping the membrane potential to a series of test potentials after activating the permeability pathway by a conditioning pulse. Whereas for  $I_{Na}$  the tail current gave large signals to measure, the  $I_K$  tail currents were not as impressive, as the repolarising potential was closer to  $E_K$  hence currents were smaller. However, they were able to plot the tail current amplitude versus the test potential and obtained a linear relationship, which passed through the voltage axis at  $E_K$ , showing that the  $K^+$  conductance was Ohmic (Fig 5.5). The conductance for  $K^+$  showed the same continuity as  $g_{Na}$ , but the rate constant of decay, although of greater value at more hyperpolarised potentials, was not as large as for  $g_{Na}$ . To test the continuity of  $K^+$  conductance, the  $E_K$  was estimated experimentally under conditions where  $I_K$  was measured in normal and choline seawater at a

variety of temperatures. The average values were consistent with higher temperatures producing more hyperpolarised values for  $E_K$  (Table 3) as predicted by the Nernst equation (Chapter 2). Altering  $[K]_o$  by factors ranging from 0.5 to 5 changed  $E_K$  in the direction predicted, but the match with Nernstian calculations was not as accurate as those for  $E_{Na}$ .

An interesting phenomenon was reported a few years after publication of this paper, which had important implications for the accuracy of the data presented. A tight membrane was proposed to fit snugly around the squid axon, which acted to concentrate the  $K^+$  released from the axon during firing of action potentials. The  $K^+$  was concentrated in a relatively small volume and acted to depolarise  $E_K$ , which altered the profile of subsequent action potentials in a train. During voltage clamp experiments the  $K^+$  increased in direct relation to the duration of the depolarising pulse, to the extent that  $E_K$  depolarised past the repolarising potential and the  $I_K$  tail current became inward after a 20 ms pulse (Frankenhauser & Hodgkin, 1956).

## Leak current

Hodgkin and Huxley then proceeded to describe the leak current, which was not discussed in much detail in these papers, and was dismissed as relatively unimportant (p.299, Hodgkin, 1992), but which plays a critical role in determination of threshold. Hodgkin and Huxley measured the current required ( $8 \mu\text{A cm}^{-2}$ ) to hyperpolarise the membrane potential from rest (-65 mV) to  $E_K$  (-78 mV) in choline seawater, reasoning that at this potential there was neither  $I_K$  nor  $I_{Na}$  present, with  $I_{leak}$  the only contributing current. However, this simple manoeuvre was insufficient to determine the reversal potential for the leak current or its conductance, as there were two unknown parameters present. To circumvent this, they then hyperpolarised the membrane potential to -149 mV and found there was no effect of altering the  $[K]_o$  by a factor of four, and thus assumed that the inward current ( $24 \mu\text{A cm}^{-2}$ ) at this potential was entirely leak current. This presented a pair of simultaneous equations, which, if solved, would provide estimates for  $E_{leak}$  and  $g_{leak}$ . This relationship is perhaps best appreciated when represented graphically as in Fig 5.6A.

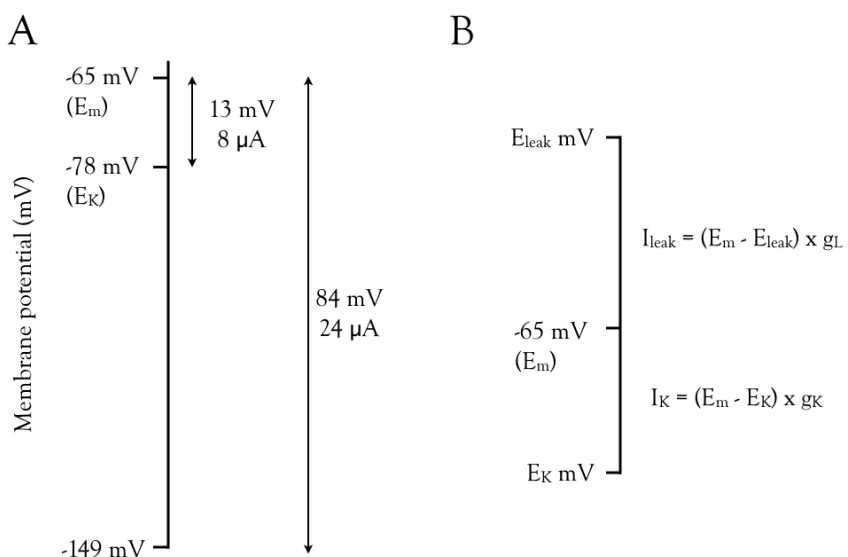


**Figure 5.6** - Schematic illustrating the measurements used to calculate  $E_{leak}$  and  $g_{leak}$ . A. The membrane potential was hyperpolarised to  $E_K$ , where the only current flowing is  $I_{leak}$ . It was then hyperpolarised to -149 mV, where no  $K^+$  current flowed and  $I_{leak}$  was the only contributing current. Solving the simultaneous equations provided values for  $E_{leak}$  and  $g_{leak}$ . B. At resting membrane potential ( $E_m$ ) only  $I_{leak}$  and  $I_K$  were open and since at this potential they must balance each other the value for  $g_K$  could be readily calculated.

Experimentally they found that

$$(-78 \text{ mV} - E_{leak}) \times g_{leak} = 8 \mu\text{A cm}^{-2}$$

and

$$(-149 \text{ mV} - E_{leak}) \times g_{leak} = 24 \mu\text{A cm}^{-2}$$

so

$$3(-78 \text{ mV} - E_{leak}) = (-149 \text{ mV} - E_{leak})$$

$$(-234 \text{ mV} - 3E_{leak}) = (-149 \text{ mV} - E_{leak})$$

$$-85 \text{ mV} = 2E_{leak}$$

$$E_{leak} = -42.5 \text{ mV}$$

$g_{leak}$  could then be calculated as

$$(-78 \text{ mV} - E_{leak}) \times g_{leak} = 8 \mu\text{A cm}^{-2}$$

$$g_{leak} = \frac{8 \mu\text{A}}{-78 \text{ mV} - (-42.5 \text{ mV})}$$

$$g_{leak} = 0.23 \text{ mS cm}^{-2}$$

The value of  $g_K$  could now be calculated from these values, but again a graphical representation illustrates more clearly the relationship between resting membrane potential,  $g_{leak}$  and  $g_K$  (Fig 5.6B). If the only permeability pathways open at rest are  $g_{leak}$  and  $g_K$ , it follows that at resting membrane potential the leak current equals the potassium current.

i.e.,  $I_{leak} + I_K = 0$  at rest, and

$$I_{leak} = g_{leak}(V - E_{leak})$$

$$I_K = g_K(V - E_K)$$

so

$$(-65 \text{ mV} - (-42.5 \text{ mV})) \times 0.23 \text{ mS} = (-65 \text{ mV} - -78 \text{ mV}) \times g_K$$

$$g_K = \frac{-22 \text{ mV} \times 0.23 \text{ mS}}{13 \text{ mV}}$$

$$g_K = 0.39 \text{ mS cm}^{-2}$$

The importance of the leak current was not described in any detail by Hodgkin and Huxley, this passive Ohmic current relegated in importance in comparison to the more dynamic active  $I_{Na}$  and  $I_K$ . However, the leak current is of fundamental importance in setting the threshold for action potential firing, which becomes apparent when one visualises the consequences of combining  $I_{Na}$  and  $I_{leak}$ . Alan Kay has covered this topic in detail in an

excellent paper (Kay, 2014), which I shall use as my template. Some of the information required to explain the effects of the leak current is contained in Chapter 7.

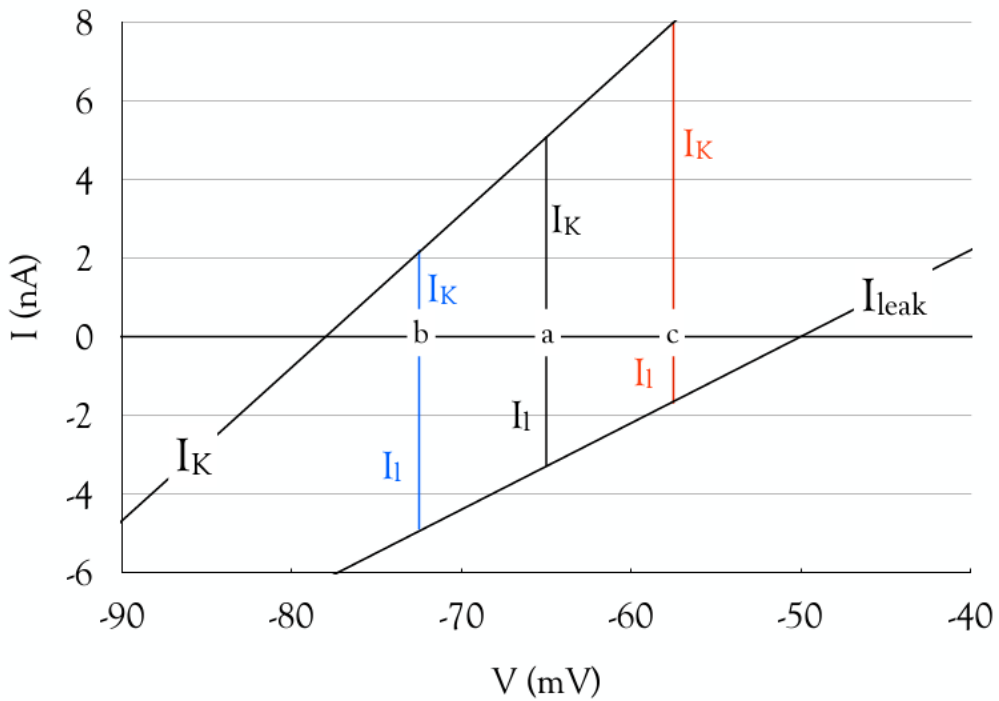


**Figure 5.7 - The effects of small voltage deviations from resting membrane potential.** This schematic illustrates the relationship shown in Fig 5.6B. If we assume that the resting membrane potential is  $-65\text{ mV}$  (a) then at this potential the  $I_{\text{leak}}$  and  $I_K$  are of opposite polarity and equal magnitude. If the membrane potential is hyperpolarised by  $7.5\text{ mV}$  to  $-72.5\text{ mV}$  (b) then the change in the contributions of  $I_{\text{leak}}$  and  $I_K$  can be visualised as the lengths of the vertical lines extending from  $-72.5\text{ mV}$  until they intercept  $I_{\text{leak}}$  and  $I_K$ . At this hyperpolarised potential the contribution of  $I_{\text{leak}}$  is greater than  $I_K$ , thus upon cessation of the imposed current the  $I_{\text{leak}}$  dominates and pulls the membrane potential in a depolarising direction until equilibrium is restored at the resting membrane potential. Similar reasoning applies to a depolarisation of  $7.5\text{ mV}$  to  $-57.5\text{ mV}$  (c), where  $I_K$  dominates on cessation of the pulse, thus  $I_K$  drives hyperpolarisation of the membrane potential to rest.

As described in the 1930s by Alan Hodgkin, small deviations in membrane potential from rest resulting from injection of depolarising or hyperpolarising pulses caused small linear changes in membrane potential, which then returned to rest when the pulse ceased (Hodgkin, 1938). The reason for this is illustrated in Fig 5.7. If we plot the values of  $I_K$  and  $I_{\text{leak}}$  versus membrane potential according to the values calculated above, which are the only currents active at rest, then the resting membrane potential at rest ( $-65\text{ mV}$ ) lies between the reversal potentials for  $I_K$  and  $I_{\text{leak}}$ . As such the magnitude of each current active at rest can be visualised by drawing a vertical line through rest (a), to intercept  $I_K$  and  $I_{\text{leak}}$ , the length of the line from rest an indication of the magnitude of the current. An injection of positive current will lead to a depolarisation of the membrane, e.g., by  $7.5\text{ mV}$  to  $-57.5\text{ mV}$ . If

## A companion guide to the Hodgkin-Huxley papers

a vertical line is extended from -57.5 mV (c) to  $I_K$  and  $I_{leak}$ , the line is longer for  $I_K$  and shorter for  $I_{leak}$  than at rest, since this voltage is further from  $E_K$  therefore increasing the driving force ( $V - E_K$ ) and hence the current, but smaller for  $I_{leak}$  since this voltage is closer to  $E_{leak}$ . On cessation of current injection, the large  $I_K$  will pull the membrane in a hyperpolarising direction, until equilibrium is re-established at the resting membrane potential of -65 mV. In a similar manner if the membrane is hyperpolarised by 7.5 mV (b) the  $I_{leak}$  dominates as the membrane potential is further from  $E_{leak}$ . On cessation of current injection, the membrane depolarises towards rest, as the  $I_{leak}$  outweighs the contribution of  $I_K$ , until equilibrium is restored. This explains the small deviations in membrane potential in response to small current injections of either polarity, or why the potential returns to rest at the end of the pulse. However, as well as setting resting membrane potential  $I_{leak}$  plays a vital role in setting the action potential threshold.

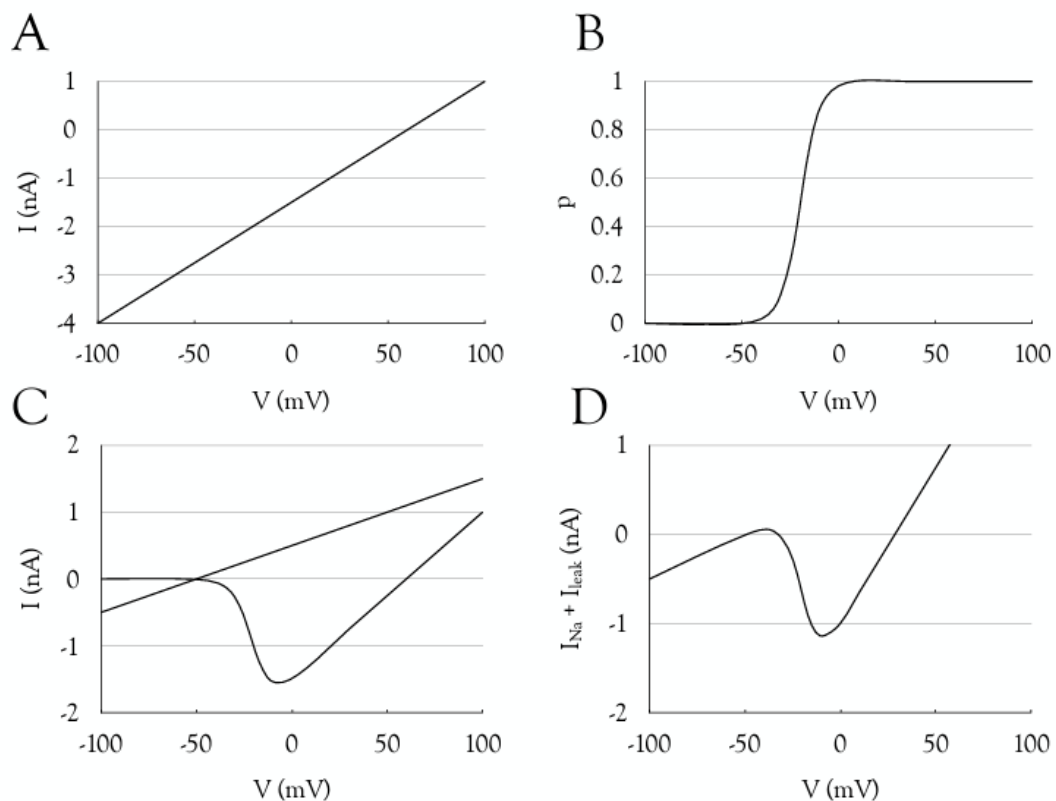


**Figure 5.8** - The effect of leak current on threshold. A. The Ohmic relationship between  $I_{Na}$  and membrane potential, where  $I_{Na}$  is calculated as  $g_{Na}(V - E_{Na})$ . B. The probability ( $p$ ) of the  $\text{Na}^+$  permeability pathway being open is described by a sigmoidal relationship relative to membrane potential. C.  $I_{Na}$  multiplied by the probability factor,  $p$ , produces the classic U-shaped relationship relative to membrane potential. The linear leak current, which crosses the voltage axis at  $E_{leak}$  is superimposed. D. Adding  $I_{leak}$  and  $I_{Na}$  provides the relationship that explains the threshold for action potential firing.

As described above the leak current can be defined as  $I_{leak} = g_{leak}(V - E_{leak})$ , which is a linear relationship when plotted against membrane potential and crosses the voltage axis at  $E_{leak} = -50$  mV (Fig 5.8C). The  $I_{Na}$  can be defined as the product of two separate components.

## A companion guide to the Hodgkin-Huxley papers

$I_{Na} = g_{Na} (V - E_{Na})$  and  $p$ . We have already described  $I_{Na} = g_{Na} (V - E_{Na})$ , which shows  $I_{Na}$  is a linear function of membrane potential that crosses the voltage axis at  $E_{Na}$  (Fig 5.8A). The function  $p$  is equivalent to the parameter  $m$ , introduced in Chapter 7, which describes the probability of the  $Na^+$  permeability pathways being open at a particular voltage. As the membrane potential depolarises from rest, the probability of the permeability pathway being open increases from 0 to 1 in a sigmoidal fashion (Fig 5.8B). The current voltage relationship of  $I_{Na}$  can be calculated by multiplying  $I_{Na}$  by  $p$  to give the U shape illustrated in Fig 5.8C. In order to describe threshold, we add the  $I_{leak}$  and  $I_{Na}$  as illustrated in Fig 5.8D to produce a profile that closely resembles that illustrated in Fig 3.3B. We ignore  $I_K$  in our ruminations on threshold as it is activated more slowly than  $I_{leak}$  and  $I_{Na}$  and therefore does not contribute during brief shocks. This is a simplification that ignores the contribution of  $I_K$  to the steady state. If  $I_K$  were included the points at which the current crosses the voltage axis would be more hyperpolarised. For those interested in a more complete description of the currents contributing to threshold details can be found in the following sources (Koch, 1999; Catterall *et al.*, 2012). The crucial consideration is that by adding the leak current to  $I_{Na}$  the combined current crosses the voltage axis at three points, the resting membrane potential, threshold and  $E_{Na}$  and introduces instability to the system (Fig 5.9A). From the point of view of threshold, it is important to realise what the slopes of the current mean when they cross the voltage axis. Both of these instances illustrate that (a) is a stable point at resting membrane potential and that small deviations along the voltage axis from this tend to be counteracted, so the membrane returns to this stable point as described above. Point (b) is also an equilibrium point. However, if sufficient positive current is injected into the axon such that the membrane potential reaches point (b), the membrane remains stable, and no action potential is evoked. However at point (b) the slope of the current is inward and results in an inherently unstable system, such that any additional inward current, no matter how small, would lead to the positive feedback cycle (Fig 2.3) causing the membrane to depolarise and an action potential to be evoked (Hodgkin, 1951). This can be seen in Fig 3.2A, where current injection in the region of threshold may or may not evoke an action potential. This can be modelled as the physical analogy of pushing a ball up a slope from a trough (Fig 5.9B). If the resting membrane potential is considered analogous to a trough, then pushing the ball up either slope from point (a) will result in the ball rolling back down the slope to rest for small deviations along the voltage axis. However, if the ball is rolled up to reach the peak (b), then a very slight movement in the depolarising direction will cause the ball to roll down the hill, activating the Hodgkin positive feedback cycle.

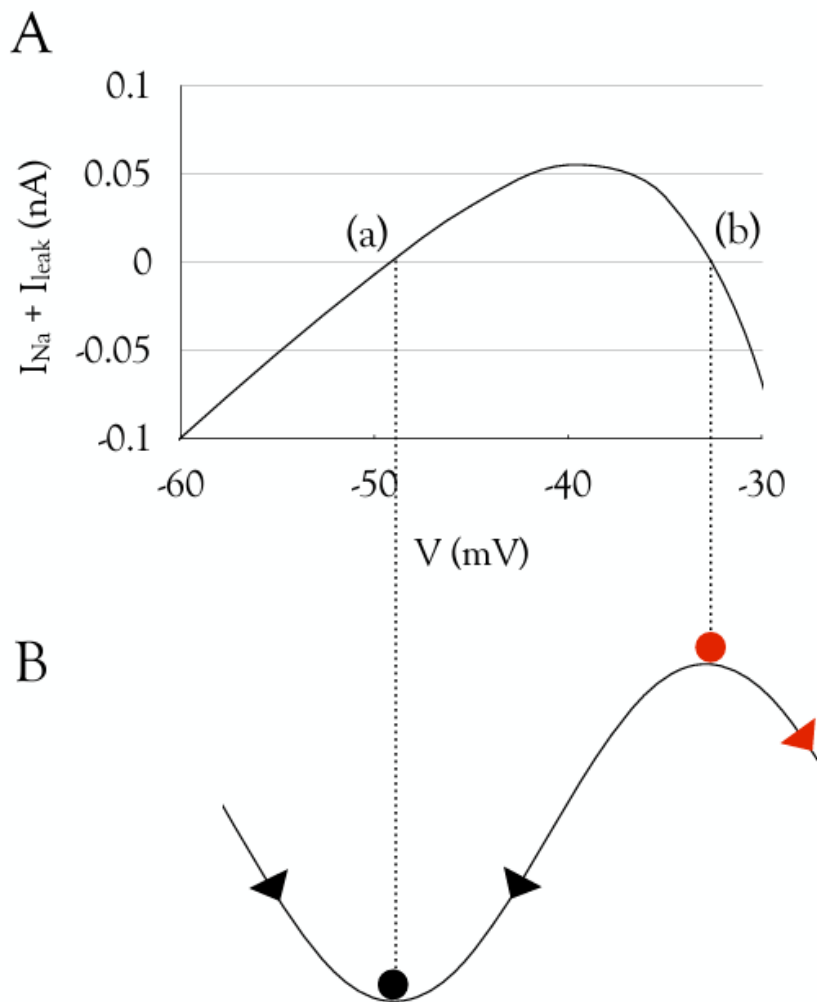


**Figure 5.9** - Action potential threshold. A. The points where the membrane current crosses the voltage axis, occur at resting membrane potential (a) and threshold (b). B. A physical model representing the stable point at resting membrane potential (black ball), and the unstable point created by negative inward current that defines threshold (red ball and arrow), which if exceeded will evoke an action potential.

## 6. THE DUAL EFFECT OF MEMBRANE POTENTIAL ON SODIUM CONDUCTANCE IN THE GIANT AXON OF *LOLIGO*

In this paper the process by which the  $\text{Na}^+$  current decreased under continued depolarisation was studied. This process clearly indicated that inherent in the permeability changes that underlie the  $\text{Na}^+$  current was a self-limiting process by which the current switched off. This is in direct contrast to the  $\text{K}^+$  current, which was maintained for the duration of the depolarising pulse. This is an extremely important distinction that Hodgkin and Huxley do not draw much attention to, since implicit in this behaviour is that the  $\text{K}^+$  current will be continuously activated, except at the most hyperpolarised of membrane potentials, hence the major contribution that  $I_K$  plays in setting the resting membrane potential as we saw at the end of the last chapter. At rest there is a tonic outwardly directed movement of  $\text{K}^+$  that will tend to keep the membrane in a hyperpolarised state, but there is also an inwardly directed leak current that tends to depolarise the cell. This leak current is Ohmic with none of the delays in activation associated with gating particles as was predicted for the  $\text{K}^+$  current (see next chapter) and thus responds instantly to changes in membrane potential. In order for an action potential to occur the inward  $\text{Na}^+$  current must exceed the  $\text{K}^+$  current.

### Time constant of inactivation

Hodgkin and Huxley investigated the turning off or ‘inactivation’ of the  $\text{Na}^+$  current by using two distinct double pulse protocols. As illustrated in *Figure 1* they held the membrane potential at -65 mV then depolarised to a test pulse of -21 mV, which evoked a large transient inward current. Introducing a conditioning pulse to -57 mV of varying durations prior to the test pulse significantly decreased the amplitude of the inward current, the longer the duration of the pulse, the smaller the current on subsequently stepping to the test pulse. Note that depolarising to -57 mV induced no  $\text{Na}^+$  current since the level of depolarisation was below threshold. The late outward current was not affected by the prepulse, which was indirect evidence that the  $\text{Na}^+$  and  $\text{K}^+$  currents were independent entities. They repeated this experiment with a hyperpolarising conditioning pulse to -96 mV of varying durations prior to the test pulse (*Figure 2*). In this instance the effect of the conditioning pulse was to increase the amplitude of the test pulse, which was dependent upon the duration of the conditioning pulse. By plotting the relative magnitude of  $I_{\text{Na}}$  during the test pulse versus the duration of the conditioning pulse to a particular potential a clear relationship was revealed in which conditioning pulses in the hyperpolarising direction led to an increased amplitude of the test current, whereas depolarising conditioning pulses led to a decrease in the test pulse amplitude. This occurred along an exponential time course with the time constant varying between 2 ms and 8 ms depending upon the magnitude of the conditioning pulse (*Figure 3*). The implications from these experiments are profound. If the membrane was held at a depolarised potential for any length of time, then a significant proportion of the permeability pathways would inactivate leading to a decrease in the  $\text{Na}^+$  current evoked by a subsequent depolarising pulse. Of equal importance is the realisation that hyperpolarising the membrane for a short period of time would remove inactivation and restore the permeability pathways to a state in which they were available for opening. In light of these observations, we can view the action potential profile from the point of inactivation. The upstroke of the action potential is the result of an influx of  $\text{Na}^+$ , an influx of  $\text{Na}^+$  that must exceed the tonic  $\text{K}^+$  current in order to exceed threshold. At the peak of the action potential the  $\text{Na}^+$  current turns off or inactivates and the  $\text{K}^+$  current activates in a delayed fashion. Since  $V$  is far from  $E_K$ , an outward current develops causing the membrane potential to hyperpolarise towards  $E_K$ , at which point we may consider the membrane exclusively permeable to  $\text{K}^+$ , before slowly returning towards resting membrane potential. This hyperpolarisation towards  $E_K$  can be explained as the means by which inactivation of

the  $\text{Na}^+$  current is removed so the optimal number of  $\text{Na}^+$  permeability pathways are primed and available for opening.

### Inactivation curve

The magnitude of the effect of the conditioning pre-pulse was investigated by imposing another double pulse protocol where a conditioning pulse was stepped to a range of potentials from -111 mV to -36 mV for 35 ms followed by a test potential to -21 mV. It should be noted that at depolarising test pulses greater than threshold (about -50 mV), a  $\text{Na}^+$  current was evoked. Plotting the normalised magnitude of the test pulse relative to a current evoked in the absence of any conditioning pulses revealed a sigmoidal relationship that decreased with depolarisation. Hodgkin and Huxley described inactivation in terms of  $h$ , which varied between 0 and 1. Thus  $(1 - h)$  was a measure of inactivation, while  $h$  was the fraction of the system that is not inactivated and available for activation. The voltage at which  $h = 0.5$  was -62.5 mV so at rest (-65 mV) about 40% of the  $\text{Na}^+$  permeability pathways were inactivated (Fig 6.1). Hodgkin and Huxley stated that the inevitable depolarisation of the membrane potential from a resting value of -65 mV during the course of the experiment could be by up to 15 mV, equivalent to  $h = 0.25$ . The importance of the AHP becomes apparent when we realise that the value of  $h$  between the resting membrane potential of -65 mV and the voltage approached at the peak of the AHP (-80 mV) increased from 0.6 to 0.9 meaning inactivation had been removed from over 90% of  $\text{Na}^+$  permeability pathways which were available for subsequent activation.

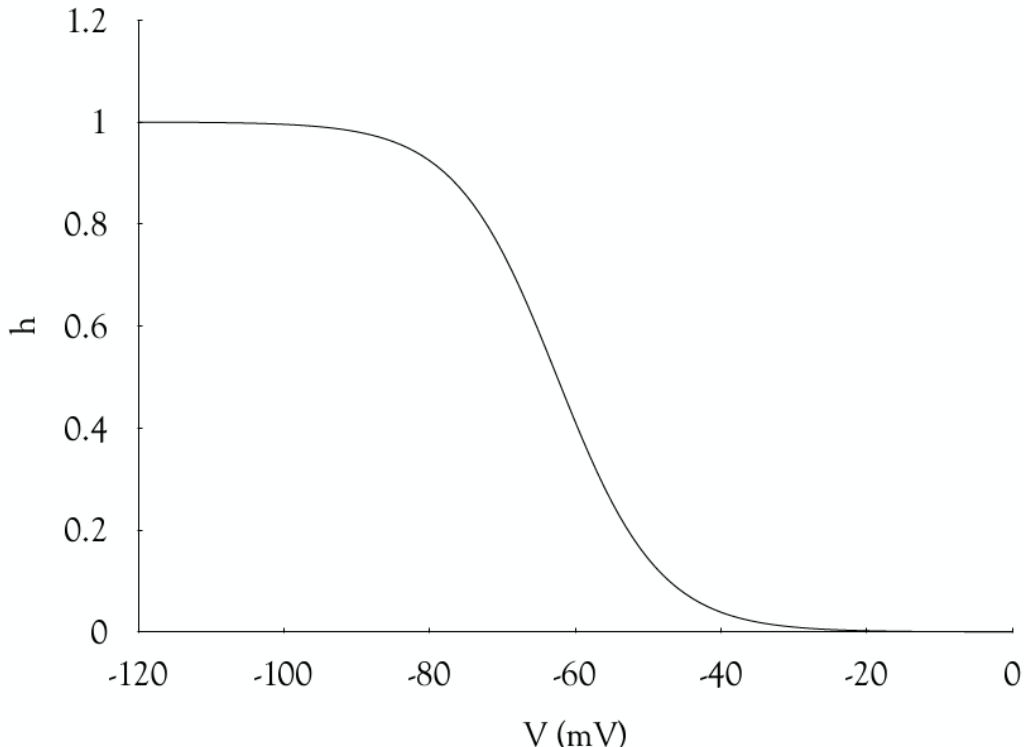


**Figure 6.1** - The  $\text{Na}^+$  permeability pathway inactivation curve is a sigmoidal relationship relative to membrane potential. At rest the value of  $h$  is about 0.6, which increases to 0.9 at  $E_K$ .

The time constant for inactivation was also investigated using a novel double pulse protocol. This required imposing two pulses to -21 mV of duration 1.8 ms, separated by a delay, the inter-pulse interval, which was sequentially decreased. At large inter pulse intervals the amplitude of the 2<sup>nd</sup> current was the same as the 1<sup>st</sup> current, but as the interval decreased below about 10 ms the 2<sup>nd</sup> pulse decreased in amplitude (Fig 6.2A). Plotting the ratio of the 2<sup>nd</sup> current versus the 1<sup>st</sup> current against the inter-pulse interval revealed an exponential relation with a time constant of about 12 ms (Fig 6.2B). The importance of this experiment was that it indicated a significant delay must occur between action potentials in order for the evoked Na<sup>+</sup> current to reach its control amplitude. The consequences of this are far reaching. If we imagine that during an action potential there is a minimum amount of Na<sup>+</sup> current required to reach threshold, and this occurs when the inward Na<sup>+</sup> current exceeds the outward K<sup>+</sup> current, then the process of inactivation reduces available Na<sup>+</sup> permeability pathways and risks reducing the Na<sup>+</sup> current to a sub-threshold amplitude. The two ways in which inactivation is removed are by hyperpolarising the membrane towards  $E_K$  as occurs during the AHP and allowing sufficient time between action potentials to permit the time dependent removal of the inactivation. In a recent paper the effect of decreasing the inter-pulse interval on compound action potential (CAP) amplitude was demonstrated in extracellular recordings of the A fibres from mouse sciatic nerve (Rich & Brown, 2018). A double pulse protocol of a similar type illustrated by Hodgkin and Huxley (Fig 6.2A) was imposed on the nerve, the difference being voltage was recorded as a result of the Na<sup>+</sup> current, whereas Hodgkin and Huxley recorded the Na<sup>+</sup> current. As the inter-pulse interval decreased the amplitude of the 2<sup>nd</sup> A fibre CAP decreased (Fig 6.2C), an indication that Na<sup>+</sup> channels were inactivating and unavailable for opening (Fig 6.2D). The effect of inter-pulse interval on the ability of a subsequent action potential to be evoked by the same amplitude of stimulus is named the refractory period and is explored in detail in the next Chapter.

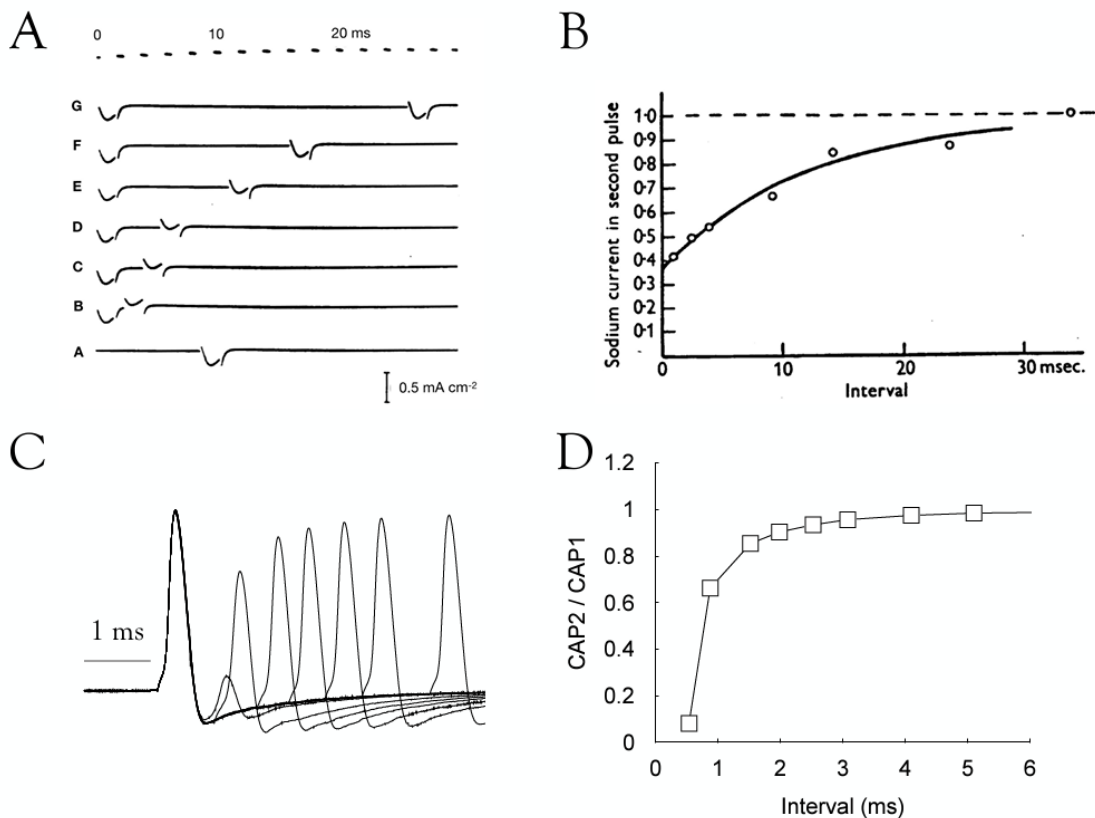


**Figure 6.2 - The effect of inter-pulse interval on  $I_{Na}$ .** A. The effect of decreasing the inter-pulse interval on the second  $I_{Na}$  was to decrease its amplitude. In this example the current was evoked at -21 mV. B. The time constant of inactivation was estimated by fitting a single exponential curve to measurements of the ratio of the 2<sup>nd</sup> current to the 1<sup>st</sup> current versus inter-pulse interval. In this example  $\tau$  was 12 ms. C. The amplitude of A fibre CAPs recorded from sciatic nerves using a similar stimulus protocol to that illustrated in A. As the inter-pulse interval decreased so did the amplitude of the 2<sup>nd</sup> CAP. D. Plotting the ratio of the two CAPs versus inter-pulse interval revealed a steep decrease at small time intervals.

# INTERLUDE

This is an appropriate point to pause and reflect on the content of the papers discussed in Chapters 2 to 6 before proceeding to describe the model proposed by Hodgkin and Huxley. Collectively the first four papers describe the use of the voltage clamp to record the trans-membrane current, which was separated into the active  $I_{Na}$  and  $I_K$  and the passive  $I_{leak}$ . The current was expressed as conductance and was assumed to reflect the permeability of the membrane. The conductance was not a function of membrane potential, which implied that membrane potential controlled the opening of the permeability pathways in order to explain the voltage dependence of the current amplitude.

**Chapter 2.** In this paper only the membrane potential was recorded. The action potential was quantified, displaying a negative resting potential and a peak that overshot 0 mV and approached  $E_{Na}$ . An AHP was present during the repolarising phase. Reducing  $[Na]_o$  in the seawater bathing the axon reduced the action potential amplitude and the rate of depolarisation, and altering  $[K]_o$  in the seawater affected the resting membrane potential, the rate of repolarisation and the AHP, clearly identifying the components of the action potential that were sensitive to  $[Na]_o$  or  $[K]_o$ . Hodgkin and Katz showed that the effects on the membrane potential in response to alterations in  $[Na]_o$  and  $[K]_o$  were in quantitative agreement to those predicted by the Nernst equation and were summarised as follows: (i) at rest the membrane was predominantly, but not exclusively, permeable to  $K^+$ , (ii) the rapid depolarisation of the membrane that initiated the action potential was due to  $Na^+$  influx driving the membrane potential towards  $E_{Na}$ , (iii) the repolarisation of the action potential was caused by an outward  $K^+$  current that drove the membrane potential towards  $E_K$ , prior to relaxing towards rest. These effects were quantified by the GHK voltage equation, which supported the assumption that the membrane potential approached the reversal potential of the ion to which it was most permeable at that instant.

**Chapter 3.** This paper was the first by Hodgkin and Huxley (and Katz) to describe ion currents recorded by using the voltage clamp technique. Recordings of membrane potential demonstrated a clear threshold, the membrane potential that must be reached in order to evoke an action potential, about 15 mV more depolarised than rest (-65 mV). Once evoked the action potentials displayed the same profile irrespective of stimulus strength. The voltage clamp data revealed a non-linear current evoked on depolarisation, which consisted of an early inward current, which decreased to become a sustained late outward current. The threshold for the early inward current was about 15 mV depolarised from rest, similar to the action potential threshold. A plot of the early current at its peak, and the late outward sustained current, versus membrane potential revealed two distinct components. The late current was outward at all membrane potentials and increased in amplitude in a linear manner with depolarisation. The inward current was more complex, increasing in amplitude, followed by a decrease, before crossing the voltage-axis at  $E_{Na}$  to become outward.

**Chapter 4.** The isolation and description of the inward current became the primary focus. In low  $[Na]_o$  seawater the early inward current disappeared, but the late outward current was relatively unaffected. The reversal potential of the inward current was measured in a variety of  $[Na]_o$  and the deviation of  $E'_{Na}$  from the  $E_{Na}$  in normal seawater agreed well with predictions by the Nernst equation of changes in  $E'_{Na}$  resulting from

decreased  $[Na]_o$ . A mathematical procedure was developed that allowed Hodgkin and Huxley to subtract the  $I'_{Na}$  in low  $[Na]_o$  from the control  $I_i$  to reveal the  $I_K$ , from which  $I_{Na}$  could be isolated from  $I_i$ . The currents were converted to conductances based on  $I_x = g_x / (V - E_x)$ , which were taken to represent the permeability of the membrane to a particular ion. The normalised conductances for  $g_{Na}$  and  $g_K$  showed a very steep relationship when plotted versus membrane potential, bearing a similar profile to the Boltzmann principle that describes the behaviour of a charged particle in an electric field.

Hodgkin and Huxley developed equations for the independence principle and compared their experimental recordings of  $I_{Na}$  in normal and low  $[Na]_o$  seawater with the model. The model was not an exact match to the data but given the limits of resolution of their electrophysiological recordings, Hodgkin and Huxley assumed that the independence principle applied to the effect of  $[Na]_o$  on  $I_{Na}$ , allowing them to treat  $I_{Na}$  and  $I_K$  as independent currents. The independence principle was revisited in two other papers in this series.

**Chapter 5.** The nature of movement of ions through the  $Na^+$  and  $K^+$  permeability pathways was quantified by using the first of a series of ingenious double pulse protocols resulting from the application of paired stimulators. The conditioning pulse activated the currents with the test pulse repolarising the membrane potential towards rest. The tail currents were the result of the test pulse changing the driving force ( $V - E_x$ ) while the permeability pathway was open. Plots of the peak tail current versus the test pulse potential revealed a linear function whose slope defined the conductance of the permeability pathway and demonstrated that the conductance was not a function on membrane potential. This implied that the voltage dependence of the current amplitude was due to the membrane potential controlling opening of the permeability pathways.

The change in  $E_K$  in voltage clamp experiments in which  $[K]_o$  was altered did not match the Nernst equation predictions for  $E_K$  in defined  $[K]_o$  as well as equivalent experiments for low  $[Na]_o$ , raising doubt that  $K^+$  was exclusively responsible for the outward current that repolarised the membrane. This uncertainty was only resolved with tracer experiments that measured the fluxes of  $Na^+$  and  $K^+$  across the membrane. In addition to the active  $Na^+$  and  $K^+$  conductances, the Ohmic leak current was quantified, establishing that  $g_K$  and  $g_{leak}$  determine the resting membrane potential.

**Chapter 6.** The process by which the  $I_{Na}$  decreased during a sustained depolarising step was described as inactivation and quantified. The inactivation process,  $h$ , had both voltage dependent and time dependent features. Hodgkin and Huxley defined  $h$  as the fraction of inactivating particles in the permissive state and  $(1 - h)$  as the fraction of inactivating particles in the non-permissive state. A sigmoidal relationship, decreasing with depolarisation, described the effect of membrane potential on  $h$ . The decrease in  $I_{Na}$  could be estimated from double pulse protocols where the amplitude of the  $I_{Na}$  versus the inter pulse interval provided the time constant at particular voltages. A full description of the relationship between membrane potential and the inactivation time constant is illustrated in the next Chapter.

# 7. A QUANTITATIVE DESCRIPTION OF MEMBRANE CURRENT AND ITS APPLICATION TO CONDUCTION AND EXCITATION IN NERVE

The final paper in the series is the most famous in the field of electrophysiology: it has been cited over 14,000 times, it introduced a new branch of physiology, membrane biophysics, and established a template for the integration of mathematical modelling with experimental data. Before describing the data in the paper in detail it is worthwhile comparing this paper with the first four papers. The first four papers in the series may be collectively considered Part I, with this paper Part II. The first four papers are experimental whereas this paper is conceptual. The first four papers deal with measurement of current whereas this paper deals with the reconstruction of voltage. If we consider the papers in terms of calculus, the first four papers deal with differentiation of the currents, whereas this paper deals with integration of the currents. The first four papers were submitted for publication on 24<sup>th</sup> October 1951 and published on 28<sup>th</sup> April 1952, whereas the final paper was submitted on 10<sup>th</sup> March 1952 and published on 28<sup>th</sup> August 1952. The reason for the delayed submission between Parts I and II will soon become apparent. When Hodgkin and Huxley concluded their acquisition of data from squid in Plymouth at the end of the summer season of 1949, they returned to Cambridge to carry out the analysis. In the era of ubiquitous desktop computers, it is difficult to appreciate the magnitude of the task that lay ahead of them. To analyse their data Hodgkin and Huxley projected their individual records onto a screen on which they superimposed a grid that delineated time and amplitude, from which they were able to make measurements. The fitting of curves required the additional complication of linear transformation of the data. In the descriptions of the experimental conditions under which data were acquired in the first four papers there are numerous references to the sub-optimal recording conditions, deterioration of axons or attenuation of the response over the course of the experiment. However, Hodgkin and Huxley could not simply carry out more experiments to acquire new data and expressed a pragmatic view of the data they had obtained. The annotation of individual axon numbers used in a particular experiment in Table and Figure legends allow an accurate estimate of the number of axons used in these studies, predominantly acquired in the summer of 1949. Although no dates are attached to the axons, we know that a total of 41 axons were notated, with good quality axons being used for multiple experimental protocols (e.g., no's 17, 18 and 41 were used in four of the five papers), but only two axons (no 31 and 38) were used in the description of inactivation of the Na<sup>+</sup> permeability pathway in Chapter 6. Some of the axons do not appear to contribute to any of the figures or tables (no's 1-10, 11, 16, 19, 22, 27, 29, 30, 32, 33, 35, 36, 40), implying that only 19 axons were used to provide data for the 5 papers.

## The computation process

This final paper has a well-earned reputation for being a challenging read. However, its most important distinction is that it won Hodgkin and Huxley the Nobel Prize, which would almost certainly not have occurred, had they only published the first four papers in the series. Indeed Huxley makes this distinction when discussing the contribution of Cole, and why Cole was not awarded the prize, concluding it was the detailed analysis of the data they carried out rather than its acquisition that was the deciding factor (Angel, 1996). What was so important about the analysis? By March of 1951 Hodgkin and Huxley had completed their derivation of the equations that described the voltage and time dependence of the conductances, the final step required to assess the predictive power of their model in comparison with experimentally acquired action potentials evoked by a variety of stimulus protocols. Their intention had been to use the EDSAC computer at the University of Cambridge in this endeavour, but it was under repair and unavailable for six months

(Hodgkin, 1992). This unfortunate situation was resolved when Huxley, in a truly monumental feat of both mental and physical prowess, decided to carry out the calculations on a Brunsviga calculator. This was a hand cranked mechanical machine that was operated by adjusting levers to appropriate positions to input numbers, then pulling a vertical lever to the horizontal to produce the result, followed by writing down of the result before proceeding to the next calculation (a video is available of the elderly Huxley demonstrating this process, while an engrossed Hodgkin looks on – see Resources Chapter 9). In his autobiography Hodgkin claims he would never have been able to carry out these calculations (Hodgkin, 1992) and it is staggering to consider that over the course of the computations it is estimated that Huxley carried out a million individual calculations (McComas, 2011). To give an idea of the sheer physical labour and mental concentration required, a space clamped axon took perhaps 8 hours to compute, but a propagated action potential took *three weeks*. In addition, any errors would have become embedded as a result of the sequential nature of the calculations, hence a complex method of forward and backward integration permitting error detection was employed to ensure accuracy. The level of resolution of the calculations was to six decimal places i.e.,  $\mu\text{V}$ . A large section of the paper is devoted to the integration process used but this is obsolete. Indeed, it is highly likely that Huxley was the only person to ever compute an action potential in this manner, and it is interesting to consider the review process of the paper. It is very obvious that given the six months between submission and publication that there was no scope for repeating Huxley's calculations, so although the process by which the reconstructions were carried out could be judged, the accuracy had to be taken on trust. However the subsequent development of computers led Cole to model a space clamped action potential (Cole *et al.*, 1955), providing extremely important independent verification of the accuracy of the Hodgkin-Huxley model. In 1964 Huxley with Frankenhauser used a computer to simulate an action potential verifying his original method (Frankenhaeuser & Huxley, 1964). The breathtaking speed of computer development meant that by the 1970s specialists could model action potentials (Fitzhugh, 1960; Noble, 1962; Cooley & Dodge, 1966; Goldman & Albus, 1968), and by the 1990s dedicated software had been developed with the sole purpose of modelling voltage and current clamp experiments, such as NEURON (Hines & Carnevale, 1997), GENESIS (Bower & Beeman, 1998) and HHsim among others, which are freely available and provide an accessible entry point for the novice to carry out reconstructions. Indeed this author demonstrated the capability to model a space clamped action potential in Microsoft Excel without the need for any programming knowledge (Brown, 2000).

## From experimental data to model

Before describing the model, it is instructive to note that Hodgkin and Huxley were interested in producing a mechanistic model of the permeability changes that underlay the action potential. They failed in this venture. They initially envisaged a carrier based mechanism for trans-membrane movement of ions, but when analysis of their data suggested that no viable mechanism could fit the data they compromised and produced a mathematical model with no underpinning mechanism, a decision that still rankled Hodgkin decades later (Hodgkin, 1992). Whereas Hodgkin and Huxley sought to reconstruct the membrane potential during an action potential they could not simply make measurements of the membrane potential to produce their model. Instead, they had to measure the membrane current of which there were 4 components, accurately analyse these currents, in the process devising the concept of gating particles in their analysis of  $I_{\text{Na}}$  and  $I_K$ , then use

## A companion guide to the Hodgkin-Huxley papers

integral calculus to quantify the effect of the simultaneous movement of these currents across the membrane on the membrane potential.

One intriguing aspect of the reconstructions was that Huxley started carrying these out in 1947, before they used the voltage clamp (Huxley, 2002). He modelled a  $\text{Na}^+$  current that inactivated, the  $\text{Na}^+$  movements were buffered by a  $\text{Na}^+$  pump, there was a lag in the  $\text{K}^+$  current, and  $E_K$  equalled the resting potential. Analysis of these simulations provided insight into potential mechanisms of the action potential and allowed fine-tuning of the voltage clamp experiments and analysis once these commenced in 1948. In describing the process by which Hodgkin and Huxley approached reconstruction of the action potential we can take a lead from Sterratt *et al.*, who describe in a logical and understandable manner, the sequence in which the Hodgkin-Huxley work was carried out (Sterratt *et al.*, 2011).

1. They recorded the current that flowed across the axon membrane over a wide range of membrane potentials using the voltage clamp technique. They were able to separate the current into its constituent parts by removing  $\text{Na}^+$  from the seawater bathing the axon, and by mathematically manipulating the current recorded under these conditions, separate the current into  $I_{\text{Na}}$  and  $I_K$ . They also quantified the Ohmic leak current that completed characterisation of the trans-membrane currents. This allowed them to represent the electrical properties of the axon membrane as an equivalent circuit (Fig 7.1), which showed that the current ( $I_m$ ) travelled through the membrane as capacitive current ( $C_M$ ) and ionic current ( $I_i$ ), where the ionic current was the sum of  $I_{\text{Na}}$ ,  $I_K$  and  $I_{\text{leak}}$ . This could be expressed algebraically as:

$$I_m = C_M \frac{dV}{dt} + I_i,$$

where

$$I_i = I_{\text{Na}} + I_K + I_{\text{leak}}$$

and

$$I_{\text{Na}} = g_{\text{Na}}(V - E_{\text{Na}})$$

$$I_K = g_K(V - E_K)$$

$$I_{\text{leak}} = g_{\text{leak}}(V - E_{\text{leak}})$$

2. The experimental records were then fit with curves to produce mathematical descriptions of  $g_{\text{Na}}$  and  $g_K$ . This involved introducing the concept of gating particles that controlled the permeability pathway. The model consisted of mathematical expressions, which combined to form a four-dimensional model comprising one non-linear differential equation

$$I_m = C_M \frac{dV}{dt} + \bar{g}_{\text{Na}} m^3 h (V - E_{\text{Na}}) + \bar{g}_K n^4 (V - E_K) + \bar{g}_{\text{leak}} (V - E_{\text{leak}}) \quad (\text{Eq. 7.1})$$

and the following three linear differential equations

$$\frac{dm}{dt} = \alpha_m(1 - m) - \beta_m m$$

$$\frac{dh}{dt} = \alpha_h(1 - h) - \beta_h h$$

$$\frac{dn}{dt} = \alpha_n(1 - n) - \beta_n n$$

3. Solving the equations to simulate the behaviour of the membrane potential. The model provided a satisfactory match of the experimental data.

In its simplest form the model may be considered as follows. The first four papers described acquisition of the raw electrophysiological data, which was processed to produce the mathematical description based on curve fitting of the membrane conductances. The model simply combined these conductances to reconstruct the action potential evoked in response to suitable stimuli.

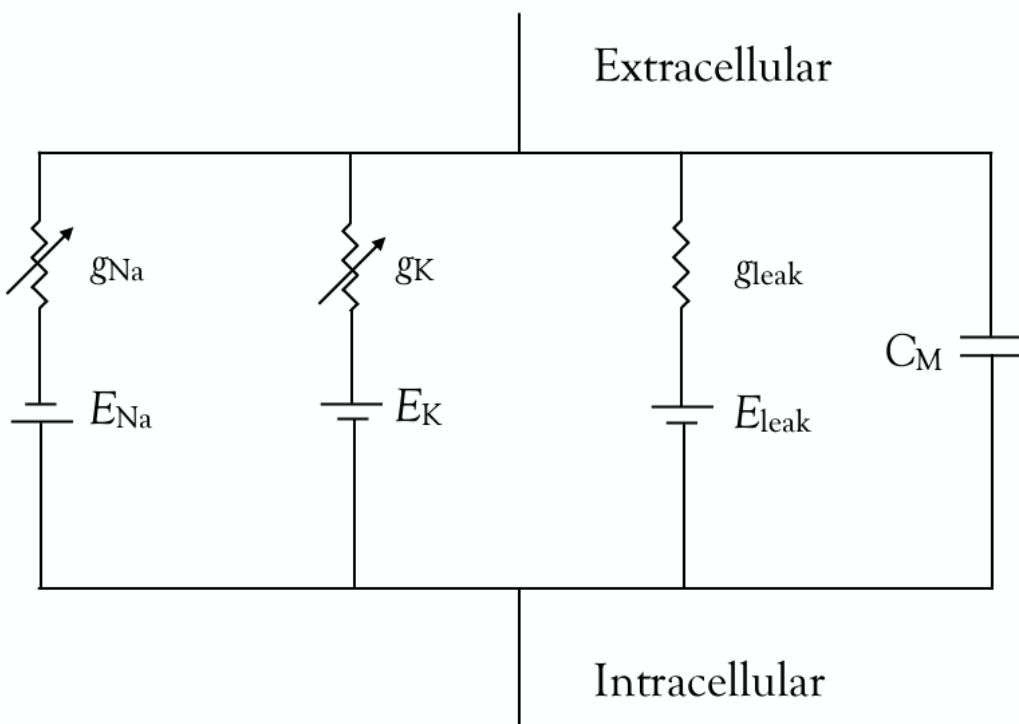


**Figure 7.1** - Equivalent circuit of the membrane current showing  $I_K$ ,  $I_{\text{Na}}$ ,  $I_{\text{leak}}$  and  $C_M$ .  $I_{\text{Na}}$  and  $I_K$  behave as variable resistors with the batteries representing the respective reversal potentials.

## The model

We shall start our description of the development of the model with the  $\text{K}^+$  conductance for the reasons that (a) it was simpler than the  $\text{Na}^+$  conductance, and (b) could be used to illuminate the more complex  $g_{\text{Na}}$ . The  $\text{K}^+$  conductance calculated in Chapter 4 displayed an intriguing time course. The rise of the conductance was sigmoidal in shape, but the fall on cessation of the depolarising pulse was a simple exponential. Hodgkin and Huxley sought to describe the conductance with a mathematical expression, but the delay in onset caused conceptual problems. It was at this point that Huxley suggested the idea of gating particles, an intuitive leap of true genius, a moment of divine inspiration that sealed their

reputations among the greats. It is instructive to make a comparison between the work of Hodgkin and Huxley, and Watson and Crick, who were working in Cambridge on another Nobel Prize winning idea at the same time as Hodgkin and Huxley carried out their reconstructions (Watson, 1968). Whereas Watson and Crick parachuted into an existing problem and solved it rapidly (Watson & Crick, 1953), had they not done so it is highly likely that others would have within a year (this is not to deny that their discovery changed the world in a way that Hodgkin and Huxley's did not). However, had Huxley not proposed gating particles would they ever have been proposed? One need only consult Cole's textbook to see the tail chasing that is inevitable in the absence of a robust hypothesis (Cole, 1968).

If we consult Eq. 7.1 the expressions for the  $\text{Na}^+$  and  $\text{K}^+$  currents are simply Ohm's law with the inclusion of letters associated with gating particles, thus the entire kinetic properties of the model are contained within these particles. These particles control the delay in the activation of the conductances, and their amplitude. The characteristics of the gating particles were developed based on the profile of the rise of  $g_K$ . This is sigmoidal in shape (Fig 7.2B), which is inconsistent with a simple exponential relationship. However if  $g_K$  is fitted with rising exponential relationships of the form  $(1 - e^{(-t/\tau_m)})^x$ , the curve approaches the experimental data best when  $x$  is increased to 4. Based on this information Hodgkin and Huxley proposed that there were 4 gating particles that controlled the movement of  $\text{K}^+$  ions through the membrane. Each gating particle was independent, but was controlled by membrane potential, and all 4 gating particles were required to be in the permissive or open state for the  $\text{K}^+$  permeability pathway to open.

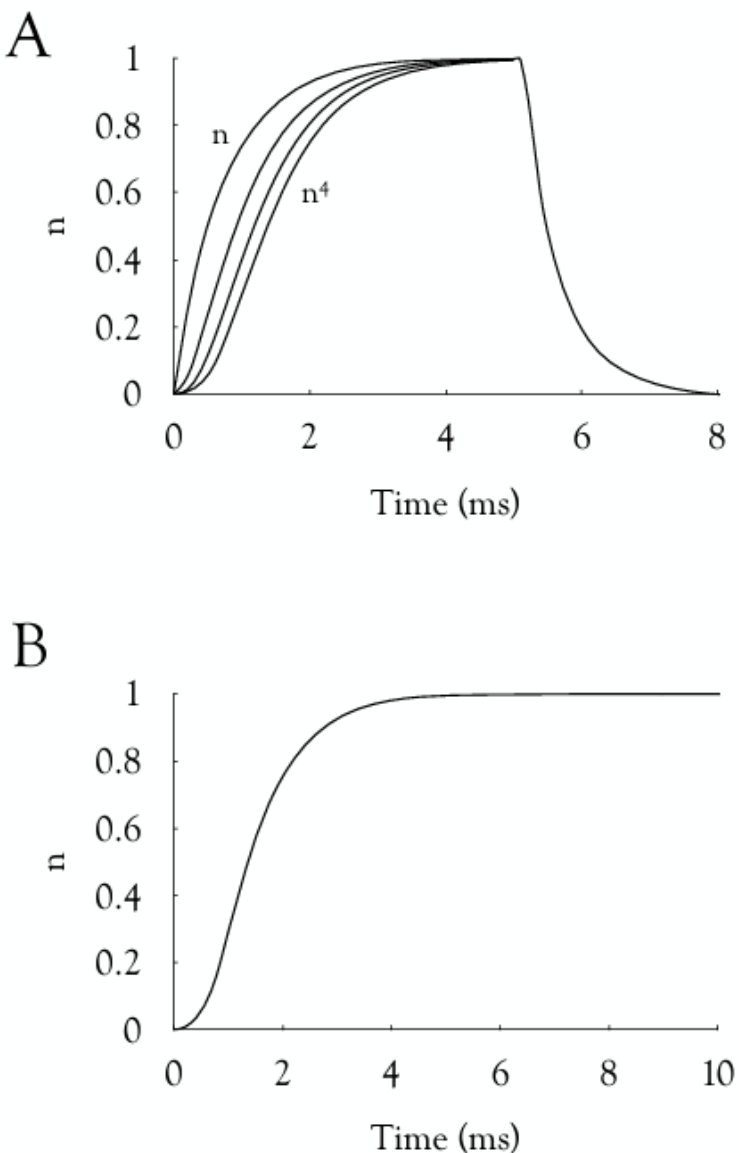


**Figure 7.2 - The gating particle for  $g_K$ .** A. The best fit for the rising phase of  $g_K$  was  $n^4$ . The alternate powers of  $n$  are shown. On repolarising  $g_K$  falls along a single exponential curve. B. On stepping from rest to a depolarised potential  $g_K$  follows a sigmoidal rise before flattening, which is modelled as  $g_\infty$  (Eq. 7.5).

### Probability theory applied to the gating particles

This introduces the concept of probability, which can be illustrated by a classic example involving playing cards. Let's assume that we want to calculate the probability that a card randomly drawn from a shuffled deck will be a Queen and a Heart. The theory of joint probability is applied when calculating the probability of two or more occurrences happening at the same time, and the probability can be calculated using the multiplication theorem (De Muth, 2006). The probability of a Heart,  $p(A)$ , occurring or the probability of a

Queen,  $p(B)$ , occurring, are independent, and therefore the probability of drawing a Queen can be expressed as:

$$p(A) = 1/13$$

and the probability of drawing a Heart is

$$p(B) = 1/4$$

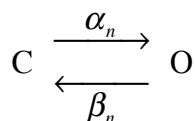
The probability of a card being a Queen and a Heart is

$$p(A \cap B) = p(A) \times p(B) = 1/13 \times 1/4 = 1/52$$

Applying this theory to the probability that all four gating particles will be in the permissive state allowing  $K^+$  ions to cross the membrane was

$$p(n \cap n \cap n \cap n) = n \times n \times n \times n = n^4.$$

Thus, the  $K^+$  conductance at any membrane potential could be expressed as  $g_K = \bar{g}_K n^4$ , where  $\bar{g}_K$  was the maximum  $g_K$ , which was measured at a depolarisation to 35 mV. The behaviour of  $g_K$ , during depolarisation and repolarisation, fitted the behaviour of a model in which four particles must all simultaneously be in the permissive state in order for the permeability pathway to open. If we next assume that the movement of the particles was a 1<sup>st</sup> order reaction and thus proportional to the concentration of the particles, then the time course of the permeability increase on stepping to a new voltage was  $n^4$ . However, only one of the particles was required to move from permissive to non-permissive for the path to close, thus the conductance decays along a single exponential, described by  $e^{(-t/\tau_n)}$ . We assume that any  $n$  particle moved between a permissive (open) and a non-permissive (closed) state, which could be described as



where O corresponded to the fraction of particles in the open state,  $n$ , and C was the fraction of particles in the closed state ( $1 - n$ ).  $n$  varies between 0 and 1, and where  $n = 1$  all particles were in the permissive state. The movement of the particles between the two states could be expressed as the 1<sup>st</sup> order kinetic equation

$$\frac{dn}{dt} = \alpha_n(1 - n) - \beta_n n \quad (\text{Eq. 7.2})$$

### Calculation of rate constants

This relationship stated that the rate at which the value of  $n$  increased was the rate at which the particle moved from the closed to the open state minus the rate at which the particle moved from the open to the closed state i.e., if the particles could only be in one of two states, then the number of particles in one state is equal to the total number of particles minus the number of particles in the other state. The rate at which the particles moved from closed to open was described by the rate constant  $\alpha_n$ , and  $\beta_n$  described the rate at which the particle moved from open to closed. The units of the rate constant were msec<sup>-1</sup>, which defined how many transitions between closed and open ( $\alpha_n$ ) and between open and closed ( $\beta_n$ ) occurred each millisecond. Thus, the main mathematical aspect of the analysis of the

## A companion guide to the Hodgkin-Huxley papers

experimental data was trying to find continuous functions of voltage to describe the effect of membrane potential on the rate constants. Knowledge of calculus was invaluable in this task. Students do not need to understand calculus to appreciate what Hodgkin and Huxley did and I will proceed without any undue explanation of the underlying mathematical processes.

The relationship in Eq. 7.2 could also be expressed as

$$\frac{dn}{dt} = \frac{n_\infty + n_0}{\tau_n}$$

where

$$\tau_n = \frac{1}{\alpha_n + \beta_n} \quad (\text{Eq. 7.3})$$

and

$$n_\infty = \frac{\alpha_n}{\alpha_n + \beta_n} \quad (\text{Eq. 7.4})$$

where  $n_\infty$  denoted the steady state value of  $n$  at a new potential,  $n_0$  denoted the steady state value of  $n$  at the original potential and  $\tau_n$  denoted the time constant for the transition from  $n_0$  to  $n_\infty$ . Upon stepping from one voltage to another as illustrated in Fig 7.2B, the time course of the change in conductance could be expressed as

$$g_K = \left[ \left( g_\infty^{\frac{1}{4}} - \left( g_\infty^{\frac{1}{4}} - g_0^{\frac{1}{4}} \right) e^{\left( \frac{-t}{\tau_n} \right)} \right) \right]^4 \quad (\text{Eq. 7.5})$$

where  $g_\infty$  was the value of  $g_K$  at the new voltage,  $g_0$  was the value of  $g_K$  at the original voltage, and  $\tau_n$  was the time constant of the transition of  $n$  to a new value at the new potential. Based on these relationships Hodgkin and Huxley had the data required to calculate  $\alpha_n$  and  $\beta_n$ . Since  $g_K = \bar{g}_K n^4$  it followed that

$$n_\infty = \sqrt[4]{\left( \frac{g_K}{\bar{g}_K} \right)} \quad (\text{Eq. 7.6})$$

thus measurement of the amplitude of  $g_K$  in the steady state i.e., where  $g_K$  asymptoted towards the end of voltage step of appropriate duration, and knowing the maximum value of  $\bar{g}_K$  gave the value of  $n_\infty$ . The relationship illustrated in Fig 4.4A, which plots the normalised  $g_K$  versus membrane potential, could be used to calculate the value of  $n$  according to Eq. 7.6. Fitting the time course of the conductance upon stepping to a new voltage gave the value of  $\tau_n$ . Based on the Eq. 7.3 and Eq. 7.4 it followed that expressions relating  $\alpha_n$  or  $\beta_n$  to  $\tau_n$  and  $n_\infty$  could be derived as follows:

$$\alpha_n + \beta_n = \frac{1}{\tau_n} \rightarrow n_\infty = \frac{\alpha_n}{\frac{1}{\tau_n}} \rightarrow n_\infty = \alpha_n \tau_n \rightarrow \alpha_n = \frac{n_\infty}{\tau_n}$$

and

$$\alpha_n + \beta_n = \frac{\alpha_n}{n_\infty} \rightarrow \beta_n = \frac{\alpha_n}{n_\infty} - \alpha_n \rightarrow \beta_n = \frac{\alpha_n}{n_\infty} - \frac{n_\infty}{\tau_n} \rightarrow \beta_n = \frac{\alpha_n}{\frac{\alpha_n}{\alpha_n + \beta_n} - \frac{n_\infty}{\tau_n}}$$

$$\beta_n = \frac{\alpha_n^2 + \alpha_n \beta_n}{\alpha_n} - \frac{n_\infty}{\tau_n} \rightarrow \beta_n = \alpha_n + \beta_n - \frac{n_\infty}{\tau_n} \rightarrow \beta_n = \frac{1}{\tau_n} - \frac{n_\infty}{\tau_n} \rightarrow \beta_n = \frac{(1 - n_\infty)}{\tau_n}$$

These rearrangements allowed values for  $\alpha_n$  and  $\beta_n$  to be calculated from experimentally measured values of  $n_\infty$  and  $\tau_n$ . From the data analysed and summarised in *Table 1* the following continuous expressions relative to membrane potential were obtained by curve fitting.

$$\alpha_n = 0.01 \frac{(V+55)}{1 - e^{(\frac{-(V+55)}{10})}} \quad (\text{Eq. 7.7})$$

and

$$\beta_n = 0.0555 e^{(\frac{-V}{80})} \quad (\text{Eq. 7.8})$$

The voltage dependence of these rate constants is shown in Fig 7.3A. The value of  $n$  could be estimated from experimental results where  $n$  was calculated from Eq. 7.6 based on records of  $g_K$  as shown in *Figure 3* or calculated from Eq. 7.4 from the rate constants (Fig 7.3B).

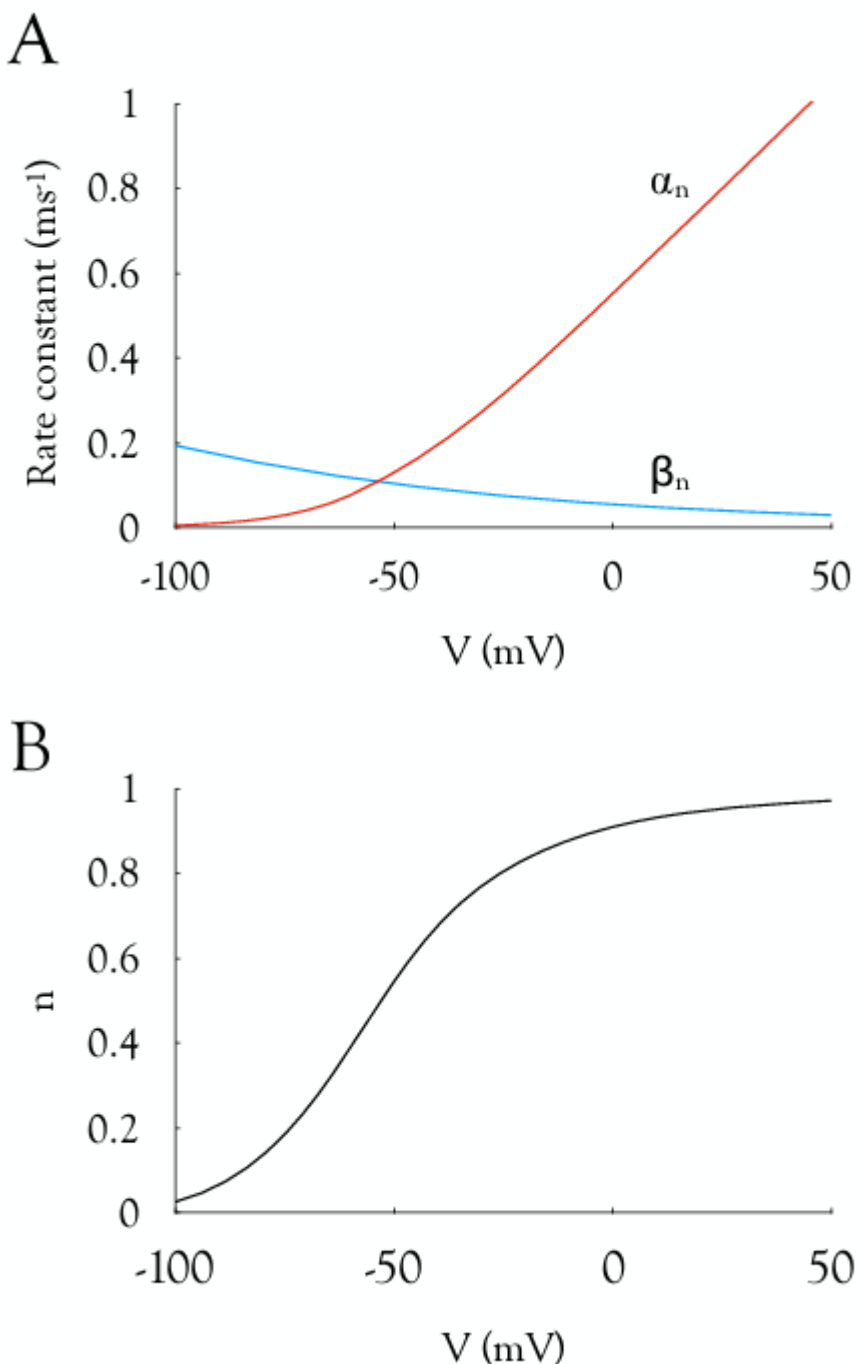


**Figure 7.3 - Rate constants for  $n$ .** A. The continuous functions describing  $\alpha_n$  (red trace) and  $\beta_n$  (blue trace) are plotted versus voltage. The fits are described by Eq. 7.7 and 7.8, respectively. B.  $n$  increases in a sigmoidal fashion on depolarising the membrane potential.  $n$  is calculated for experimental data according to Eq. 7.6 or based on the rate constants according to Eq. 7.4.

More complete accounts of this analysis are available (Aidley, 1996; Fain, 1999; Koch, 1999; Hille, 2001; Byrne & Roberts, 2009; Sterratt *et al.*, 2011; Raman & Ferster, 2021).

An equivalent process was carried out for the  $\text{Na}^+$  conductance with the exception that in addition to an activation gating particle,  $m$ , an inactivation particle,  $h$ , was introduced, where  $m$  was an equivalent particle to  $n$ , but  $h$  controlled the inactivation process of closing the  $\text{Na}^+$  permeability pathway. Based on the probability theory described above the rising then falling profile of  $g_{\text{Na}}$  was described according to  $m^3h$ , where the activation particle was raised to the power 3 (compared to 4 for the  $n$  particle) and the inactivation particle was raised to the power 1. The rising and falling shape of  $g_{\text{Na}}$  was fit by the equation

$$g_{\text{Na}} = \left(1 - e^{\left(\frac{-t}{\tau_m}\right)}\right)^3 e^{\left(\frac{-t}{\tau_h}\right)} \quad (\text{Eq.7.9})$$

This is graphically illustrated in Fig 7.4.

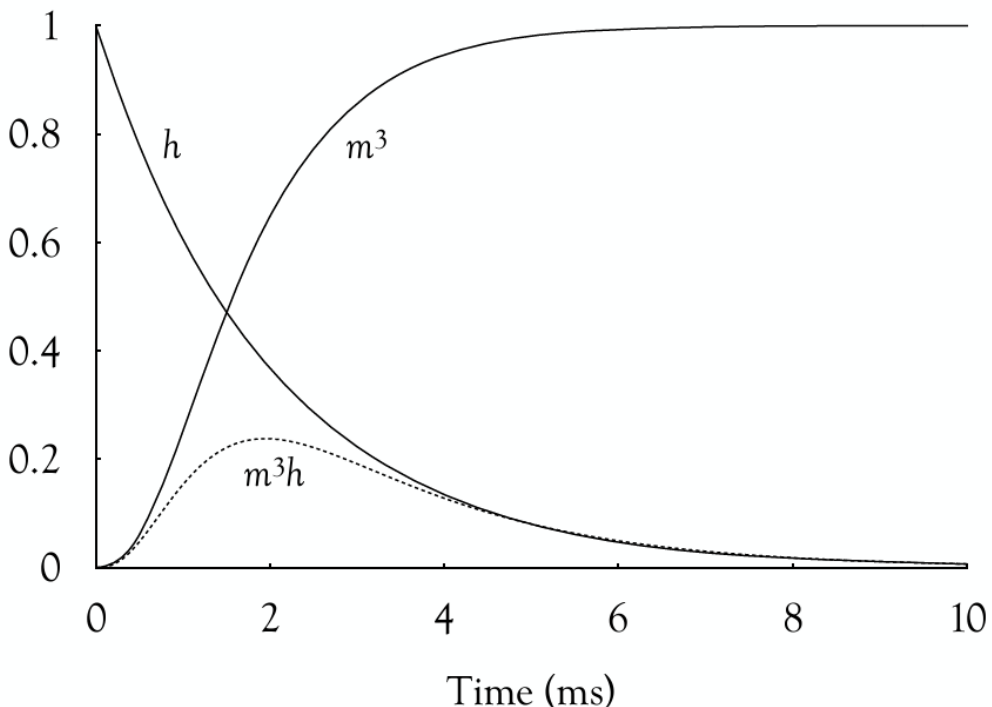


**Figure 7.4** - Gating particles governing  $g_{\text{Na}}$ . Plots of the activation particle  $m^3$  and inactivation particle  $h$ . The product of these particles,  $m^3h$ , shows a delayed rising then falling phase according to Eq. 7.9.

An equivalent mathematical approach to that described for  $g_K$  was applied to the  $g_{\text{Na}}$  data to derive the rate constants for  $\alpha_m$  and  $\beta_m$ . As illustrated in Fig 7.4 a complication arose in that inactivation prevented the value of  $g_{\text{Na}}$  reaching its maximum value according to  $m^3$ , thus Hodgkin and Huxley fit the data by assuming that the value of  $h$  was fixed at 1, such that  $g_{\text{Na}}$  in the absence of inactivation was

$g_{\text{Na}} = \bar{g}_{\text{Na}} \left(1 - e^{\left(\frac{-t}{\tau_m}\right)}\right)^3$  as illustrated in Fig 7.4. Once this was complete, they incorporated  $h$ , which allowed them to fit curves to define the value of  $\tau_h$ . In this manner they were able

to obtain values for  $\alpha_m$ ,  $\beta_m$ ,  $\alpha_h$  and  $\beta_h$ , from which they could calculate  $\tau_m$   $\tau_h$ ,  $m_\infty$  and  $h_\infty$ , using Eq. 7.3 and 7.4, expressed for  $m$  and  $h$  (Fig 7.5A & C). The value for  $m$  could be estimated from experimental records of  $g_{Na}$ , based on a similar method to that used to calculate  $n$  for  $g_K$ . Alternatively,  $m$  could be calculated from the equivalent relationship to Eq. 7.4 expressed for  $m$  (Fig 7.5B). As described in Chapter 6, Hodgkin and Huxley had carried out experiments using double pulse protocols to independently measure the values of  $h_\infty$  and  $\tau_h$ . The value for  $h_\infty$  was measured based on the pre-pulse experiments shown in *Figure 4*, (Hodgkin & Huxley, 1952c), which revealed a sigmoidal shape of  $h_\infty$  relative to membrane potential.  $h_\infty$  could also be calculated based on Eq. 7.4 expressed for  $h$ , which provided a very good match (Fig 7.5B) when overlaid on the experimental data summarised in *Table 1* (Hodgkin & Huxley, 1952c). These experiments involved stepping to a conditioning voltage for a variety of durations, followed by a test pulse to a depolarised voltage that elicited a large  $I_{Na}$ . If the ratio of the  $I_{Na}$  in the absence of the conditioning pulse was compared to the  $I_{Na}$  evoked following the conditioning pulse, and plotted against the duration of the conditioning pulse, a smooth curve was obtained for that particular conditioning potential. The time constant could be obtained by fitting a single exponential curve. In this manner the time constants for a series of conditioning voltages could be estimated. Plotting these values versus the membrane potential produced an  $n$  shaped relationship that was accurately described by Eq. 7.3 expressed for  $h$  (Fig 7.11C). The rate constants were derived as

$$\alpha_m = \frac{0.1(V+40)}{1-e\left(\frac{-V+40}{10}\right)} \quad (\text{Eq.7.9})$$

$$\beta_m = 0.108e\left(\frac{-V}{18}\right) \quad (\text{Eq.7.10})$$

$$\alpha_h = 0.0027e\left(\frac{-V}{20}\right) \quad (\text{Eq.7.11})$$

$$\beta_h = \frac{1}{1-e\left(\frac{-V+35}{10}\right)} \quad (\text{Eq.7.12})$$

and are displayed in Figs 7.5A and C.

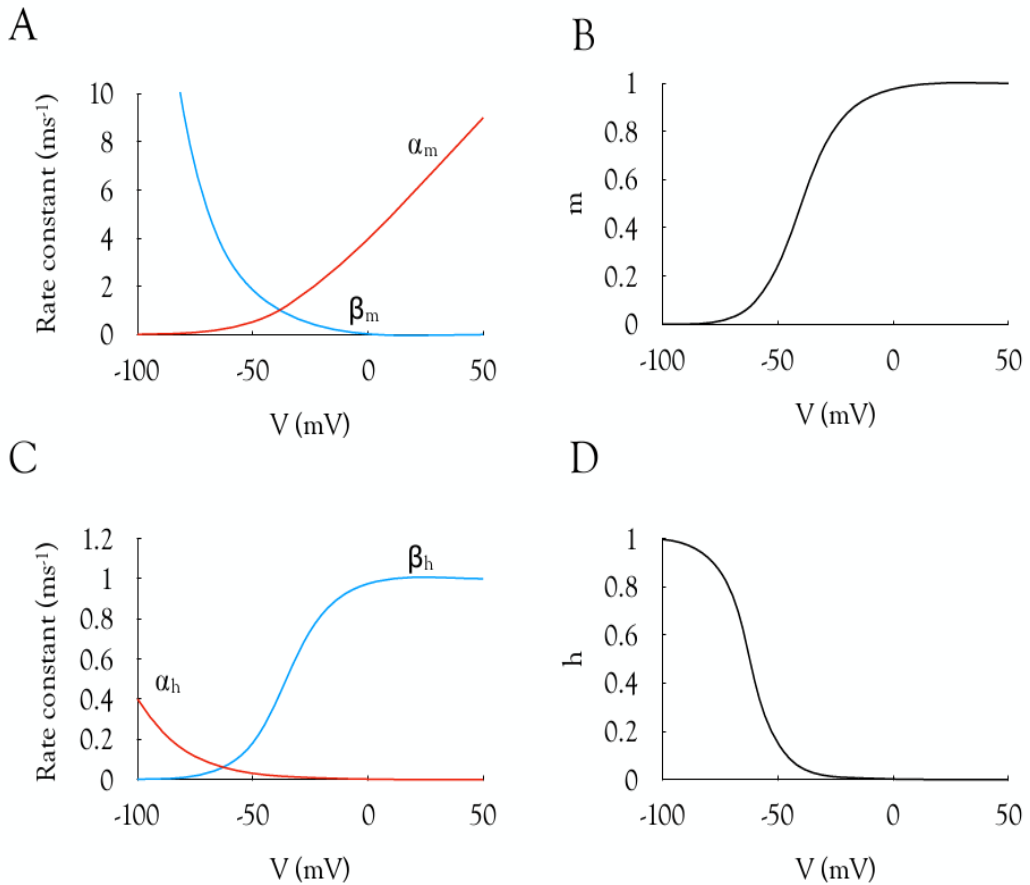


**Figure 7.5** - Rate constants for  $I_{Na}$ . A.  $\alpha_m$  (red trace) and  $\beta_m$  (blue trace), and (C)  $\alpha_h$  (red trace) and  $\beta_h$  (blue trace) are plotted versus membrane potential according to Eq. 7.9, and 7.10, and Eq. 7.11 and 7.12, respectively. B and D.  $m$  and  $h$ , respectively, plotted versus membrane potential.

## The complete model

The complete Hodgkin-Huxley model comprised the following non-linear differential equation

$$I_m = C_M \frac{dV}{dt} + \bar{g}_{Na} m^3 h (V - E_{Na}) + \bar{g}_K n^4 (V - E_K) + \bar{g}_{leak} (V - E_{leak})$$

and the following three linear differential equations

$$\frac{dm}{dt} = \alpha_m (1 - m) - \beta_m m$$

$$\frac{dh}{dt} = \alpha_h (1 - h) - \beta_h h$$

$$\frac{dn}{dt} = \alpha_n (1 - n) - \beta_n n$$

where the rate constants (Eq. 7.9 to 7.12) were continuous functions of voltage. The constants required to complete the model were

$$C_M = 1 \mu\text{F cm}^{-2}$$

$$E_{Na} = 50 \text{ mV}$$

$$E_K = -77 \text{ mV}$$

$$E_{leak} = -54.4 \text{ mV}$$

$$\bar{g}_{Na} = 120 \text{ mS cm}^{-2}$$

$$\bar{g}_K = 36 \text{ mS cm}^{-2}$$

$$\bar{g}_{leak} = 0.3 \text{ mS cm}^{-2}$$

## Action potential reconstruction

The second part of the paper involved calculating the response of the membrane potential to a variety of stimuli. The calculation was based on the following reasoning. According to Eq. 7.1 if  $I_m$  was known then  $V$  could be calculated by integration of the sum of the membrane currents. This process can be readily understood if we sequentially list each calculation carried out in order. The first step involved selecting an appropriate membrane potential for the axon i.e.,  $V_1$

Calculate  $\alpha_m$ ,  $\beta_m$ ,  $\alpha_h$ ,  $\beta_h$ ,  $\alpha_n$  and  $\beta_n$  for  $V_1$

Calculate  $m$  as  $\alpha_m / (\alpha_m + \beta_m)$

Calculate  $h$  as  $\alpha_h / (\alpha_h + \beta_h)$

Calculate  $n$  as  $\alpha_n / (\alpha_n + \beta_n)$

Calculate  $g_{Na}$  as  $120m^3h$ ,

Calculate  $g_K$  as  $36n^4$

Calculate  $I_{Na}$  as  $g_{Na}(V_1 - E_{Na})$

Calculate  $I_K$  as  $g_K(V_1 - E_K)$

Calculate  $I_{leak}$  as  $g_{leak}(V_1 - E_{leak})$

Input stimulating current as  $I_{inj}$

Calculate the total current as  $I_{Na} + I_K + I_{leak} + I_{inj}$

Enter  $C_M$

Integrate the total currents to calculate new voltage  $V_2$

Loop to start and repeat for  $V_2$  as voltage etc.

Repeat for the duration of the simulation. The time step was 0.01 ms at the start of the action potential and 0.02 ms during the rising phase of the action potential.

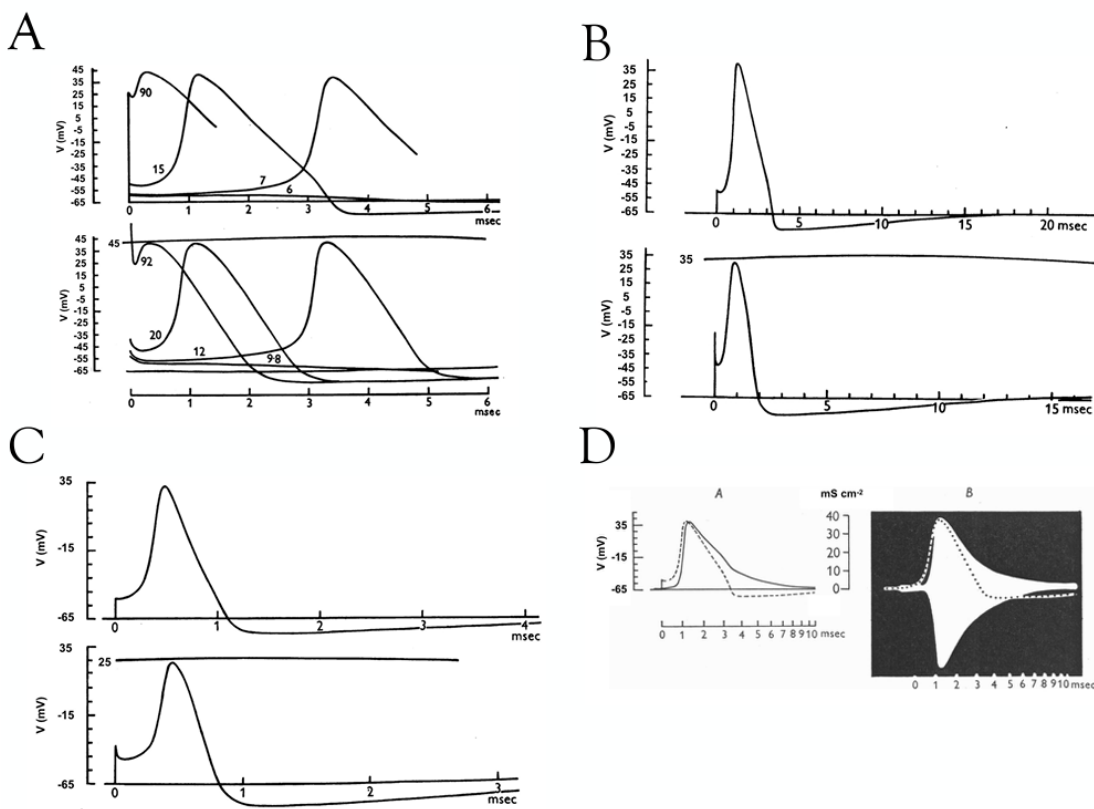


**Figure 7.6** - Reconstructions of the space clamped action potential in response to brief shocks. A. Action potentials evoked by stimulus of varying intensities (upper) are a good match for experimental records of equivalent stimuli (lower traces). B. Longer duration reconstructions of the action potential show the AHP is a good match for the experimental data. C. Simulations and experiment carried out at 18°C are comparable with experimental data. D. Plot of total conductance superimposed on a record of an action potential is a good representation of the classic Cole image measured experimentally (Cole & Curtis, 1949).

The first set of simulations may be grouped together (Figures 12, 13, 14, 16) and described action potentials evoked from rest by brief shocks (Fig 7.6). Figure 7.6A illustrates a comparison of the computed action potentials from Eq. 7.1 evoked by three stimuli of increasing strength by varying the value of  $I_{inj}$  in the model, compared with experimental records of action potentials evoked by equivalent stimuli. The simulation matched closely the experimental action potential in profile, magnitude, threshold, and time course. The model also reproduced a key aspect of the experiments in that once evoked the action potentials shared the same profile, a rapid depolarisation followed by a slower repolarisation beyond rest, the AHP. An indication of the labour involved in reconstructing the action potential is evident from Huxley's decision to truncate two of the reconstructed action potential mid-way through the repolarising phase on account of the similarity of this phase with the one completed action potential. The simulation of the AHP, which had a longer duration than the action potential, was also a close match to the experimental data (Fig 7.6B). Accounting for a temperature of 18°C, by using the  $Q_{10}$  value described in Chapter 3, reproduced an accurate action potential (Fig 7.6C) and in an act of homage, confirmation or simply completing the circle, the superimposition of the total conductance on an action

potential reproduced Cole's famous impedance image that so excited Hodgkin over a decade before (Fig 7.6D). These simulations model a space clamped axon in which the membrane potential is uniform across the entire axon.

## Propagated action potential

The next simulation was of a propagated action potential where the membrane was not clamped, and the action potential propagated along the length of the axon using local circuits. This process was described by

$$I_m = C_M \frac{dV}{dt} + \bar{g}_{Na} m^3 h(V - E_{Na}) + \bar{g}_K n^4 (V - E_K) + \bar{g}_{leak}(V - E_{leak}) + \frac{d}{4R_a} \frac{\partial^2 V}{\partial x^2}$$

(Eq. 7.13)

where  $R_a$  was the axoplasmic resistance,  $d$  was the axon diameter and  $x$  was the distance travelled along the axon. This was a far more complex procedure, as it required calculation of  $V$  sequentially along the axon in small increments as the propagation of the axial current excited neighbouring regions. This process took three weeks to complete, but was rewarded with an accurate representation of the action potential profile and AHP, and an astonishingly accurate estimate of conduction velocity relative to that calculated experimentally:  $18.8 \text{ ms}^{-1}$  versus  $21.2 \text{ ms}^{-1}$  (Fig 7.7), according to Cronin the most impressive aspect of the reconstructions (Cronin, 1987).

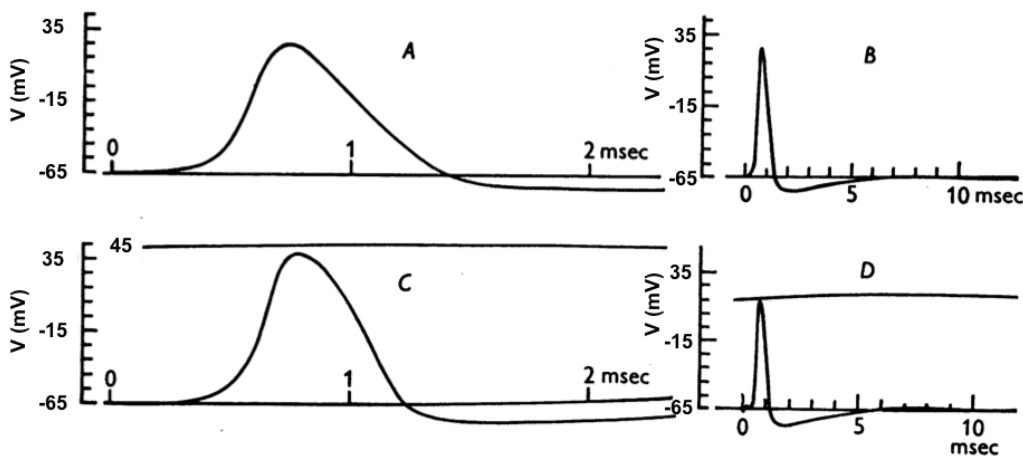


**Figure 7.7 - Propagated action potential.** The reconstructed propagated action potential (upper) is a good match for the experimental record (lower) showing similar properties of depolarisation, repolarisation, AHP and conduction velocity.

## Ion conductances

The ability to superimpose the individual conductances on the action potential allowed for demonstration of several important points. The first was that  $g_{Na}$  did not start to

rise until the membrane potential was significantly depolarised, evidence of the role of local circuits in bringing the membrane potential to threshold, revisiting the results in Hodgkin's first paper (Hodgkin, 1937a). Threshold was not the potential at which  $I_{Na}$  was activated, but rather the potential at which  $I_{Na}$  exceeded  $I_K$ . The peak  $g_{Na}$  coincided with the peak of the action potential and the rise of  $g_K$  was later than  $g_{Na}$  due to the difference in the time constants for activation relative to  $g_K$  (Fig 7.11C). The  $g_K$  maintained significant amplitude when  $g_{Na}$  had returned to zero, explaining the presence of the AHP, whose decline mirrored the fall of  $g_K$  (Fig 7.8A).

In addition to resolving the individual conductances underlying the action potential the components of the membrane currents were also resolved. The time course of  $I_K$  and  $I_{Na}$  were consistent with  $g_{Na}$  and  $g_K$  i.e.,  $g_K$  and  $I_K$  were delayed relative to  $g_{Na}$  and  $I_{Na}$ , where  $I_{Na}$  displayed a small notch due to the repolarisation of the action potential increasing the driving force, as the membrane potential moved away from  $E_{Na}$  whilst the  $\text{Na}^+$  permeability path was still open, hence a transient increase in the current that soon fell as the  $\text{Na}^+$  permeability pathway inactivated (Fig 7.8B). In this manner the model was shown to accurately reproduce key aspects of space clamped and propagating action potentials with regard to stimulus intensity and temperature sensitivity.

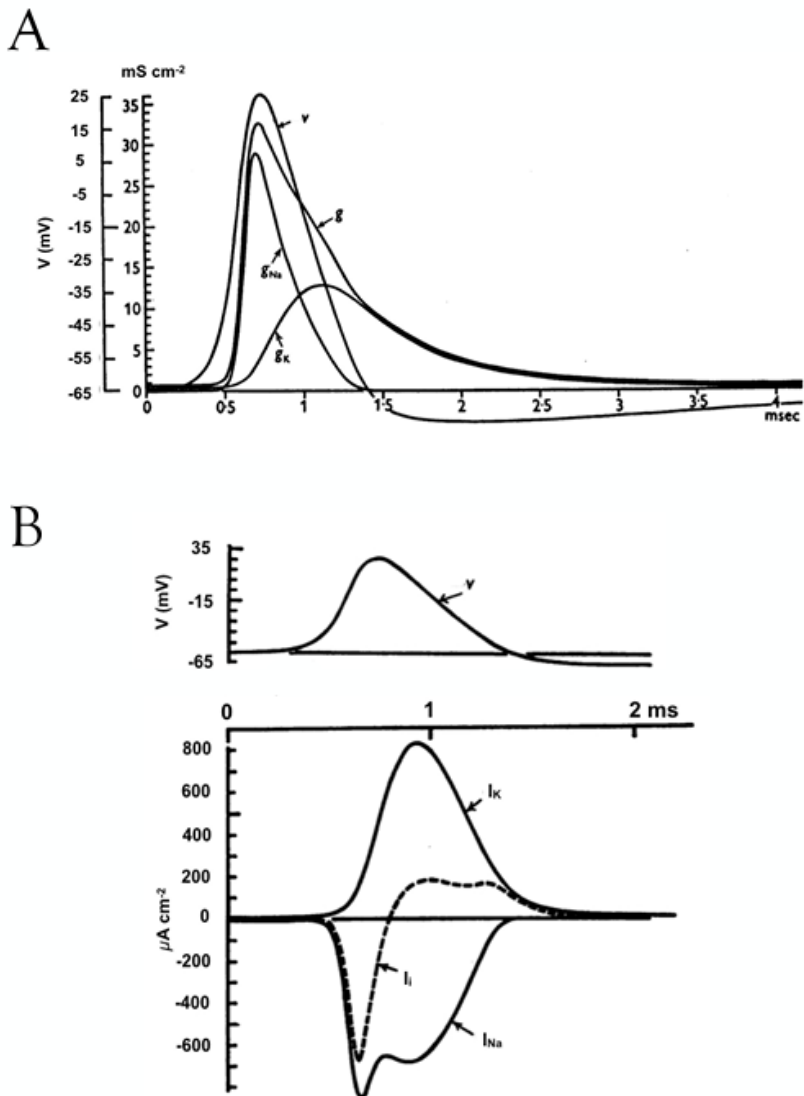
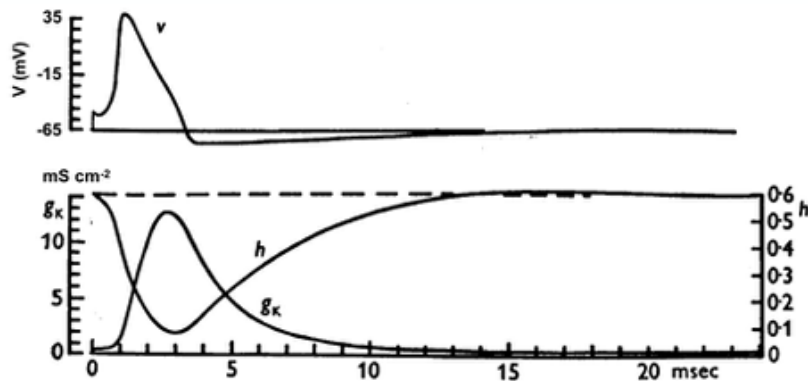


**Figure 7.8** - Conductance and currents underlying the action potential. A. The time course of  $g_{Na}$  and  $g_K$  overlying the action potential show the rise of  $g_{Na}$  and delayed fall in  $g_K$  produce the AHP. B.  $I_{Na}$  and  $I_K$ , with  $I_{Na}$  showing a notch where sudden increase in driving force temporarily increases  $I_{Na}$ .

The next phase of their reconstructions demonstrated the advantages of modelling, where behaviour of the membrane potential was explained based on data derived from the model, which could not itself be experimentally demonstrated e.g., gating particles. In the first part of this paper Hodgkin and Huxley described the conductances underlying the membrane current in terms of activation and inactivation (for  $g_{Na}$ ), but modelling allowed for their roles in governing activity to be demonstrated. For example, the phenomenon of the refractory period was adequately explained from the point of view of inactivation and  $g_K$ . This concept could be executed in the squid axon by determining the response of the axon to two stimuli, the first of which evoked an action potential, and the second of which could be varied in amplitude and latency. Examining the underlying conductances and gating particles offered a ready explanation for the behaviour.

A



B

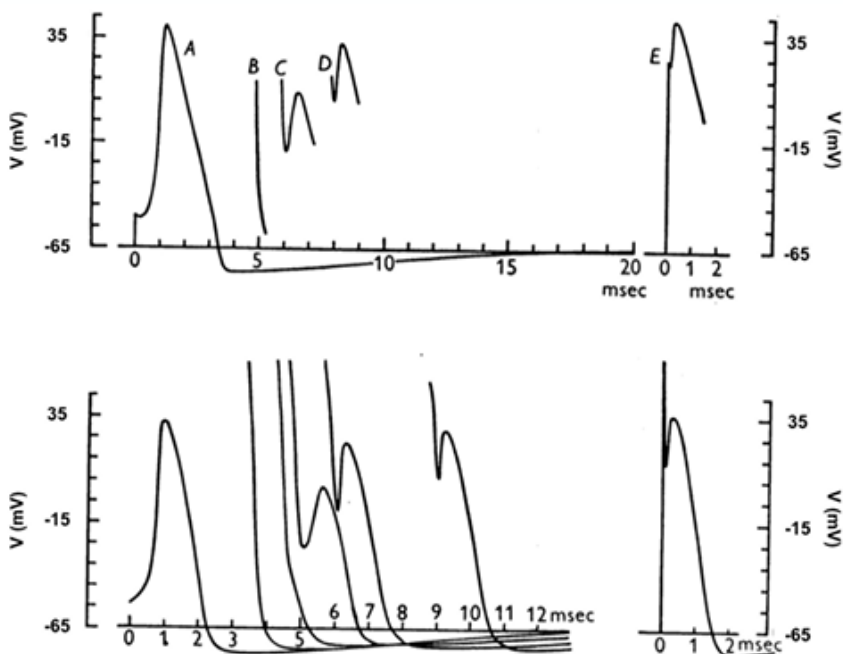


**Figure 7.9 - Refractory period.** A. Stimulus evoked action potential with  $g_{Na}$  and  $h$ , showing delay in  $g_K$  returning to rest after the action potential, and  $h$  is close to zero following the action potential. B. Reconstruction of the action potential (upper) where the second shock follows the first with varying latency. During the relative refractory period small action potentials can be evoked if the shock intensity is increased.

### Refractory period

The two factors that controlled the generation of the subsequent spike were  $g_K$  and  $h$ . Figure 7.9A displays an action potential evoked from rest at 6°C by a depolarisation of 15 mV, with the underlying  $g_K$  and the state of the gating particle  $h$ , superimposed on the same time scale. Since  $h$  had been quantified it provided vital information as to the degree by

which  $h$  had to fall in order to prevent an action potential from firing. Remember  $h$  is the probability of the  $\text{Na}^+$  permeability pathway not being inactivated, where  $(1 - h)$  denoted the fraction of the system that was inactivated, so low values of  $h$  were correlated with a large fraction of inactivation. The value of  $h$  at rest was 0.6, which was comparable with a membrane potential of -65 mV in *Figure 10*, thus this was a value of  $h$  that was consistent with action potential firing. As previously shown the activation of  $g_K$  lagged the action potential depolarisation, but once activated stayed open for over 10 ms. Exactly what the limits were in recruiting a subsequent action potential was investigated by modelling the action potential evoked by a subsequent stimulus at a defined latency after the first. Figure 7.9B shows that a delay of 5 ms evoked no action potential, which corresponded to an  $h$  value of about 0.25. A delay of 6 ms evoked an action potential but the peak was attenuated (Fig 7.9B). Thus, at the latency of 6 ms where  $h$  was approximately 0.35 and  $g_K$  was 3 mS cm<sup>-2</sup> threshold is reached. It is important to realise that at these short intervals the stimulus occurred during the AHP when  $g_K$  exceeded its resting level. However, for intervals of up to 10 ms the second action potential was smaller than the first, which was an indication of a decrease in the number of available  $\text{Na}^+$  permeability pathways i.e., decreased  $\text{Na}^+$  conductance, since the trans-membrane concentration of  $\text{Na}^+$  ions were unchanged, thus  $E_{\text{Na}}$  was in the vicinity of 50 mV. In data derived from a model of squid axon (Brown, 2000) the conductances can be viewed more clearly than in the Hodgkin and Huxley paper, by superimposing values of  $g_K$  and  $h$  on the action potential (Fig 7.10A). A single pulse evoked an action potential, which showed the fall of  $h$  towards 0 and delayed rise in  $g_K$ . Imposing a second stimulus of the same amplitude failed to evoke a second action potential, as  $h$  was still at a low value and  $g_K$  was still activated. However, an action potential could be evoked if the amplitude of the second stimulus was increased in order to overcome the hyperpolarising effect of  $g_K$ , although the action potential was smaller.  $\text{Na}_{i/o}$  have not changed, thus the  $E_{\text{Na}}$  remained about 50 mV, but the action potential did not approach  $E_{\text{Na}}$  as there are limited permeability pathways available, as demonstrated by the attenuated value of  $g_{\text{Na}}$  associated with the second action potential (Fig 7.10B). The absolute refractory period refers to the process where no stimulus, however large, was capable of evoking an action potential, and this corresponded to small values of  $h$  and large values of  $g_K$ . The relative refractory period referred to the ability to evoke a subsequent action potential, but its amplitude was smaller and larger stimulus pulses were required (Fig 7.10B). However, the large stimulus currents shown in Fig 7.10C were un-physiological, so under physiological conditions the absolute refractory period extended into the hypothetical relative refractory period, where increased stimuli were required to counteract the large  $g_K$  present during the AHP. The  $\text{Na}^+$  permeability pathway inactivation was solely responsible for the absolute refractory period, as there were few available  $\text{Na}^+$  permeability pathways to carry the  $\text{Na}^+$  current. The relative refractory period was a product of decreasing  $g_K$  and increasing  $h$ . As such the absolute refractory period controls the maximum firing frequency. The brain processes incoming sensory information via frequency encoding in which the firing frequency is related to the magnitude of the stimulus, and the refractory period plays a vital role in how this information is transmitted. For example, increased pressure will cause mechanoreceptors to fire at higher frequency, and higher pitches will cause increased firing frequency in cochlear nerve fibres (Kandel *et al.*, 2013b).

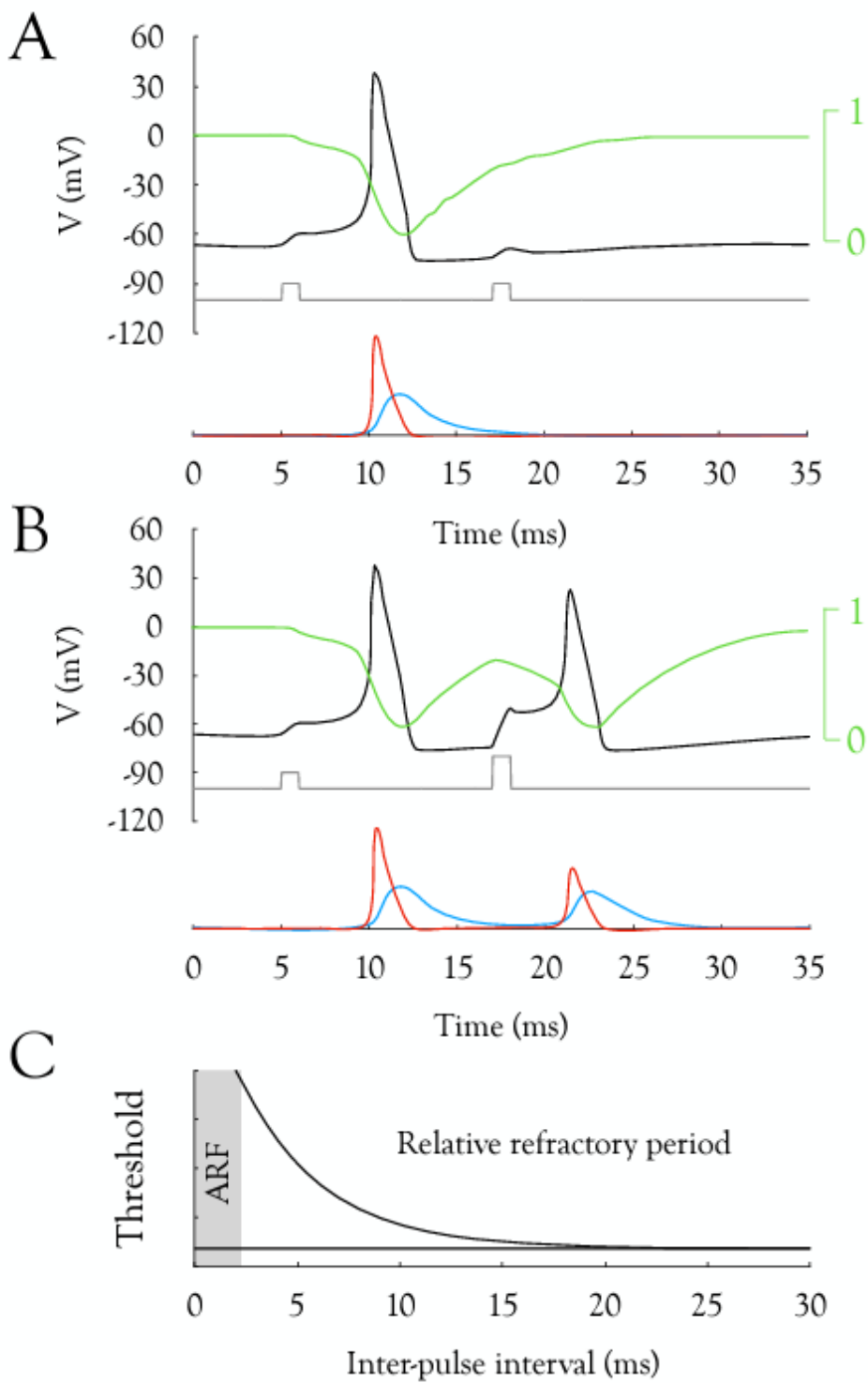


**Figure 7.10** - Relative refractory period. A. Stimulus evoked an action potential (black trace), with  $h$  (green trace) and the stimuli (grey trace) superimposed. The lower trace shows  $g_K$  (blue trace) and  $g_{Na}$  (red trace). During a second stimulus of the same amplitude an action potential was not evoked, as the value of  $g_K$  was still high i.e., second stimulus occurred during AHP, and  $h$  was at a low value. B. Increased stimulus amplitude evoked a smaller second action potential due to small  $g_{Na}$ , since limited permeability pathways were available as  $h$  was smaller than its resting value of 0.6. C. Plot of the ratio of the stimulus required to

evoke a 2<sup>nd</sup> action potential versus the stimulus required to evoke the 1<sup>st</sup> action potential. The absolute refractory period (ARF) is the period when no action potential can be evoked, and the relative refractory period refers to the period when increased stimulus is required to evoke a second action potential. The horizontal line is the stimulus intensity required to evoke an action potential under baseline conditions.

## Anode break excitation

In the updates of the classic papers, I excluded all mention of the terms anode and cathode, as these are antiquated and can be confusing as they can have different meanings depending upon context. Expressions such as 'under a cathode' were replaced by the terms depolarising or hyperpolarising as these are easier to understand. The exception to this was retention of the phrase 'anode break excitation', as it was easily understood. The anode referred to passing a current such that the membrane hyperpolarised, to about -95 mV, for a significant period of time e.g., 10 ms. The sudden release of this hyperpolarising current evoked an action potential (Fig 7.11A). This is initially a perplexing result as all the experimental data indicate that membrane depolarisation precipitates action potential firing. However, if we examine the underlying properties, namely the inactivation particle  $h$  (Fig 7.11A), the leak current and the time constants for  $g_{Na}$  and  $g_K$  (Fig 7.12C), a ready explanation is available. Threshold is not a fixed value and varies depending upon the numerous factors including membrane potential, state of the gating particles and magnitude of active conductances at the instant of stimulus. For example, in the case of anode break excitation the membrane hyperpolarisation reduced the value of  $g_K$  and increased the value of  $h$ . This meant two things, first that there were more  $Na^+$  permeability pathways available for activation so the resulting  $I_{Na}$  would be larger, and that the  $g_K$  was small, which meant that less  $I_{Na}$  would be required to take the membrane potential to threshold. This can be appreciated by referring to Fig 7.11C, which is a cartoon of the relationship between membrane potential and threshold. Upon hyperpolarising the membrane potential, the threshold for evoking an action potential was decreased and fell below the resting membrane potential for the reasons described. Release of the voltage clamp was an instantaneous affair, whereas the threshold relaxed to a new value determined by the response time of  $g_K$ , governed by  $\tau_n$ , which would be comparatively slow compared to the Ohmic  $I_{leak}$ . Under these circumstances the membrane potential temporarily exceeded threshold evoking an action potential (Aidley, 1996).

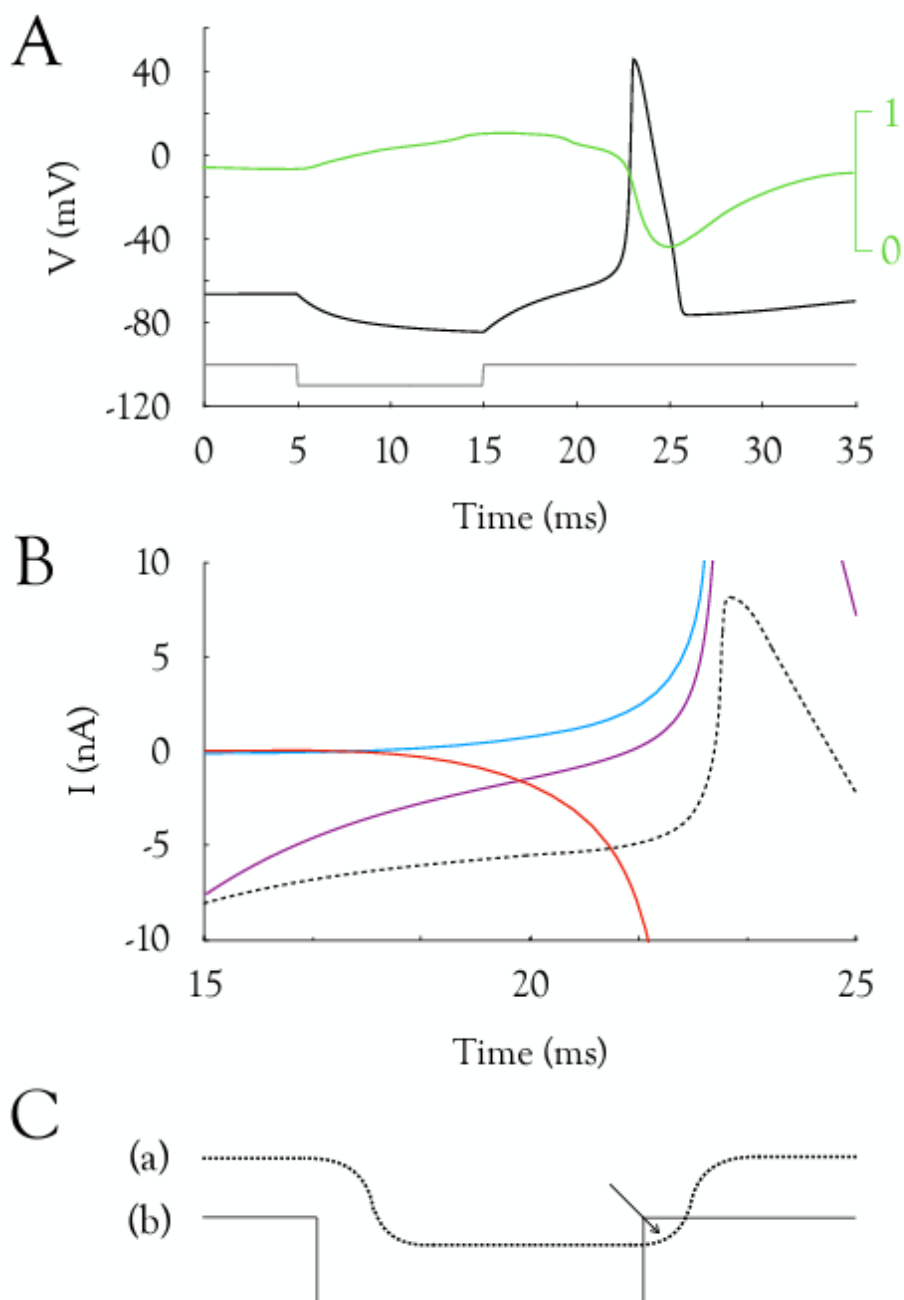


**Figure 7.11** - Anode break excitation. A. Passing a hyperpolarising current pulse (grey trace) for 10 ms increases the value of  $h$  towards 1 (green trace and scale) and  $g_K$  decreases towards zero. On release of the current the membrane potential rebounds and an action potential is evoked. B. On release of the hyperpolarising current there is a large inwardly directed leak current (purple trace) that drives the membrane potential (black dotted trace) towards  $E_{leak}$  (-55 mV). Note how the leak current depolarises the membrane potential, activating the inward  $g_{Na}$  (red trace) before outward  $g_K$  (blue trace), which takes the membrane potential towards threshold and evokes an action potential. C. Representation of the effect of membrane hyperpolarisation (b) reducing threshold (a) below the resting membrane potential, resulting in the release of the clamp causing membrane potential to temporarily exceed threshold (arrow).

It is illuminating to overlay the values of  $m$  and  $h$ ,  $m$  and  $n$  and  $\tau_m$ ,  $\tau_h$  and  $\tau_n$  as shown in Fig 7.12. These comparisons illustrate several key principles, which include (A) at rest (-65 mV)  $m$  is close to zero meaning no  $\text{Na}^+$  permeability pathways are activated. However, since  $h$  is 0.6 about 40% of the  $\text{Na}^+$  permeability pathways are unavailable for opening. To increase the per cent of available permeability pathways the membrane potential must be hyperpolarised for a finite period of time. (B) A comparison of the value of  $n$  versus  $m$  at rest shows that there is a significant portion of  $I_K$  tonically active at rest, since  $g_K$  does not inactivate. Thus, outward  $K^+$  conductance contributes to the resting membrane potential and must be exceeded by inward  $I_{\text{Na}}$  for an action potential to be evoked. (C) The  $\tau$  for  $I_{\text{Na}}$  is faster than that for  $I_K$  so  $I_{\text{Na}}$  turns on more quickly than  $I_K$  during a depolarisation, hence the  $\text{Na}^+$  upstroke precedes the outward  $K^+$  repolarisation. The values for  $\tau_h$  and  $\tau_n$  are comparable and both contribute to restoring the membrane potential towards rest.

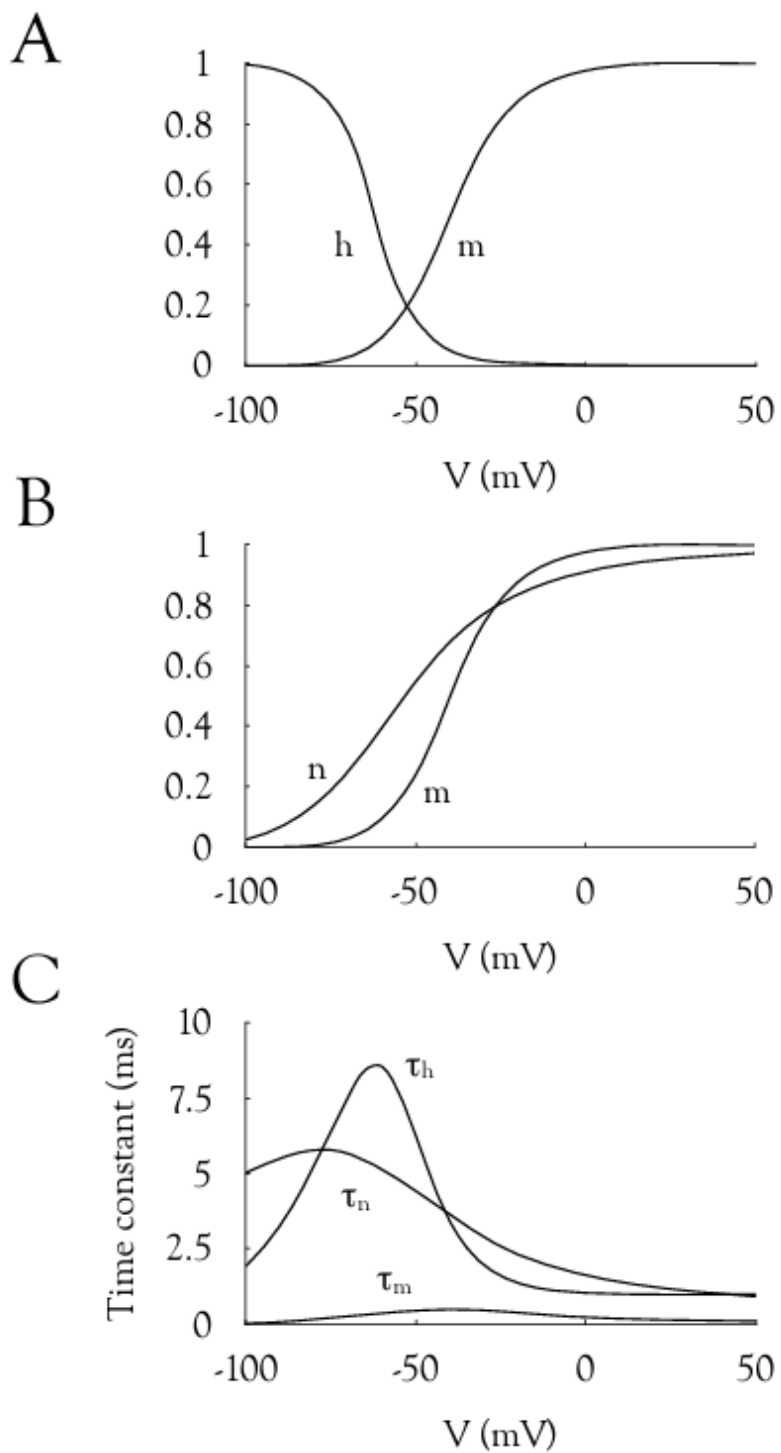


**Figure 7.12** - Comparison of gating particles. A. Values of  $m$  and  $h$  at rest show that 40% of the  $\text{Na}^+$  permeability pathways are inactivated, and  $m$  is close to zero. B.  $n$  is about 0.4 at rest so tonic  $I_K$  contributes to the resting membrane potential. C.  $\tau_m$  is small and  $\tau_n$  is high, which means that  $I_{\text{Na}}$  is activated before  $I_K$  when the membrane is depolarised leading to  $I_{\text{Na}}$  depolarising the membrane, followed by  $I_{\text{Na}}$  inactivation (slow  $\tau_h$ ) and  $I_K$  causing repolarisation.

## 8. THE POTASSIUM PERMEABILITY OF A GIANT NERVE FIBRE

Although I have completed the description of the five seminal Hodgkin and Huxley papers, as well as the introductory Hodgkin and Katz paper, I have included this paper for the following reasons. Huxley described his decision to investigate the mechanism underlying muscle contraction in 1952 as being prompted by the feeling that the work on axon excitability had reached a natural conclusion. Watson and Crick's work would not to be published for another year (Watson & Crick, 1953) so there was no genetic way to study excitability, the carrier molecules that they had considered likely to transfer ions across the membrane would occur in too low a density to measure, the gating currents that were associated with voltage dependent increases in permeability were too small to measure with their techniques (Angel, 1996), and the sharp electrode was introduced (Ling & Gerard, 1949) after completion of their experimental acquisition of data in 1949, but prior to publication of the results.

### The late outward current and K<sup>+</sup>

The incentive for this paper was rather unusual. Hodgkin considered that there were certain issues relating to the action potential that were unresolved, principally the role of K<sup>+</sup> ions in the late outward current that facilitated the repolarising phase of the action potential. The electrophysiological data used to illustrate this was not as convincing as the data showing the early inward current that produced the upstroke of the action potential was due to Na<sup>+</sup> influx. This was reflected in the inaccurate experimental estimates of changes in  $E_K$  as a result of varying [K]<sub>o</sub> compared to Nernstian predictions of  $E_K$ . However, in mitigation it must be realised that the relationship between the membrane potential and Na<sup>+</sup> and K<sup>+</sup> fluxes offered some stark contrasts. The  $E_{Na}$  was distant from the resting membrane potential (about 100 mV separated the two potentials) and there was no net Na<sup>+</sup> influx into the axon at rest. In addition, the [Na]<sub>o</sub> could be substantially altered without harming the axon. However,  $E_K$  was close to the resting membrane potential, and since the membrane was primarily permeable to K<sup>+</sup> at rest, Hodgkin and Huxley were limited to the degree by which they could alter [K]<sub>o</sub> without damaging the axon. In addition, since [K]<sub>o</sub> effectively set the resting membrane potential the two parameters were interlinked and could not be studied in isolation. Coupled with these difficulties was the large margin of error of their experimental results due to axon damage and run down of the membrane potential during their electrophysiological recordings. Hodgkin and Huxley had addressed the issue of K<sup>+</sup> loss from axons during the repolarising phase when they quantified the amount of K<sup>+</sup> that left an axon during an action potential using electrophysiological techniques (Hodgkin & Huxley, 1947). Indeed Hodgkin and Huxley returned to the putative contribution of K<sup>+</sup> to the late outward current in no less than three publications (Hodgkin & Huxley, 1947, 1952a; Hodgkin & Huxley, 1953) prior to this paper (Hodgkin & Keynes, 1955). As well as carrying out the experimental work described in the preceding chapters, Hodgkin had also supervised the Ph.D. of Richard Keynes at this time. Keynes was the great grandson of Charles Darwin and was an important influence as he decided to explore the mechanisms underlying electrical excitability using radiotracer methods, rather than using the conventional electrophysiological techniques. This added an extra experimental dimension that allowed both confirmation of electrophysiology results using an independent technique and the opportunity of an alternate experimental approach to study the trans-membrane ion movements. Clearly dissatisfied with their electrophysiological data Hodgkin and Huxley, under advice from Keynes, used the tracer technique to measure the efflux of K<sup>+</sup> from axons at rest, and from axons stimulated with a depolarising current, where the difference between the two was taken as the K<sup>+</sup> efflux from the axon in response to the current. By varying the levels of current imposed the K<sup>+</sup> efflux could be correlated with the magnitude of

the current. Under these conditions the charge transfer i.e.,  $K^+$  efflux across the membrane was

$$Q = CV \quad \text{Eq. 8.1}$$

where  $Q$  is charge,  $C$  is membrane capacitance and  $V$  is potential difference across the membrane. This expression was adapted to account for the number of moles transferred across the membrane as

$$n = CV/F \quad \text{Eq. 8.2}$$

where  $n$  is the number of moles and  $F$  is the Faraday constant ( $96,485 \text{ C mol}^{-1}$ ), a measure of the charge on a mole of ions. This can be rearranged as

$$F = Q/n \quad \text{Eq. 8.3}$$

A plot of the relationship between the magnitude of the imposed current ( $\text{C sec}^{-1}$ ) and the outward  $K^+$  flux (moles  $\text{sec}^{-1}$ ) demonstrated that the slope of the relationship was equal to the Faraday constant (Eq. 8.1), convincing evidence that  $K^+$  contributed exclusively to the outward flux (Hodgkin & Huxley, 1953). However by this time Keynes had demonstrated both  $\text{Na}^+$  influx and  $K^+$  efflux in cuttlefish axons using the radiotracer method (Keynes, 1951a, b).

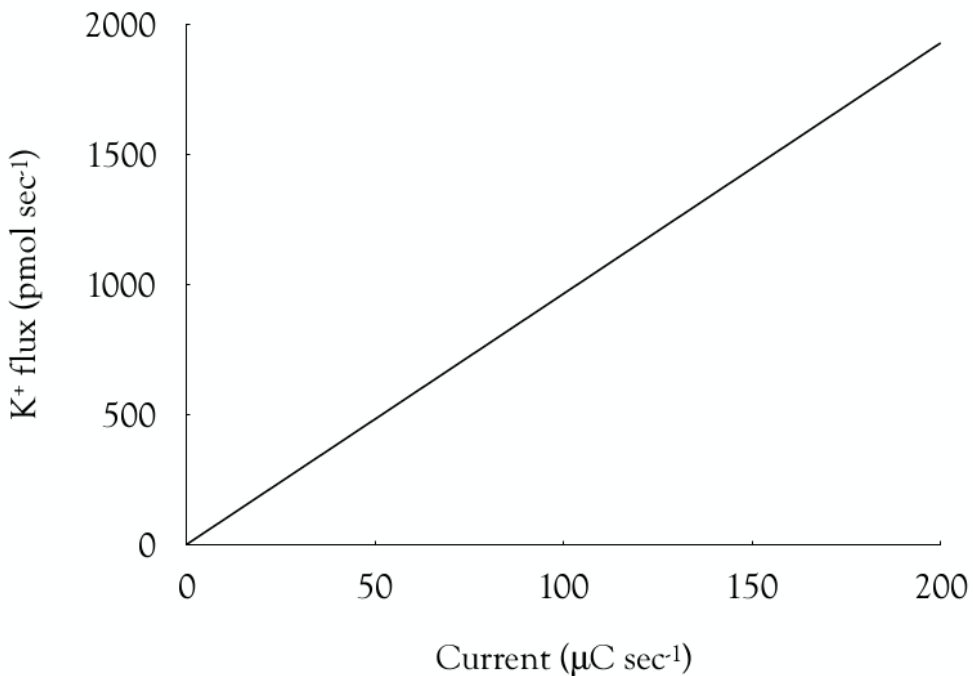


**Figure 8.1** - The relationship between the magnitude of the depolarising current imposed on the axon and the amount of  $K^+$  release from the axon. The slope of the relationship matches the Faraday constant ( $96,485 \text{ C mol}^{-1}$ ).

The success of the 1953 paper must have encouraged Hodgkin to explore the independence principle using this tracer technique, which promised greater resolution than electrophysiological recording, a particularly appealing aspect being the less invasive nature of the experimental protocol. The penetration of the axon with a large microelectrode as required for electrophysiological recordings inevitably damaged the axon and led to a slow decrease in the membrane potential over time, measured as 2 mV hour (Hodgkin *et al.*, 1949). Indeed in the preceding papers axons were described as being in a derelict state (Figure 10 legend, Hodgkin & Huxley, 1952d), the membrane potential depolarised by up to 15 mV over the course of the experiment (Hodgkin & Huxley, 1952c) and replacing seawater with low Na<sup>+</sup> seawater resulted in a 30% decrease in the current amplitude on restoring seawater (Hodgkin & Huxley, 1952a).

From the independence principle Hodgkin and Huxley were able to derive a model (Equation 12, Hodgkin & Huxley, 1952b) that predicted the effect of [Na]<sub>o</sub> on the sodium current, which they were able to test experimentally. They measured the peak  $I_{Na}$  in seawater at a variety of voltages using the voltage clamp technique. These control currents were scaled according to the model and compared to the  $I_{Na}$  recorded in low Na<sup>+</sup> seawater, where the majority of the Na<sup>+</sup> was replaced by the impermeant choline. The model would only converge with the experimental data if a scaling factor was introduced (Figure 13, Hodgkin & Huxley, 1952b). The experiments in which the instantaneous IV of the Na<sup>+</sup> current was explored were technically flawed and no conclusions could be drawn (Figure 7, Hodgkin & Huxley, 1952a). Thus, based on the electrophysiology data the applicability of the independence principle was considered unresolved.

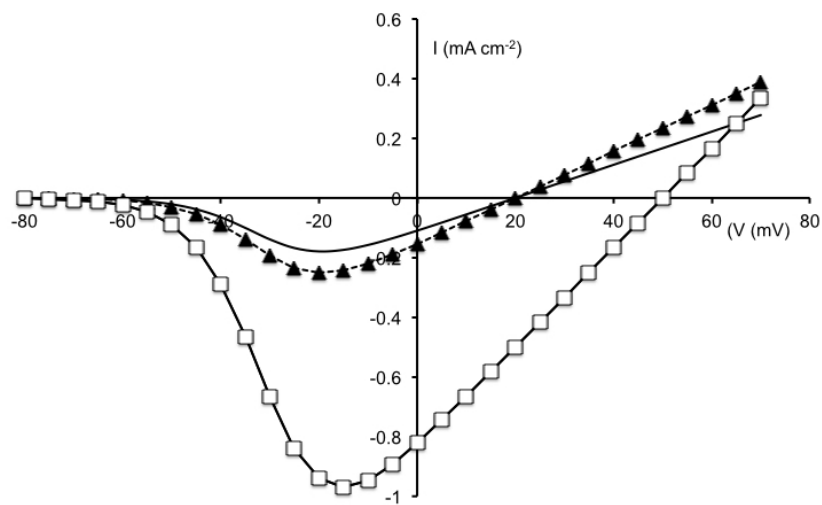


**Figure 8.2** - Test of the ‘independence principle’ applied to  $I_{Na}$  recorded with electrophysiological techniques. Peak amplitude of control sodium currents recorded in normal seawater plotted against test potential (-□-). Sodium current amplitude recorded from axons bathed in 30% Na<sup>+</sup> seawater (-▲-). The continuous line is the peak  $I'_{Na}$  in 30% Na<sup>+</sup> seawater calculated from control  $I_{Na}$  according to the independence principle and scaled appropriately to fit the experimental data recorded in 30% Na<sup>+</sup> seawater (dashed line). Note how reducing [Na]<sub>o</sub> decreases the value of  $E_{Na}$  as predicted.

## The tracer method

Although Hodgkin and Huxley used the inward  $\text{Na}^+$  current to explore the independence principle with electrophysiological techniques, Hodgkin and Keynes used the outward  $\text{K}^+$  current to investigate the principle with tracers. This was primarily because the  $\text{K}^+$  permeability pathways did not inactivate whereas those for  $\text{Na}^+$  did, thus  $\text{Na}^+$  flux would be more difficult to measure and limited in a way that that  $\text{K}^+$  was not. The pathway through which the  $\text{K}^+$  ions moved was the voltage-dependent  $\text{K}^+$  conductance, which was initially described in the squid axon (Hodgkin & Huxley, 1952d), and was also known as the delayed rectifier in reference to its delayed activation compared to the  $\text{Na}^+$  conductance (Fig 7.8). Hodgkin and Keynes never explicitly stated this, and readers may be confused into thinking that the  $\text{K}^+$  ions moved through the leak conductance pathway, since the  $\text{K}^+$  movements are referred to as passive. This was not the case. According to Fig 7.3 a significant portion of the  $\text{K}^+$  permeability pathway was open at rest, allowing long duration experiments to be performed in which the flux of  $\text{K}^+$  could be measured for significant periods of time, thereby increasing the signal to noise ratio.

The principle behind the tracer method was to expose radiolabelled isotope to the tissue, which could be quantified using a Geiger counter. Influx could be measured as the accumulation of the tracer inside the tissue after external exposure to the tracer, whereas efflux could be measured as the loss of tracer from preloaded tissue into tracer-free solution. Measuring the influx and efflux of an ion allowed estimation of the flux ratio as proposed in the flux-ratio criterion (Ussing, 1949). If there was no coupling i.e., if the independence principle applied, then the flux ratio should equal the ratio of the ion concentrations according to Eq. 4.9. In the experiments the axon was bathed in a solution containing labelled  $^{42}\text{K}$  for a finite period of time. The axon was subsequently removed from the bath, washed, and its radioactive content measured, which allowed the rate of influx to be quantified ( $\text{mol cm}^{-2} \text{s}^{-1}$ ). Efflux was calculated by loading the axon with  $^{42}\text{K}$  as described above, then placing it in solution for fixed periods of time. The accumulation of radioactive tracer in these solutions allowed estimates of the rate of  $\text{K}^+$  efflux from the axon. In these experiments Hodgkin and Keynes used axons from *Sepia* (cuttlefish), rather than squid axons for practical rather than scientific reasons, as it allowed them to remain in Cambridge to carry out the experiments rather than relocating to Plymouth. This convenience was offset by the disadvantage that the smaller *Sepia* axons could not be penetrated with an electrode in the manner that the squid axon could be, and was thus not amenable to voltage clamping, a considerable disadvantage as we shall see. The aim of the paper was to measure both the influx and efflux of  $\text{K}^+$  ions when not in equilibrium, in order to compare the experimentally acquired data with the model of independence over a wide range of driving forces. With the tracer method Hodgkin and Keynes could test the independence principle more rigorously than with electrophysiology. A key test of the independence principle was that the fluxes should be directly proportional to the ion concentrations. However, if the independence principle did not apply i.e., ions did affect the movement of other ions, then these effects should be amplified as the concentration of ions was increased. In order to rigorously test the principle a variety of scenarios would be tested where the ion concentrations were raised. It was straightforward to increase  $[\text{K}]_o$  but  $[\text{K}]_i$  was fixed, as the ability to exchange axoplasm with artificial seawater lay in the future (Baker *et al.*, 1962). Ideally, they would measure  $\text{K}^+$  fluxes where  $[\text{K}]_o$  was changed independently of the driving force ( $V - E_{\text{Na}}$ ), and where the driving force was changed while  $[\text{K}]_o$  was unaltered.

## Electrical measurements

As a first test Hodgkin and Keynes recorded the resting membrane potential from axons bathed in seawater containing varying  $[K]_o$ . Instead of using an intracellular electrode as in the previous experiments with squid axon, which was not possible with the small *Sepia* axons, they used the newly developed glass microelectrode of tip diameter about  $1\text{ }\mu\text{m}$  filled with 3 M KCl solution to measure the membrane potential (Ling & Gerard, 1949). This method was likely more accurate than the previous intracellular technique due to its less invasive nature, and with 10.4 mM as the basal level of  $[K]_o$ , they recorded a resting membrane potential of -62 mV. These glass microelectrodes did not require correction for junction potentials, thus the technique (assuming squid and *Sepia* axons have similar  $[K]$ ) was up to 10 mV more accurate than intracellular electrodes. They reproduced the curved relationship between membrane potential and  $[K]_o$  (Hodgkin *et al.*, 1949). The deviation was greatest at the lowest  $[K]_o$ , but above about 50 mM the membrane potential was very close to  $E_K$  (Fig 8.2). This meant that at these high values of  $[K]_o$  an equilibrium would exist where influx = efflux, and under such circumstances only limited information could be obtained. At the resting potential of -65 mV in squid axon the  $g_K$  is about 35 % of  $\bar{g}_K$  (Hodgkin & Huxley, 1952d). A complication in interpreting the results was that as  $[K]_o$  increased the axon depolarised and  $g_K$  increased, a phenomenon recognised by Hodgkin and Keynes.

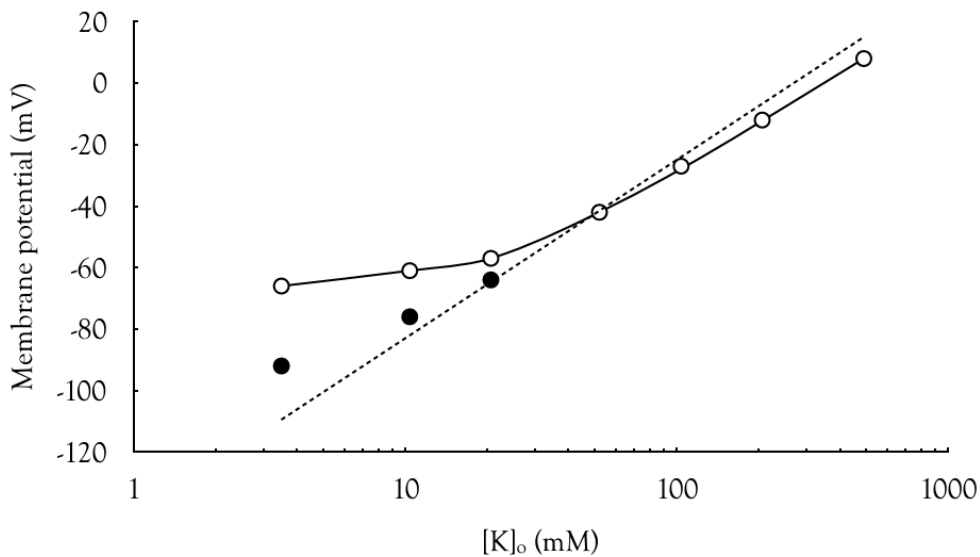


**Figure 8.3** - A plot of *Sepia* axon membrane potential recorded using sharp glass microelectrodes in axons bathed in seawater containing a variety of  $[K]_o$ . The dotted line indicates the Nernstian potential calculated using the value of  $[K]_i$  measured in the axon at the end of the experiment. The open circles are measurements of the membrane potential at rest and the filled circles are measures of the peak AHP.

In order to measure the flux ratio at a wide range of external  $[K]_o$  without altering the driving force, Hodgkin and Keynes had to somehow uncouple the membrane potential from  $[K]_o$ . The most obvious method was to voltage clamp the axon with intracellular electrodes then vary  $[K]_o$ , but the small diameter of the *Sepia* axon precluded this. Instead, they devised two methods by which membrane potential could be isolated from  $[K]_o$ .

### The flux ratio under varying $[K]_o$

Maintain constant membrane potential ( $E$ ) while varying  $[K]_o$ . This ingenious method involved threading the axon through two holes in a 2 mm diameter glass capillary tube in which seawater containing labelled  $^{42}\text{K}$  flowed. The capillary was bathed in another chamber, which contained 104 mM [K], the assumption being that given the relatively large axonal length constant,  $E$  would be determined by the [K] in the outer bath irrespective of the [K] in the capillary tube (Fig. 8.4). This allowed Hodgkin and Katz to maintain a constant  $E$  whilst varying  $[K]_o$  in the capillary tube. Under such circumstances the flux ratio (efflux/influx) could be expressed in terms of electrochemical activities of the ions inside and outside the axon.

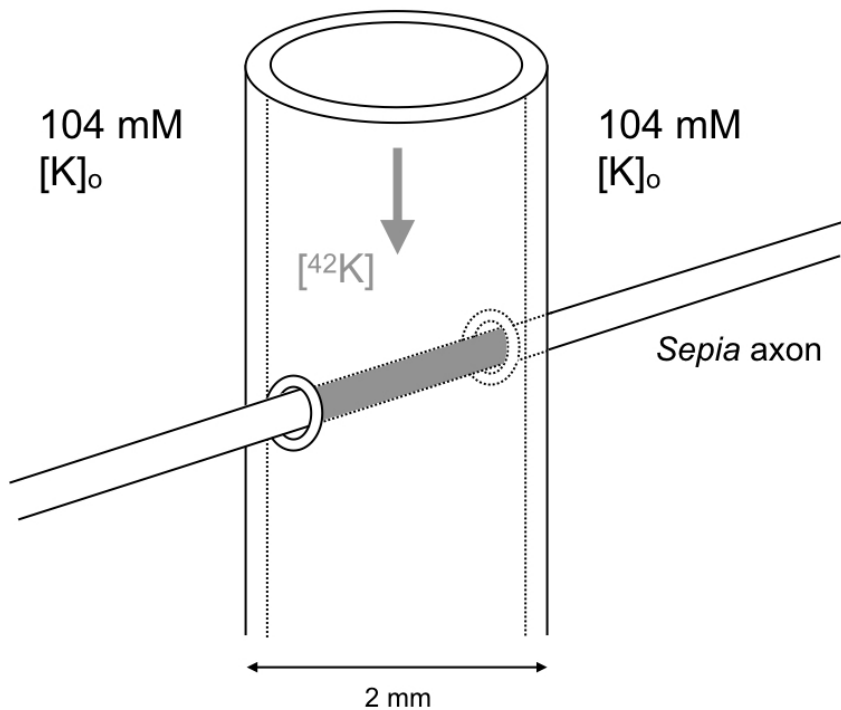


**Figure 8.4** - Model of the method used to load Sepia axons with  $^{42}\text{K}$ . A 2 mm diameter glass capillary tube had two holes of about 300  $\mu\text{m}$  diameter drilled on opposite sides. A Sepia axon was threaded through the holes and the capillary was perfused with seawater containing 104 mM  $^{42}\text{K}$ . The grey colouring indicates the section of axon loaded with  $^{42}\text{K}$ . The axon outside the capillary was bathed in a chamber containing 104 mM K. The [K] content in the capillary was changed from 104 mM to 10.4 mM and the influx and efflux were measured.

From Chapter 4 (Eq. 4.9) we have seen

$$\frac{M_2}{M_1} = \frac{c_2}{c_{*1}} e^{\left[ \frac{EF}{RT} \right]} \quad (\text{Eq. 8.4})$$

where  $c_2$  is the internal [K] and  $c^*_1$  is the external [K]. The equation predicts that for a 5-fold decrease in  $[K]_o$  the flux ratio ( $M_2/M_1$ ) should increase by a factor of 5, specifically that  $M_1$  should decrease by a factor of 5 and  $M_2$  should be unchanged.

## The flux ratio under varying driving forces

Maintain constant  $[K]_o$  while varying  $E$ . This method required application of a current across the axon via the forceps that secured the axon in place, allowing them to alter  $E$  by up to  $\pm 10$  mV, whilst maintaining constant  $[K]_o$ . Under these conditions the flux ratio could be expressed relative to the electrochemical driving force ( $E - E_K$ ).

An expression for this can be derived from Eq. 4.9

$$\frac{M_2}{M_1} = \frac{c_2}{c^*_1} e^{\left[ \frac{EF}{RT} \right]}$$

and we have seen in Chapter 4 that

$$\frac{c_1}{c_2} = e^{\left[ \frac{E^*F}{RT} \right]}$$

thus it follows that

$$\frac{c_2}{c_1} = e^{\left[ \frac{-E^*F}{RT} \right]}$$

Substituting into Eq. 4.9 gives

$$\begin{aligned} \frac{M_2}{M_1} &= e^{\left[ \frac{EF}{RT} \right]} \times e^{\left[ \frac{-E^*F}{RT} \right]} \\ \frac{M_2}{M_1} &= e^{\left[ \frac{(E-E^*)F}{RT} \right]} \end{aligned} \tag{Eq. 8.5}$$

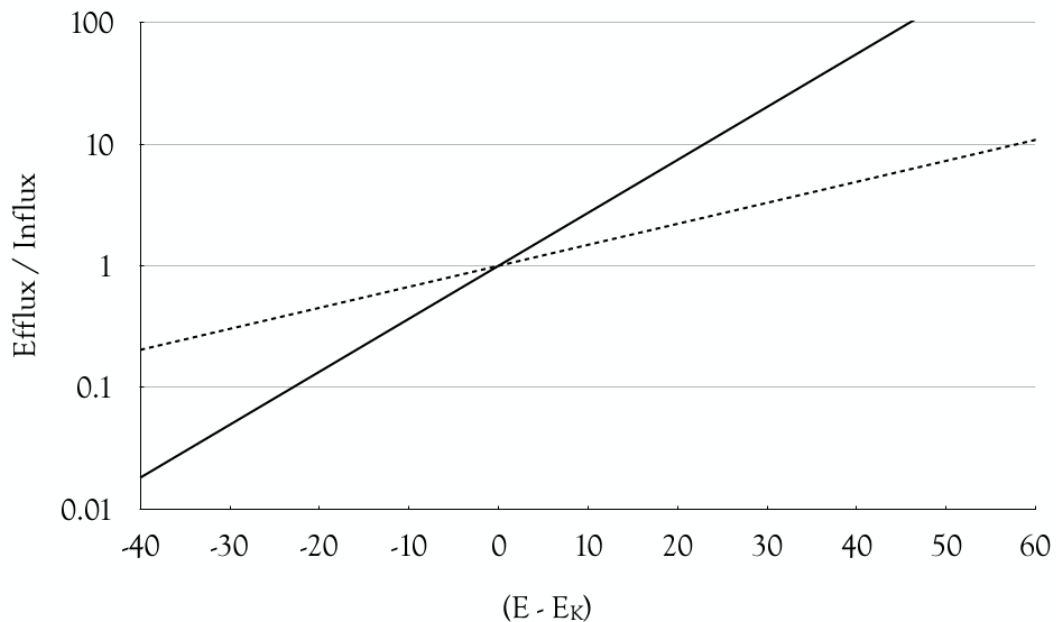


**Figure 8.5** - The effect of driving force, as depicted in Eq. 8.5, on the efflux/influx ratio. The continuous line illustrates the Nernstian relationship with a slope of 58 mV, whereas the dotted line describes the experimental data, which has a slope of 23 mV.

## Evidence of interaction

According to Hodgkin and Keynes if the independence principle applied “the chance that any individual ion will cross the membrane in a specified time interval is independent of the other ions which are present.” Hodgkin and Keynes’ results were presented in a series of exhaustive and rather confusing tables, which can be summarised as follows: (1) increasing  $[K]_o$  whilst maintaining constant  $E$  reduced  $K^+$  efflux, (2)  $K^+$  influx at constant  $E$  was greater than predicted when  $[K]_o$  was increased, and (3) the effect of driving force ( $E - E_K$ ) was greater than predicted. The experimental data did not follow the predictions indicating that the independent movement of ions did not apply (Fig 8.5). A possible explanation for this observation was based upon the means by which  $K^+$  ions were thought to cross the membrane. Hodgkin and Keynes proposed that narrow pores facilitated ion movements across the membrane. If the pores were assumed to be narrow (the width of one  $K^+$  ion) and long (the length of several  $K^+$  ions laid end to end) then the process of flux coupling would interfere with free movement of ions through the pore. If ions moved through the pore in single file (Fig 8.6B) then the movement would be influenced by other ions present in the pore, and such coupling would reduce the movement of ions in the pore. As the independence principle did not apply Hodgkin and Keynes proposed ions moved through pores, which we can consider as channels. In order to explain these results Hodgkin and Keynes proposed that  $K^+$  ions moved through the membrane via a narrow pore in single file and that the pore was occupied by about three  $K^+$  ions at any time. To support their premise they devised a famous mechanical model whose simple elegance was still a source of pride to its creator many years later (Hodgkin, 1992).

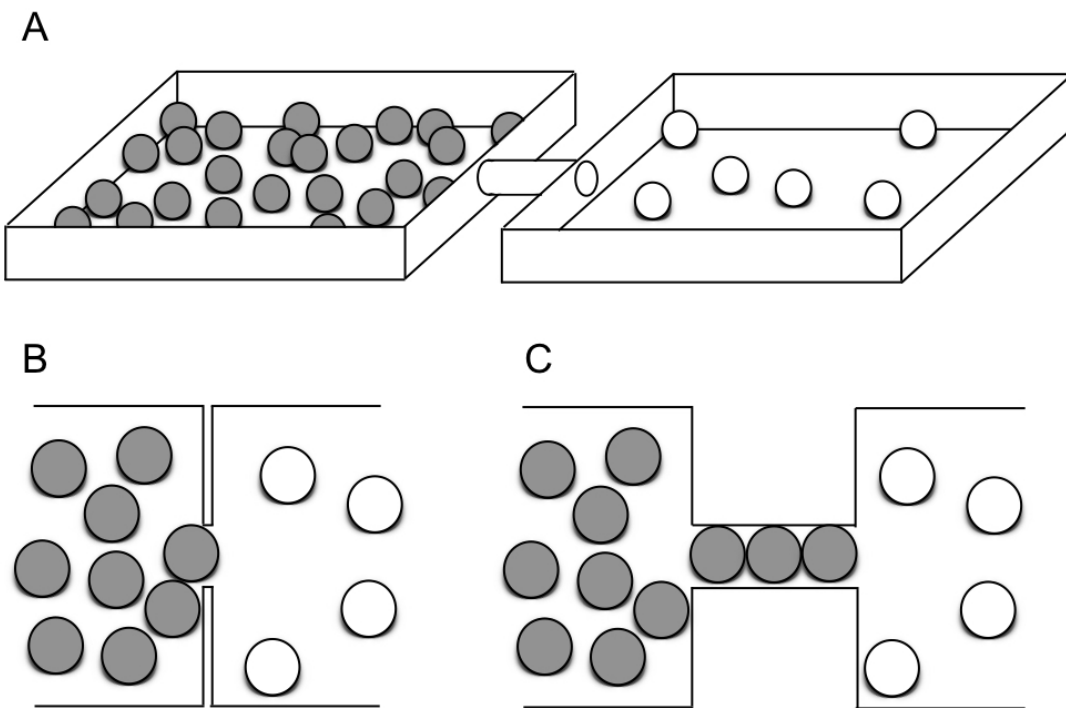


**Figure 8.6** - A representation of the mechanical model devised by Hodgkin and Keynes to demonstrate the long pore effect. (A). Two compartments were interconnected via a tube. The compartments contained different coloured ball bearings in known ratios. The length of the connecting tube could be altered from a (B) short gap, where only one collision between a ball bearing and the gap is required to move a ball bearing from one compartment to the other, to a (C) long gap where four successive collisions are required to move a ball bearing from one compartment to the other.

Briefly, the model comprised two compartments containing ball bearings of different colours to facilitate identification of ball bearing movement. The model was vigorously shaken to facilitate ball bearing movement. A tube whose diameter was equal to the diameter of a ball bearing and whose length could be varied connected the compartments (Fig 8.6A). If the length of the tube was much less than the diameter of one ball bearing, a short gap (Fig 8.6B), the number of ball bearings crossing between compartments was directly related to the number of ball bearings in each compartment. For example, if there were 100 ball bearings in each compartment then shaking the apparatus resulted in an equal number of ball bearings moving from left to right as those from right to left. This was due to the random ‘Brownian’ motion of the ball bearings causing collisions with the gap, the number of collisions being governed by the number of ball bearings in each compartment. If there were twice as many ball bearings in one compartment than the other, then twice as many ball bearings would move from that side to the other. However, if the length of the tube was increased to equal the diameter of three ball bearings, a long gap (Fig 8.6C), then the number of ball bearings moving into each compartment was now no longer directly related to the ratio of the number of ball bearings in each compartment. With the

long gap four consecutive collisions are required to move one ball bearing from one compartment to the other. It is much more likely that this will occur in the compartment that has the most ball bearings, and can be quantified as

$$\frac{flux_{12}}{flux_{21}} = \left[ \frac{bb_1}{bb_2} \right]^n$$

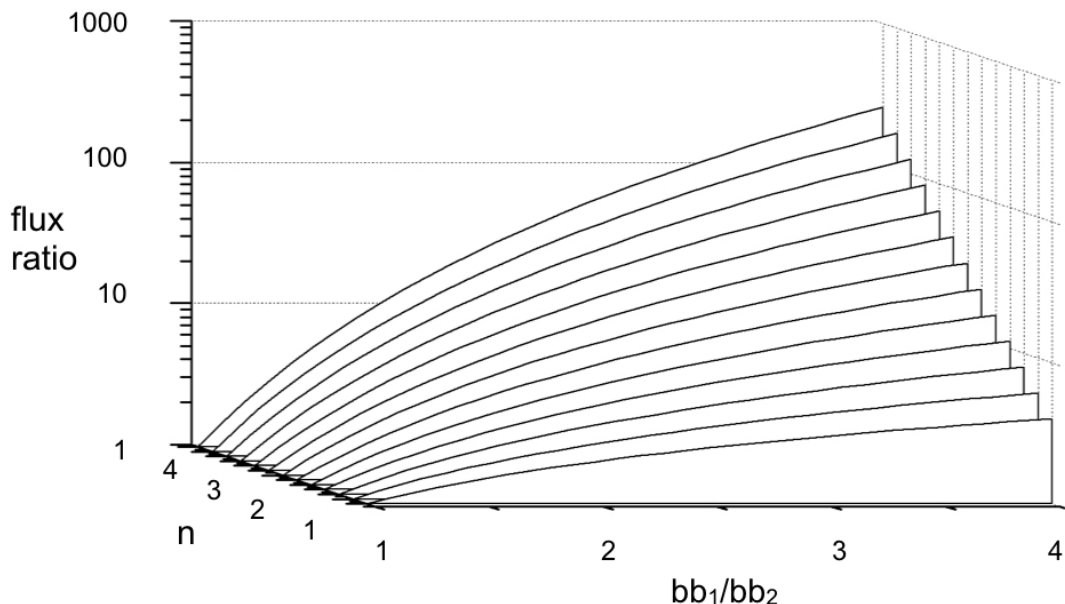


**Figure 8.7** - The non-linear relationship between the flux ratio (y axis, log scale), the ratio of ball bearings in each compartment (x axis), and the length of the pore (z axis), which dictates the number of collisions required to move a ball bearing from one compartment to the other (Eq. 8.2) The simulated flux ratio of 2.7 obtained by Hodgkin and Keynes for the short gap suggests that the thickness of the walls of the container contributed to the gap length explaining the calculated number of collisions as 1.43.

where  $flux_{12}$  is the movement of ball bearings from compartment 1 to 2,  $flux_{21}$  applies to movement in the opposite direction,  $bb_1$  and  $bb_2$  are the number of ball bearings in compartments 1 and 2, respectively, and  $n$  is the number of collisions required to move a ball bearing through the gap from one compartment to the other. The principle underlying the non-independence of movement was that in the compartment with the higher number of ball bearings there was an increased likelihood of the collisions that will move the ball bearings one place further along the pore towards the other compartment. Even though collisions on the other side will occur they are less likely, and the net movement of ball bearings favours that from higher concentration to low concentration, i.e., the movement of one ion through the pore assists the movement of other ions in the same direction. In this way Hodgkin and Keynes predicted the manner in which  $K^+$  ions traverse the membrane through channels, which was verified over four decades later when the structure of  $K^+$  channels elucidated by X ray crystallography showed the channel was occupied by three  $K^+$  ions (Doyle *et al.*, 1998).

## 9. CONCLUSION

The Hodgkin-Huxley model was a quantitative account of the voltage and time dependence of  $g_{Na}$  and  $g_K$  used to reconstruct accurately the action potential in response to a variety of discrete stimuli. An appreciation of the limited electrophysiological techniques available to Hodgkin and Huxley only increases our admiration for this accomplishment. The manner in which the work was conducted pointed the way to which research into neuronal excitability is currently undertaken. Hodgkin and Huxley successfully combined electrophysiology with mathematical modelling, a multi-disciplinary strategy that is now commonplace, with the tools currently available including fluorescence imaging, molecular biology, patch clamping, mathematical modelling, and X-Ray crystallography. The element of luck played an important role when reviewing Hodgkin and Huxley's work. It was no exaggeration by Hodgkin to claim that the introduction of the squid axon as the model of choice was a critical development in studies on membrane excitability (Keynes, 2005), and its (re)discovery by Young in 1936 occurred at exactly the right time. The squid was the optimal model for this work for the following reasons. Its cylindrical shape made it amenable to penetration by long, thin electrodes and facilitated space clamp in a way that a branching structure would not. This was crucial as it allowed the axon to be voltage clamped and therefore space clamped simultaneously, which simplified interpretation of the recorded currents. Another advantage of the squid axon was its limited complement of only two types of voltage gated current,  $I_{Na}$  and  $I_K$ , as well as an Ohmic leak current. Using ion substitution Hodgkin and Huxley were able to separate the currents, which then allowed them to quantify the conductances. Had the squid contained just one additional active conductance, e.g., the  $I_A$  current (see below), such separation would have provided an insurmountable impediment to characterisation of individual conductances. We now know there are hundreds of different voltage gated ion channels, but most are present in the soma (Kandel *et al.*, 2013b). This allows processing of the numerous synaptic inputs that principally occur in the dendritic tree, but the resulting deflections in membrane potential travel to the soma, where neuronal integration occurs. Such integration can be considered a decision-making algorithm with only two possible outcomes - fire, or not fire, an action potential in response to the inputs. As such the axon carries out the comparatively simple role of transmitting propagating action potentials down the axon, which Hodgkin and Huxley showed only requires two active conductances. In the wake of the Hodgkin-Huxley model others applied their voltage clamp technique to disparate preparations. The first of these was Dodge and Frankenhauser who showed that the Hodgkin-Huxley model was applicable to frog nerve (Dodge & Frankenhauser, 1958), and frog muscle was also later shown to also conform to the Hodgkin-Huxley model (Adrian *et al.*, 1970). In the early 1960s Denis Noble applied the Hodgkin-Huxley equations to study the ion channels underlying the mechanisms of heartbeat (Noble, 1962), his lifelong devotion to the topic culminating in development of the virtual heart (Noble, 2007).

### Currents that control firing frequency

The giant axons of the squid are activated by a single pair of first order giant nerve cells that result in synchronised contraction of the mantle, the resulting expulsion of water through a funnel rapidly propelling the squid in a direction determined by the position of the funnel. The giant size of the axons enables rapid contraction of the mantle, ensuring rapid movement, the escape of the squid sometimes occluded by the release of ink (Young, 1938). This rapid contraction is achieved via short high frequency bursts of action potentials. Hodgkin had reported that the response of crab axons to sustained current injection could be classified into three categories, (i) axons displayed a wide ranging of firing frequencies, (ii)

axons displayed a limited range of frequencies, with an abrupt onset of firing, (iii) axons fired limited action potentials and only fired repetitively with high current strength (Hodgkin, 1948). The squid axon falls into the second category, which may be explained by its function, to briefly fire a high frequency volley of action potentials, in order to activate the escape mechanism. A plot of the squid axon action potential frequency versus stimulating current strength produces an  $f$ - $I$  curve (Fig 9.1A), which illustrates the following properties, (i) the abrupt onset of high frequency firing, (ii) the limited range of high frequency firing, and (iii) the absence of any firing at low stimulus strengths (Koch, 1999). The classic studies of Chuck Stevens at the University of Washington, Seattle, highlights one of the criticisms of the Hodgkin–Huxley model, namely that there are currents present in neurones that were not described by Hodgkin and Huxley. Stevens carried out electrophysiological recordings from the neural cell body of the marine gastropod *Anisidoris*, which displayed a firing pattern that conforms to category (i) described by Hodgkin. Stevens used the voltage clamp technique to describe (Connor & Stevens, 1971a) and then model (Connor & Stevens, 1971b) the  $I_A$  current, which was an inactivating  $K^+$  current that controlled firing activity, by contributing hyperpolarising current during the inter-pulse interval that counteracted membrane depolarisation, limiting the firing frequency (Fig 9.1B). Axons that exhibit the firing patterns described in category (i) possess membrane currents in addition to those described by Hodgkin and Huxley in the squid axon. These additional currents that control firing frequency are predominantly  $K^+$  channels (Schwindt *et al.*, 1988a; Schwindt *et al.*, 1988b), such as the  $I_A$  current described above, but  $Ca^{2+}$  currents (Huguenard & McCormick, 1992; McCormick & Huguenard, 1992) and  $Na^+$  currents (Crill, 1996) can also participate.

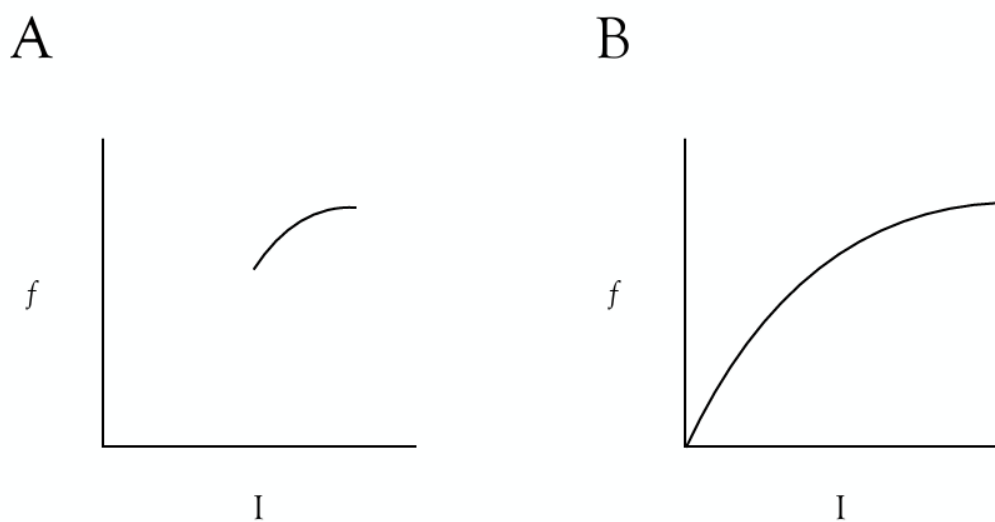


**Figure 9.1** -  $f$ - $I$  curves. A. The  $f$ - $I$  curve for the Hodgkin-Huxley axon showing type (ii) firing with a rapid onset of firing, limited range of firing frequencies and abrupt cut-off. Note the axon cannot fire at low frequencies. B. The  $f$ - $I$  curve for an axon containing the  $I_A$  current, which shows a wide range of firing frequencies and the ability to fire at low frequency in response to small, injected currents.

While it is true that the Hodgkin-Huxley model was unsuitable for modelling the firing frequency of trains of action potentials due to the presence of only two currents in the axons, it must be appreciated that the  $I_A$  current is expressed in the neuronal cell body of *Anisidoris* not the axon. Criticism that Hodgkin and Huxley did not model high frequency firing fails to appreciate the original intentions of the model. When one considers that it took Huxley 8 hours to reconstruct a single action potential of 5 ms duration, any thoughts of reconstructing trains of action potentials lasting hundreds of milliseconds is wildly unrealistic. However, this difficulty in reconstruction may have been a blessing since it limited the complexity of the model. Hodgkin and Huxley pitched their model appropriately - it was complicated, but not too complicated to be experimentally testable and to be at least conceptually understood by the scientific community. Had there been a means of faster computation Hodgkin and Huxley may have been tempted to try to optimise the model by including additional parameters. When assessing the mismatch between the lag in the onset of  $g_K$  compared to their model of  $n^4$  (Figure 2, Hodgkin & Huxley, 1952d) they state 'Better agreement might have been obtained with a fifth or sixth power, but the improvement was not considered to be worth the additional complication.' We can appreciate their pragmatic view that the model was accurate enough, and any gains in accuracy would have been offset by additional complexity and computing time. In 1960 Cole and Moore investigated this lag period in the onset of  $g_K$  after a hyperpolarising pulse, prior to the depolarising voltage step. This phenomenon, known as the Cole-Moore effect, is still unexplained, and although raising  $n$  to the power 25 improves the fit of the model to the data (Hoshi & Armstrong, 2015), it is inconsistent with the structure of the  $K^+$  channel (see below).

### Application of the Hodgkin-Huxley model to mammalian neurones

The glass microelectrode was an important technological advance as it allowed recordings from smaller mammalian neurones and revealed currents measured could generally be modelled with Hodgkin-Huxley style equations, demonstrating the universal application of the model. In the late 1950s Wilfred Rall started investigating the cable properties of dendrites using mathematical analysis (Rall, 1977). His method was to reduce the dendritic tree to a series of compartments that were each modelled as cylinders. This allowed him to model mammalian neurones of complex shape whilst maintaining the computations at a manageable level (Moore, 2010). The combination of the glass microelectrode and an improved understanding of current flow in dendrites facilitated the introduction of realistic models of neurones with complex morphologies.

The Hodgkin-Huxley model was also shown to apply to myelinated (also referred to as medullated) axons, where the vast majority of the axon surface is covered with myelin, with only the exposed nodes containing high densities of  $Na^+$  channels (Rasband & Shrager, 2000). In these instances, the propagation of the action potentials jumps from node to node, known as saltatory conduction, rather than spreading as a propagating wave, but the currents present adhere to the Hodgkin-Huxley model. An unusual aspect of the location of channels present in myelinated axons is that the delayed rectifier  $K^+$  channels are not located at the node, but instead are present in the juxtaparanodal region underlying the myelin, and appear to play no role in action potential repolarisation (Ritchie, 1995), which is facilitated by rapid  $I_{Na}$  inactivation and a large leak current (Bakiri *et al.*, 2011; Kolarik *et al.*, 2013).

## Predictions of ion channel selectivity

Hodgkin and Keynes's proposal that ions move through pores or channels in single file posed multiple questions, the most obvious one being, are the channels selective for a particular ion? Hodgkin and Huxley's experiments separated the trans-membrane current into  $I_K$  and  $I_{Na}$ , implying there were two independent conductance pathways that must show a preference for  $K^+$  ions over  $Na^+$  ions and vice versa. Hodgkin and Huxley stated their measurements 'were not at all accurate', and their incorrect claims that  $Na^+$  ions moved independently across the membrane can be explained by insufficient resolving powers of their method. Nearly 15 years elapsed until this topic was studied in detail, when Bertil Hille used the voltage clamp technique to record  $Na^+$  currents from frog node of Ranvier. He compared the currents recorded with  $Na^+$  Ringer's solution to those in which  $Na^+$  was substituted with equimolar concentrations of other test ions. An important finding was that non-physiological ions could carry a current implying that selectivity was based on chemical structure rather than physiological relevance. By plotting the peak current amplitude versus voltage, the difference between the reversal potential for  $Na^+$  versus the test ions was measured, from which estimates of the relative permeabilities of the test ions could be made:

$$E_X - E_{Na} = 55.2 \text{ mV} \times \log_{10} P_X \frac{[X]_o}{[Na]_o} \text{ or } P_X = 10^{\left[ \frac{(E_X - E_{Na})}{55.2 \text{ mV}} \right]} \quad (\text{Eq. 9.1})$$

where  $E_{Na}$  and  $E_X$  are the equilibrium potentials for  $Na^+$  and the test ion, respectively,  $[Na]_o$  and  $[X]_o$  are the extracellular concentrations of  $Na^+$  and the test ion, respectively, and  $P_X$  is the relative permeability of the test ion compared with  $Na^+$  (Fig 9.2). This relationship is derived using the same ingenious manipulation of the 1<sup>st</sup> and 2<sup>nd</sup> laws of logarithms to exclude unknown terms that Hodgkin and Katz applied (Chapter 2) to assess if the action potential peak in different  $[Na]_o$  was carried by  $Na^+$  ions (Hodgkin *et al.*, 1949). The relative permeability of the test ion provided important insights into what chemical properties/structure were important in relation to permeability.

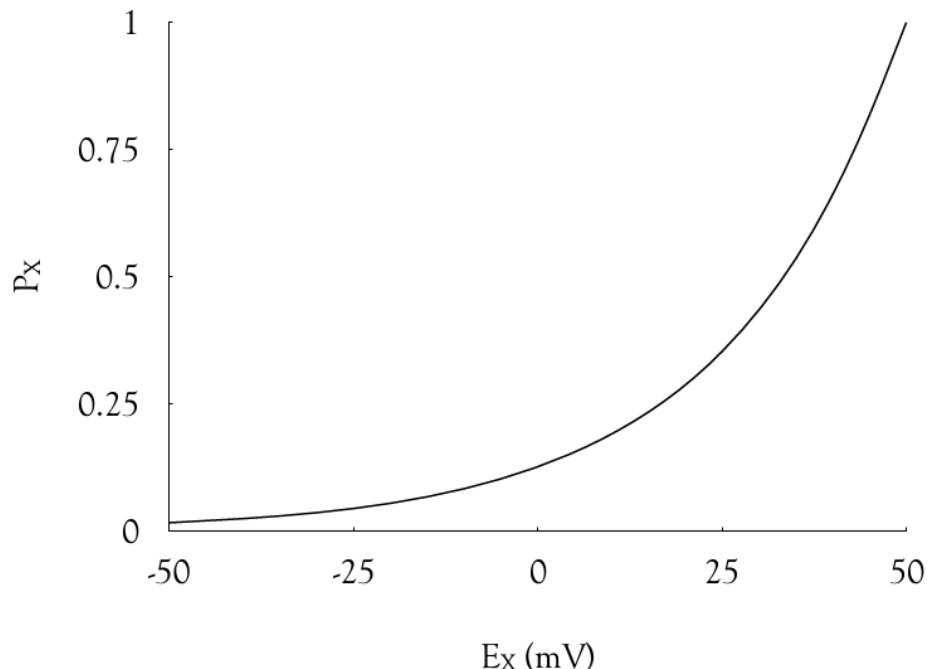


**Figure 9.2** - The permeability of ions at the  $\text{Na}^+$  channel as calculated by Eq. 9.1. The x-axis denotes the reversal potential for the ions tested ( $E_x$ ). The  $E_{\text{Na}}$  is 50 mV and there is a rapid decrease in the relative permeability of ions as the measured reversal potential deviates from  $E_{\text{Na}}$ .

## Ion channel structure

The existence of ion channels moved from theory to reality in the 1980s, with the advent of the patch clamp technique and advances in molecular biology. The combination of these techniques was extremely powerful as they revealed the amino acid sequence, then structure of the channels, and allowed the measurement of ion movement through the channel. Mutagenesis studies revealed the amino acids responsible for a variety of ion channel properties including drug binding sites, voltage sensors, and inactivation, among others. Over the last three decades a detailed picture has emerged of the intimate relationship between structure and function of ion channels (Catterall, 2012). One of the most intriguing is the idea that Hodgkin and Huxley predicated the structure of voltage gated  $\text{K}^+$  and  $\text{Na}^+$  channels, since the four subunits that comprise the pore region of these channels matches the number of gating particles predicted to control opening and closing of the channels in the model. This must be tempered with the realisation that powers other than four may provide a better fit of the experimental data. However, we can certainly credit Hodgkin and Huxley with applying fictive particles to the model that did prove to be components of the channel that governed activation. Although Hodgkin and Huxley did not describe gating particles (their technique was not sensitive enough to measure these) they did predict their existence, and the small currents associated with movement of these sensors in response to membrane potential (Armstrong & Bezanilla, 1973). Molecular

biology has revealed that there are three main parts of an ion channel, the pore, the voltage sensor, and the gate. The functional relationship between these components is as follows. In a channel at rest (closed) a depolarisation of the membrane is sensed by the voltage sensor, which reacts via the movement of positive charges. The charges cause a conformational change in the gate, causing it to open allowing ions to pass through (Bezanilla, 2005). The general structure of a voltage gated  $\text{Na}^+$  channel comprises 4 subunits, each of which contains 6 membrane-spanning domains (Fig 9.3).

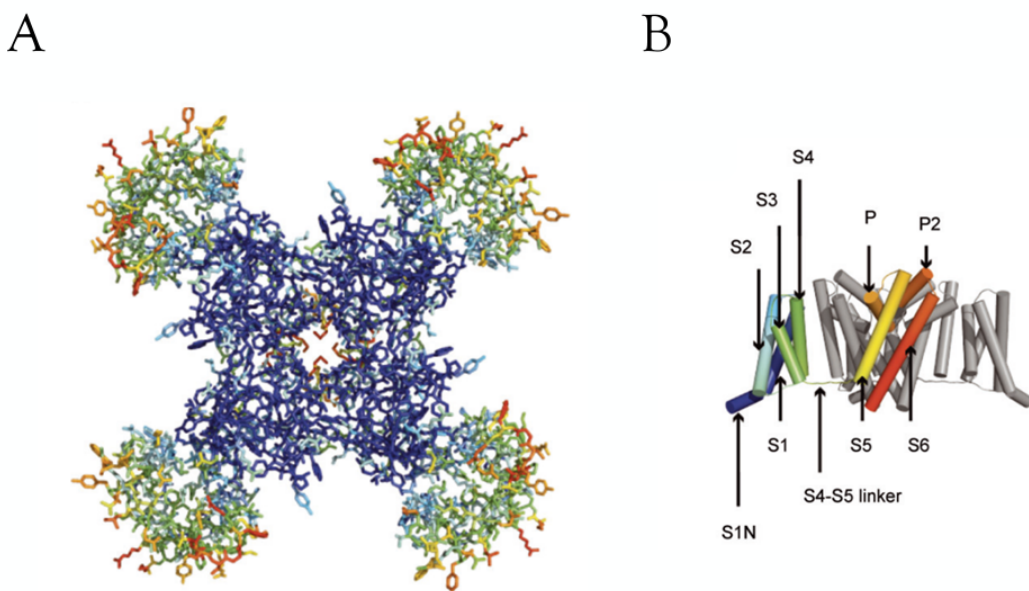


**Figure 9.3 - Structure of the voltage gated  $\text{Na}^+$  channel.** A. View from above clearly identifies the 4 subunits that comprise the pore forming region of the channel. B. The components of an individual subunit are shown where the trans-membrane spanning region S4 denotes the voltage sensor (Catterall, 2012).

The selectivity of the  $\text{Na}^+$  channels for  $\text{Na}^+$  ions was investigated by Hille, who proposed several properties to explain the phenomenon. A puzzle was that  $\text{K}^+$  channels exclude  $\text{Na}^+$  ions although  $\text{Na}^+$  is a smaller ion than  $\text{K}^+$ , so clearly factors other than simple ionic size were involved. Hille realised that because of its smaller size  $\text{Na}^+$  attracted a larger number of water molecules such that the hydrated  $\text{Na}^+$  was larger than the hydrated  $\text{K}^+$  ion. For the channel to be so selective Hille proposed there must exist an intimate relationship between the channel and the ion. A particularly notable finding was that the large molecule aminoguanadinium was permeable whereas smaller methylated cations such as methylamine were not (Hille, 1971). Hille proposed that there were two features of ions that determined permeability: shape and chemical nature. For channels to be selective they must be small, and there must be an intimate interaction between the channel and the ion for it to be sensed. This suggested that not only did the  $\text{Na}^+$  ion lose its water molecules i.e., becomes dehydrated, it also suggested the existence of a selectivity filter, which inhibited access of large molecules. A circular ring of oxygen dipoles that served as the selectivity filter, to which ions passing through the channel make hydrogen bonds was proposed (Fig

9.4). The chemical nature of methylated compounds dictated that they were incapable of forming such bonds, satisfactorily explaining their marginal permeability (Hille, 2001).

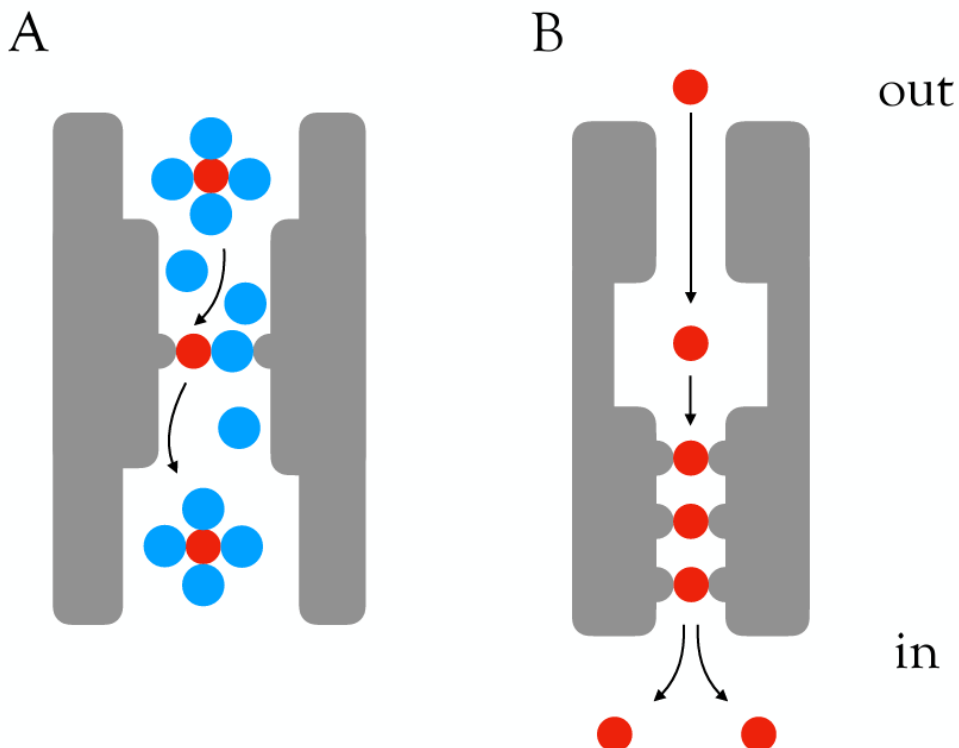


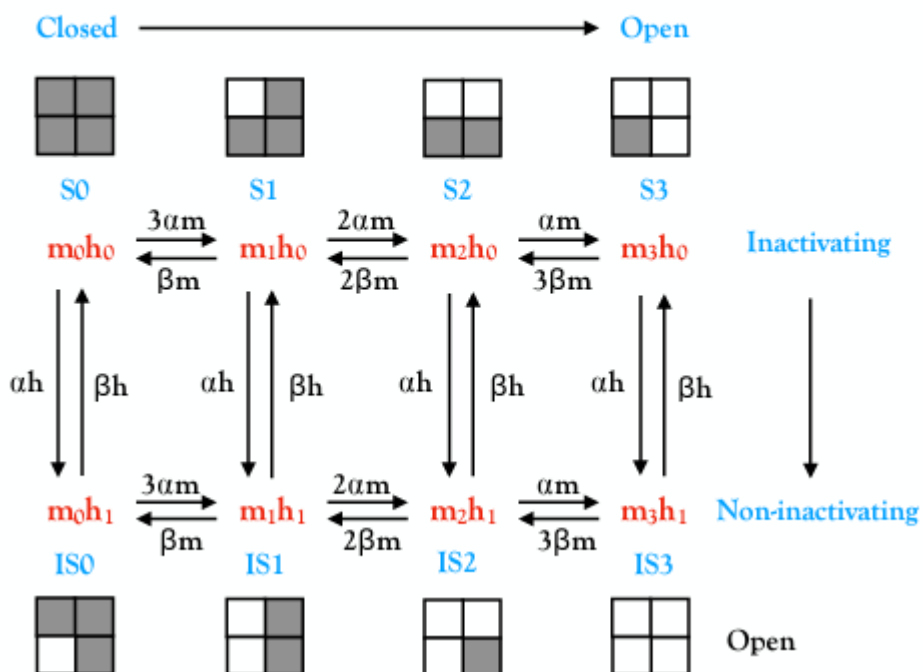
**Figure 9.4** - A schematic view of a  $\text{Na}^+$  channel. A. The hydrated  $\text{Na}^+$  ions enter the vestibule and shed water molecules. In this dehydrated state they pass through the selectivity filter where they transiently bind to an active site before rehydrating. The red circles denote the  $\text{Na}^+$  and the blue circles denote water molecules. The narrow region denotes the selectivity filter. B. Permeation of  $\text{Na}^+$  through the channel involves  $\text{Na}^+$  ions moving in single file - when one ion enters the channel another is propelled inwards.

### Application of the Hodgkin-Huxley model to ion channels

In Chapter 8 we saw that Hodgkin and Keynes proposed ions move through pores or channels, with the implication that the macroscopic current was the sum of the active microscopic currents that occurred across the membrane through channels. The application of Hodgkin-Huxley style rate constants to models of individual channels evolved in the wake of the first patch clamp recordings of individual ion channels (Neher & Sakmann, 1976). Ion channels can exist in two conductive states, open and closed, and channels can switch between these states randomly i.e., at a fixed voltage the channel can move from open to closed in a stochastic fashion, where the probability of such transitions is controlled by voltage dependent rate constants. As such the probability of a channel changing state can be assigned a numerical value based on the rate constants that govern the transition between the states. At a depolarised voltage there is a high probability that the channel will switch from closed to open, whereas at membrane potentials close to rest the probability for such an occurrence is lower, the likely movement between states being from open to closed. We

can apply similar reasoning to the gating of the inactivation particle. At depolarised membrane potentials there is a greater likelihood that the inactivation particle will switch to the closed state. Systems like these, which move sequentially through various states, can be described as Markov processes (Koch, 1999). A key aspect of these processes is that the previous state the channel existed in has no bearing on the next state the channel will move to i.e., there is no memory, and that the transitions between states are governed by a single time constant, which can be calculated based on the rate constants (Eq. 7.3).

A



B

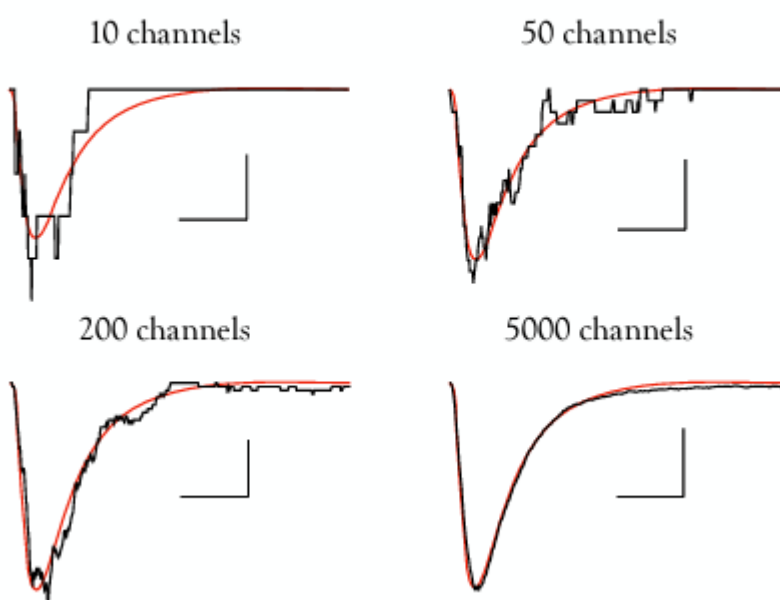


**Figure 9.5 - Kinetic diagram of  $I_{Na}$  using a Markov scheme to model single channel transitions based on the rate constants.** A. Since the scheme contains 3  $m$  particles and an inactivating  $h$  particle there are 8 separate states. As  $\alpha_m$  controls the transition from closed to open, moving towards the right indicates an opening of the channel. Similarly, since  $\alpha_h$  controls the move from the inactivated to non-inactivated state moving from top to bottom moves to the non-inactivated open state. B. Markov simulation showing the current resulting from simulations with 10, 50, 200 or 5,000 channels (black lines) with the scaled macroscopic current according to Eq. 9.2 (red lines) overlaid.

The model illustrated in Fig 9.5A is the simplest model that incorporates inactivation for the  $\text{Na}^+$  channel. There are three  $m$  states and one  $h$  state. Since  $m$  is the particle that controls the transition from closed to open, the rate constant  $\alpha_m$  is the probability that this transition will occur, and conversely  $\beta_m$  is the probability that the  $m$  particle will transition from open to closed. In addition, the  $h$  particle controls whether the inactivation particle is in the open (bottom row) or closed (top row) state, controlled by the rate constants  $\alpha_h$  and  $\beta_h$ , respectively. Thus, moving from left to right in Fig 9.5A is indicative of the transition of the  $m$  particle from closed to open, whereas moving from top to bottom is indicative of the transition of the  $h$  particle from inactivated to non-inactivated. The only state in which the channel is open is the lower right ( $m_3 h_1$ ), where all three  $m$  particles and the  $h$  particle are in the open state. There are numerous examples of the Markov process applied to ion channels (Neher & Stevens, 1977; Strassberg & DeFelice, 1993; Fain, 1999; Hille, 2001; Sterratt *et al.*, 2011), many displaying far more complex states than that shown in Fig 9.5. An excellent access point for novices in such schemes is contained in the following paper, which provides examples of code and illustrates several different kinetic schemes (Elliott & Brau, 1997). The principle by which such models operate is fairly straightforward. A state is assigned by random number generation, based on the value of the rate constants at the selected voltage. Once the state has been assigned, the duration for which it stays in this state is determined by random number generation applied to the time constant for that voltage. The next state is chosen based on the probability of transition determined by the rate constants, and so on. The value of such schemes is that they use Hodgkin-Huxley style rate constants, determined from macroscopic current records, to produce a stochastic model of single channel behaviour. We now know that the deterministic current is the sum of all the  $\text{Na}^+$  channels in the membrane, which behave in a stochastic manner, determined by the voltage dependence of the rate constants. If the model is run 5,000 times the duration and latencies of the openings and closings of the channel would vary among the sweeps, but the sum of these 5,000 traces would converge on the Hodgkin-Huxley deterministic current described by the following relationship (Fig 9.5B):

$$I_{Na} = \left(1 - e^{\left(\frac{-t}{\tau_m}\right)}\right)^3 e^{\left(\frac{-t}{\tau_h}\right)}$$
(Eq. 9.2)

### J Walter Woodbury and the Nobel Prize nomination

The work of Hodgkin and Huxley was so novel and unfamiliar that it did not make any immediate impact at the level of undergraduate teaching. This situation changed dramatically in 1960 when J Walter Woodbury, a faculty member of the Physiology and Biophysics Department at the University of Washington in Seattle, was invited to contribute two chapters on the work of Hodgkin and Huxley to the 18<sup>th</sup> edition of the textbook '*Medical*

*Physiology and Biophysics'* edited by Ruch and Fulton. Woodbury was aware of Hodgkin and Huxley's work, having met Hodgkin at the 1952 Cold Spring Harbour Symposium and been sent preprints of the papers by Hodgkin in autumn 1952. Woodbury, who possessed a bachelor's degree in physics, was the ideal advocate, his chapters based on a successful and popular lecture course in Seattle. Woodbury recognised the novelty and difficulty of this work and took the trouble to explain in a detailed and methodical manner the theory behind the papers. The chapters were important in introducing the work of Hodgkin and Huxley to a globally receptive audience in an accessible manner. An unexpected but far-reaching consequence of this was an invitation on behalf of the Nobel Prize committee requesting that Woodbury nominate suitable candidates for the prize. Unsurprisingly Woodbury nominated Hodgkin and Huxley and they were duly awarded the prize in 1963. It is fascinating to trace the evolution of Woodbury's chapters to the 19<sup>th</sup> edition of the book, where the concept of ions channels had been accepted and was now incorporated into his description. Bertil Hille joined the faculty of the Department of Physiology and Biophysics at the University of Washington, Seattle, in 1968, and assumed responsibility for the excitable membrane chapters in the subsequent 20<sup>th</sup> and 21<sup>st</sup> editions of the textbook renamed '*Physiology and Biophysics'* and edited by Ruch and Patton. Hille subsequently published his own book, '*Ionic Channels of Excitable Membranes*' in 1984. This book was a critical factor in promoting the soon burgeoning area of ion channel research in the mid 1980s, and it is difficult to exaggerate its importance in attracting researchers to the field. Hille skilfully wove together the disparate areas of electrophysiology, electrochemical principles, and models of permeability theory to provide researchers with a single source of all the basic information they were ever likely to require. It progressed through two subsequent editions, in 1992 and 2001, that incorporated updated information regarding ion channel structure from molecular biology techniques, revealing mechanisms underlying permeability, selectively, gating and action of drugs. During an interview I conducted with Bertil over 10 years ago (Brown, 2010), he showed me a letter sent to him by Marni, Hodgkin's wife, after Hodgkin's death. She wrote: "But he (Hodgkin) followed your career with great interest and latterly with a faintly disapproving feeling that you were writing too much and experimenting too little, but then experimental scientists always do feel like that." This was one of the few errors in judgment displayed by Hodgkin, since Hille's book has sold in excess of 20,000 copies and inspired a generation of researchers (including this author) to devote their careers to ion channel research. Hille's decision to write such a specialised book was based on his feeling that biophysicists were talking in an inaccessibly complex language coupled with the realisation that the Hodgkin and Huxley papers were inaccessible to most biologists. This book is a model of clarity and contains within its covers all (and a lot more besides) that students could wish to know on the topic. The last edition was published in 2001 and although there have since been significant advances in our understanding of ion channels; it remains the best textbook on the topic.

## Autobiographical Chapters

For the interested reader there is a rich source of autobiographical material from the key researchers. Hodgkin was the most prolific in this regard publishing two large reviews (Hodgkin, 1976, 1983). The first described experiments that he carried out between 1934 and 1952, not surprisingly focussing on the squid work with Huxley, whereas the latter was a more personal reflection on his early years up to 1947. Both reviews served as the foundation for his autobiography, '*Chance and Design*', published in 1992 (Hodgkin, 1992).

Hodgkin was at pains to emphasize the role that chance played in his research, which contrasts with the accepted view of Hodgkin's razor-sharp intellect directing each twist and turn of his research based on rigorous mathematical principles. Readers can draw their own conclusions, but Hodgkin's achievements, particularly in contrast to the failings of his contemporaries, speak for themselves. He also wrote a monograph based on lectures given at the University of Liverpool. This has a more didactic approach than the discursive autobiography, and focuses mainly on his experiments, but includes additional information to provide the appropriate background (Hodgkin, 1964). There is a review for the Society for Neuroscience's History of Neuroscience in Autobiography Series (Hodgkin, 1996), and a touching biographical chapter written by Huxley, which exudes their mutual respect (Huxley, 2000). Huxley contributed an autobiographical chapter to the Society for Neuroscience (Huxley, 2004) and a fascinating short review in which he divulged unpublished elementary action potentials calculated prior to the voltage clamp experiments (Huxley, 2002). These gave important insights into the potential permeability mechanisms and informed on fine-tuning the voltage clamp experiments and analysis. Cole published several reviews, which have a rather defensive tone (Cole, 1979, 1982). It is indeed unfortunate that the reputation of Cole, who contributed so much to the field, has diminished when compared to his contemporaries. This is mainly due to his reluctance to accept the  $\text{Na}^+$  theory. The infamous paper from 1942 specifically stated that the action potential peak exceeded the value of  $E_{\text{Na}}$ , which was later attributed to a technical error (Cole, 1968), and that the action potential was not affected by the replacement of seawater with dextrose i.e., removing  $\text{Na}^+$  from the perfusate (Curtis & Cole, 1942). Of this Cole claimed 'I neither understand nor remember' (Cole, 1979). Although Marmont invented and built the voltage clamp (a term Cole disliked) under Cole's supervision, Cole was only able to carry out a few experiments as Marmont favoured using the amplifier in the current clamp mode to measure membrane voltages (Marmont, 1949). However Cole showed an early transient inward current followed by the late outward current was evoked by membrane depolarisation to a steady voltage (Cole & Curtis, 1949), which was the basis of Hodgkin and Huxley's experiments. Hodgkin communicated with Cole in 1947 with Cole recalling 'Hodgkin told me of his  $\text{Na}^+$  results but I was more impressed with my own', and explained his reluctance to believe the  $\text{Na}^+$  theory, as 'I was addicted to  $\text{Ca}^{2+}$  which had such dramatic effects' (Cole, 1982). In addition Lorente de No did not believe the  $\text{Na}$  theory was relevant to frog as the nerves continued to produce action potentials for extended periods when bathed in dextrose, although we know this was because de No had not removed the perineurium surrounding the nerve trunk, which served as a  $\text{Na}^+$  reservoir enabling continued activity (McComas, 2011). McComas explains the confusion relating the spurious claim of the action potentials being unaffected by removal of  $\text{Na}^+$  by the fact that Curtis had left Cole's lab, and when writing the paper imagined he had carried out an experiment which he had not. On receiving the manuscript Cole must have believed the experiments had been carried out and developed his hypothesis based on this results (McComas, 2011). The confusion associated with long distance communication by letter in a time of war is understandable, but it had a disastrous effect on Cole's thinking and on his reputation, a matter to which Huxley later alluded (Angel, 1996). However Cole contributed two immortal images that are present in all major Neuroscience textbooks (Fig 7D and Fig 8.3) and generously supported Hodgkin's studies with invaluable advice and guidance, a gesture that was not reciprocated (McComas, 2011). He also trained future scientists who made important contributions to the field of neuroscience, notably graduate student David Goldman, whose 1943 paper (Goldman, 1943) paved the way for Hodgkin and Katz's estimations of changes in  $\text{Na}^+$  permeability during an action potential, Clay Armstrong, who along with Bertil Hille proposed the presence and fundamental properties of ion

channels (Armstrong & Hille, 1998), and John Moore, who devised the NEURON simulator (Moore, 2010).

## Specialist texts

All standard Neuroscience textbooks devote at least a chapter to the Hodgkin-Huxley work, but I find these on the whole disappointing. The requirement to compress a considerable amount of information into a standard textbook chapter ensures that much relevant data is omitted and most books have settled for reporting a simplistic description of the separation of the membrane current into  $I_{Na}$  and  $I_K$  and reconstruction of the action potential. The best accounts of the Hodgkin-Huxley work occur in specialist textbooks that devote appropriate space to the principles underlying the experiments and explaining the results in detail. The books by Sterratt (Sterratt *et al.*, 2011), Koch (Koch, 1999) and the relevant chapters in Byrne and Roberts (Baxter & Byrne, 2009) are admirable in this respect, explaining the Hodgkin-Huxley work in a logical step-by-step format. There is a glorious historical account of electrophysiology from Galvani to the present day by Alan McComas, who worked with Huxley, which is a treasure trove of information on the science and personalities behind the experiments (McComas, 2011). In addition there are books, which use the Hodgkin-Huxley model as a starting point to develop complex mathematical models; these books are for specialists only (Cole, 1968; Adelman, 1971; Jack *et al.*, 1983; Lakshminarayanaich, 1984; Cronin, 1987; Wallisch *et al.*, 2014; Borgers, 2017).

## Resources

### Video

In addition to books and journal articles there are several fascinating videos recorded at the Plymouth Marine Laboratory in the 1970s that feature key contributors to the field (Video-1). These include:

1. JZ Young demonstrates dissection of squid and how electrical stimulus of a giant axon causes contraction of the mantle (Video-2).
2. Hans Meves demonstrates dissection and removal of the squid axon (Video-3).
3. Peter Baker shows the Perspex bath set up used by Hodgkin and Huxley to record from squid axons, and Alan Hodgkin demonstrates inward and outward currents recorded using the voltage clamp technique (Video-4).
4. Hodgkin and Huxley are filmed in an extended conversation during which Huxley demonstrates the Brunsviga calculator (Video-5).

### Software

There are a number of freely available resources that allow the modelling of experiments under both voltage clamp and current clamp conditions. Among the most popular are:

1. HHsim (Software-1). This is the simplest simulation software as the user interacts via a set of GUIs. However, it lacks flexibility.
2. Genesis (Software-2). This requires the user to type code so is not for beginners, but is flexible and can create multi-compartment and multi-cellular models
3. NEURON (Software-3). This is perhaps the best simulator, as it is accompanied by a wide range of resources that are available via the web site, including a large database of simulations. The moderately steep learning curve is well worth the effort, as it opens the potential not only to create new simulations but to modify existing simulations and create bespoke models.

## Conclusion

The era in which these papers were written is often referred to as the golden age of electrophysiology, with the principal participants Cambridge University students and academics. The exception was Bernard Katz, a refugee from Nazi Germany, who was embraced into the fold. This elite band enjoyed the numerous advantages that the English class system had to offer, ensuring that they benefitted from family connection, social position, and excellent educational opportunities. It was a blessed existence, evoked in the contemporaneous novel *Brideshead Revisited*, when the only prospect for a large proportion of their peers was unemployment. They also possessed good genes; in fact a more superior set is difficult to imagine. Andrew Huxley, whose half-brother Aldous wrote *Brave New World* in 1932, was the great grandson of TE Huxley, known as Darwin's bulldog, and a founder of The Physiological Society; Alan Hodgkin's ancestors include his great-great uncle Thomas Hodgkin who described the eponymous lymphoma in 1832. It was the brother of JZ Young's great-great grandfather who deciphered the Rosetta Stone, and perhaps most impressively, Richard Keynes was the great grandson of Charles Darwin. However, this English dominance was short lived and faded rapidly in the aftermath of Hodgkin and Huxley's work as a consequence of myopic attitudes to funding in the UK. The newly created field of membrane biophysics was soon dominated by researchers working in America; Stephen Kuffler, Bertil Hille and Clay Armstrong were joined by Bill Catterall, Richard Aldrich, Rod McKinnon *et al.*, benefitting from more generous funding schemes. The field of membrane biophysics reached its apotheosis with the invention of the patch clamp technique by Neher and Sakmann in the 1970s (Nobel Prize for Physiology or Medicine in 1991), allowing measurement of the function of an individual protein for the first time, and our story reaches a natural conclusion with the use of X-Ray crystallography by Rod McKinnon (Nobel Prize for Chemistry in 2003) to reveal at high resolution the 3-D molecular structure of the K<sup>+</sup> channel.

## REFERENCES

- Adelman WJ. (1971). *Biophysics and Physiology of Excitable Membranes*. Von Nostrand Reinhold Company, New York.
- Adrian RH, Chandler WK & Hodgkin AL. (1970). Voltage clamp experiments in striated muscle fibres. *J Physiol* **208**, 607-644.
- Aidley DA. (1996). *The Physiology of Excitable Cells*. Cambridge University Press, Cambridge.
- Angel A. (1996). An interview with Sir Andrew Huxley  
[https://static.physoc.org/app/uploads/2019/03/22194446/Sir\\_Alexander\\_Huxley.pdf](https://static.physoc.org/app/uploads/2019/03/22194446/Sir_Alexander_Huxley.pdf)
- Armstrong CM & Bezanilla F. (1973). Currents related to movement of the gating particles of the sodium channels. *Nature* **242**, 459–461.
- Armstrong CM & Hille B. (1998). Voltage-gated ion channels and electrical excitability. *Neuron* **20**, 371-380.
- Attwell D & Laughlin SB. (2001). An energy budget for signaling in the grey matter of the brain. *J Cereb Blood Flow Metab* **21**, 1133-1145.
- Baker PF, Hodgkin AL & Shaw TI. (1962). Replacement of the axoplasm of giant nerve fibres with artificial solutions. *J Physiol* **164**, 330-354.
- Bakiri Y, Karadottir R, Cossell L & Attwell D. (2011). Morphological and electrical properties of oligodendrocytes in the white matter of the corpus callosum and cerebellum. *J Physiol* **589**, 559-573.
- Baxter DA & Byrne JH. (2009). Dynamical properties of excitable membranes. In *From Molecules to Networks*, 2nd edn, ed. Byrne JH & Roberts JL, pp. 181-215. Academic Press, London.
- Bernstein J. (1902). Untersuchungen zur Thermodynamik der bioelektrischen Ströme: Erster Theil. *Pflugers Arch* **92**, 521–562.
- Bernstein J. (1971). Investigations on the thermodynamics of bioelectric currents. In *Founders of Experimental Physiology*, ed. Boylan JW, pp. 258-299. J.F. Lehmanns Verlag, Munich.
- Bernstein J. (1979). Investigations on the thermodynamics of bioelectric currents. In *Cell Membrane Permeability and Transport*, ed. Kepner GR, pp. 184-1210. Dowden, Hutchinson and Ross, Stroudsbury, PA.
- Bezanilla F. (2005). Voltage-gated ion channels. *IEEE Trans Nanobioscience* **4**, 34-48.
- Borgers C. (2017). *An Introduction to Modeling Neuronal Dynamics*. Springer, New York.
- Boron WF & Boulpaep EL. (2009). *Medical Physiology*. Elsevier, New York.

## A companion guide to the Hodgkin-Huxley papers

- Bower JM & Beeman D. (1998). *The Book of GENESIS*. Springer-Verlag Publishers, Santa Clara, CA.
- Brown AM. (2000). Simulation of axonal excitability using a spreadsheet template created in Microsoft Excel. *Comp Meth Prog Biomed* **63**, 47-54.
- Brown AM. (2010). What makes ion channels exciting - a penetrating interview with Bertil Hille. *Physiol News* **81**, 13-16.
- Brown AM. (2018). Flowcharts to aid student comprehension of Nernst equation calculations. *Adv Physiol Educ* **42**, 260-262.
- Brown AM. (2019a). The classics updated, or an act of electrophysiological sacrilege? *J Physiol* **597**, 2821-2825.
- Brown AM. (2019b). Ion channels: the concept emerges. *J Physiol* **597**, 5725-5729.
- Brown AM. (2022). The Hodgkin and Huxley papers: still inspiring after all these years. *J Physiol* **600**, 173-174.
- Byrne JH & Roberts JL. (2009). *From Molecules to Networks*. Elsevier, New York.
- Cardozo D. (2016). An intuitive approach to understanding the resting membrane potential. *Adv Physiol Educ* **40**, 543-547.
- Catterall WA. (2012). Voltage-gated sodium channels at 60: structure, function and pathophysiology. *J Physiol* **590**, 2577-2589.
- Catterall WA, Raman IM, Robinson HP, Sejnowski TJ & Paulsen O. (2012). The Hodgkin-Huxley heritage: from channels to circuits. *J Neurosci* **32**, 14064-14073.
- Cole KC & Curtis HJ. (1949). Electric impedance of the squid giant axon during activity. *J Gen Physiol* **22**, 649-670.
- Cole KS. (1949). Dynamic electrical characteristics of the squid axon membrane. *Arch Sci Physiol* **3**, 253-258.
- Cole KS. (1968). *Membranes, Ions and Impulses*. University of California Press, Berkeley, CA.
- Cole KS. (1979). Mostly membranes. *Ann Rev Physiol* **41**, 1-24.
- Cole KS. (1982). Squid axon membrane: impedance decrease to voltage clamp. *Ann Rev Neurosci* **5**, 305-323.
- Cole KS, Antosiewicz HA & Rabinowitz P. (1955). Automatic computation of nerve excitation. *J Soc Indust Appl Math* **3**, 153-172.
- Connor JA & Stevens CF. (1971a). Prediction of repetitive firing behaviour from voltage clamp data on an isolated neurone soma. *J Physiol* **213**, 31-53.

- Connor JA & Stevens CF. (1971b). Voltage clamp studies of a transient outward membrane current in gastropod neural somata. *J Physiol* **213**, 21-30.
- Cooley JW & Dodge FA. (1966). Digital computer solutions for excitation and propagation of the nerve impulse. *Biophys J* **6**, 583-599.
- Crill WE. (1996). Persistent sodium current in mammalian central neurons. *Annu Rev Physiol* **58**, 349-362.
- Cronin J. (1987). *Mathematical Aspects of Hodgkin-Huxley Neural Theory*. Cambridge University Press, Cambridge.
- Crowther GJ. (2017). Which way do the ions go? A graph-drawing exercise for understanding electrochemical gradients. *Adv Physiol Educ* **41**, 556-559.
- Curtis HJ & Cole KS. (1942). Membrane resting and action potentials from the squid giant axon. *J Cell Comp Physiol* **19**, 135-144.
- De Muth JE. (2006). *Basic Statistics and Pharmaceutical Statistical Applications*. Chapman & Hall, Boca Raton.
- De Palma A & Parieti G. (2011). Bernstein's long path to membrane theory: radical change and conservation in nineteenth-century German electrophysiology. *J Hist Neurosci* **20**, 306-337.
- Dempster J. (1993). *Computer Analysis of Electrophysiological Signals*. Academic Press, London.
- Dodge FA & Frankenhauser B. (1958). Membrane currents in isolated frog nerve fibre under voltage clamp conditions. *J Physiol* **143**, 76-90.
- Elliott JR & Brau ME. (1997). A beginner's guide to computer simulation of voltage-gated ion conductances. *Prog Neurobiol* **52**, 469-484.
- Erlanger J, Gasser H, S. with the collaboration, in some experiments of & Bishop GH. (1924). The compound nature of the action current of nerve as disclosed by cathode ray oscillograph. *Am J Physiol* **70**, 624-666.
- Erlanger J & Gasser HS. (1937). *Electrical Signs of Nervous Activity*. Univ. of Pennsylvania Press, Philadelphia.
- Fain GL. (1999). *Molecular and Cellular Physiology of Neurons*. Harvard University Press, Cambridge, MA.
- Faraday M. (1834). Experimental researchers in electricity. Seventh series. *Trans Roy Soc London* **124**, 77-79.
- Fitzhugh R. (1960). Thresholds and plateaus in the Hodgkin-Huxley nerve equation. *J Gen Physiol* **43**, 867-896.

## A companion guide to the Hodgkin-Huxley papers

- Frankenhaeuser B & Huxley AF. (1964). The action potential in the myelinated nerve fibre of *Xenopus laevis* as computed on the basis of voltage clamp data. *J Physiol* **171**, 302-315.
- Frankenhauser B & Hodgkin AL. (1956). The after-effects of impulses in the giant nerve fibres of *Loligo*. *J Physiol* **131**, 341-376.
- Gasser H & Grundfest H. (1939). Axon diameters in relation to spike dimensions and the conduction velocity in mammalian A fibers. *Am J Physiol* **127**, 393-414.
- Gasser HS & Erlanger J. (1927). The role played by the sizes of the constituent fibers of a nerve trunk in determining the form of its action potential wave. *Am J Physiol* **80**, 522-547.
- Goldman DE. (1943). Potential, impedance, and rectification in membranes. *J Gen Physiol* **27**, 37-60.
- Goldman LR & Albus JS. (1968). Computation of impulse conduction in myelinated fibers; theoretical basis of the velocity-diameter ratio. *Biophys J* **8**, 596-607.
- Hille B. (1971). The permeability of the sodium channel to organic cations in myelinated nerve. *J Gen Physiol* **58**, 599-619.
- Hille B. (1972). The permeability of the sodium channel to metal cations in myelinated nerve. *J Gen Physiol* **59**, 637-658.
- Hille B. (2001). *Ion Channels of Excitable Membranes*. Sinauer Associates Inc., Sunderland, MA, USA.
- Hines ML & Carnevale NT. (1997). The NEURON simulation environment. *Neural Comput* **9**, 1179-1209.
- Hodgkin AL. (1937a). Evidence for electrical transmission in nerve: Part I. *J Physiol* **90**, 183-210.
- Hodgkin AL. (1937b). Evidence for electrical transmission in nerve: Part II. *J Physiol* **90**, 211-232.
- Hodgkin AL. (1938). The subthreshold potentials in a crustacean nerve fibre. *Proc Roy Soc B* **126**, 87-121.
- Hodgkin AL. (1939). The relation between conduction velocity and the electrical resistance outside a nerve fibre. *J Physiol* **94**, 560-570.
- Hodgkin AL. (1948). The local electrical changes associated with repetitive firing action on non-medullated axons. *J Physiol* **107**, 165-181.
- Hodgkin AL. (1951). The ionic basis of electrical activity in nerve and muscle. *Biol Rev* **26**, 339-409.

- Hodgkin AL. (1964). *The Conduction of the Nerve Impulse: The Sherrington Lectures VII.* Liverpool University Press, Liverpool.
- Hodgkin AL. (1976). Chance and design in electrophysiology: an informal account of certain experiments on nerve carried out between 1934 and 1952. *J Physiol* **263**, 1-21.
- Hodgkin AL. (1983). Beginning: some reminiscences of my early life (1914-1947). *Ann Rev Physiol* **45**, 1-16.
- Hodgkin AL. (1992). *Chance & Design: Reminiscences of Science in Peace and War.* Cambridge University Press, Cambridge UK.
- Hodgkin AL. (1996). Sir Alan Hodgkin. In *The History of Neuroscience in Autobiography Vol 1*, ed. Squires L, pp. 252-293. Society for Neuroscience, Washington.
- Hodgkin AL & Horowitz P. (1959). Movements of Na and K in single muscle fibres. *J Physiol* **145**, 405-432.
- Hodgkin AL & Huxley AF. (1939). Action potentials recorded from inside a nerve fibre. *Nature* **144**, 710-711.
- Hodgkin AL & Huxley AF. (1945). Resting and action potentials in single nerve fibres. *J Physiol* **104**, 176-195.
- Hodgkin AL & Huxley AF. (1947). Potassium leakage from an active nerve fibre. *J Physiol* **106**, 341-367.
- Hodgkin AL & Huxley AF. (1952a). The components of membrane conductance in the giant axon of *Loligo*. *J Physiol*, 55-80.  
<https://physoc.onlinelibrary.wiley.com/hub/journal/14697793/classicsupdated>
- Hodgkin AL & Huxley AF. (1952b). Currents carried by sodium and potassium ions through the membrane of the giant axon of *Loligo*. *J Physiol*, 29-54.  
<https://physoc.onlinelibrary.wiley.com/hub/journal/14697793/classicsupdated>
- Hodgkin AL & Huxley AF. (1952c). The dual effect of membrane potential on sodium conductance in the giant axon of *Loligo*. *J Physiol*, 81-91.  
<https://physoc.onlinelibrary.wiley.com/hub/journal/14697793/classicsupdated>
- Hodgkin AL & Huxley AF. (1952d). A quantitative description of membrane current and its application to conduction and excitation in nerve. *J Physiol* 92-136.  
<https://physoc.onlinelibrary.wiley.com/hub/journal/14697793/classicsupdated>
- Hodgkin AL & Huxley AF. (1953). Movement of radioactive potassium and membrane current in a giant axon. *J Physiol* **121**, 403-414.
- Hodgkin AL, Huxley AF & Katz B. (1949). Ionic currents underlying activity in the giant axon of the squid. *Arch Sci Physiol* **3**, 129-150.

## A companion guide to the Hodgkin-Huxley papers

- Hodgkin AL, Huxley AF & Katz B. (1952). Measurement of current–voltage relations in the membrane of the giant axon of *Loligo*. *J Physiol*, 1-28.  
<https://physoc.onlinelibrary.wiley.com/hub/journal/14697793/classicsupdated>
- Hodgkin AL & Katz B. (1949a). The effect of sodium ions on the electrical activity of the giant axon of the squid. *J Physiol*.  
<https://physoc.onlinelibrary.wiley.com/hub/journal/14697793/classicsupdated>
- Hodgkin AL & Katz B. (1949b). The effect of temperature on the electrical activity of the giant axon of the squid. *J Physiol* **109**, 240-249.
- Hodgkin AL & Keynes RD. (1955). The potassium permeability of a giant nerve fibre. *J Physiol*.  
<https://physoc.onlinelibrary.wiley.com/hub/journal/14697793/classicsupdated>
- Hodgkin AL & Nastuk WL. (1950). The electrical activity of single muscle fibres. *J Cell and Comp Physiol* **35**, 39-73.
- Hoshi T & Armstrong CM. (2015). The Cole-Moore effect: Still unexplained? *Biophys J* **109**, 1312-1316.
- Huguenard JR & McCormick DA. (1992). Simulation of the currents involved in rhythmic oscillations in thalamic relay neurons. *J Neurophysiol* **68**, 1373-1383.
- Huxley AF. (2000). Alan L Hodgkin. *Biogr Mem Soc R Soc* **46**, 219-241.
- Huxley AF. (2002). From overshoot to voltage clamp. *TiNS* **25**, 553-558.
- Huxley AF. (2004). Sir Andrew Huxley. In *The History of Neuroscience in Autobiography Vol 4*, ed. Squires L, pp. 282-319. Society for Neuroscience, Washington.
- Jack JJB, Noble D & Tsien RW. (1983). *Electric Current Flow in Excitable Cells*. Oxford University Press, Oxford.
- Kandel ER, Schwartz JH, Jessell TM, Siegelbaum SA & Hudspeth AJ. (2013a). Membrane Potential and the Passive Electrical Properties of the Neuron. In *Principles of Neural Science*, Fifth edn, ed. Kandel ER, Schwartz JH, Jessell TM, Siegelbaum SA & Hudspeth AJ, pp. 126-147. McGraw Hill, New York.
- Kandel ER, Schwartz JH, Jessell TM, Siegelbaum SA & Hudspeth AJ. (2013b). *Principles of Neural Science*. McGraw-Hill, New York.
- Katz B. (1947). The effect of electrolyte deficiency on the rate of conduction in a single nerve fibre. *J Physiol* **106**, 411-417.
- Kay AR. (2014). What gets a cell excited? Kinky curves. *Adv Physiol Educ* **38**, 376-380.
- Keynes RD. (1951a). The ionic movements during nervous activity. *J Physiol* **114**, 119-150.

- Keynes RD. (1951b). The leakage of radioactive potassium from stimulated nerve. *J Physiol* **113**, 99-114.
- Keynes RD. (2005). J.Z. and the discovery of squid giant nerve fibres. *J Exp Biol* **208**, 179-180.
- Koch C. (1999). *Biophysics of Computation*. Oxford University Press, Oxford.
- Kolarik KV, Thomson G, Edgar JM & Brown AM. (2013). Focal axonal swellings and associated ultra-structural changes attenuate conduction velocity in central nervous system axons: a computer modeling study. *Physiol Reports* **1** e00059.
- Kuffler SW, Nicholls JG & Orkand RK. (1966). Physiological properties of glial cells in the central nervous system of amphibia. *J Neurophysiol* **29**, 768-787.
- Lakshminarayanaich N. (1984). *Equations of Membrane Biophysics*. Academic Press, Orlando, FL.
- Ling G & Gerard RW. (1949). The normal membrane potential of frog sartorius fibres. *J Cell Comp Physiol* **34**, 383-396.
- Marmont G. (1949). Studies on the axon membrane; a new method. *J Cell Comp Physiol* **34**, 351-382.
- McComas AJ. (2011). *Galvani's Spark*. Oxford University Press, Oxford.
- McCormick DA & Huguenard JR. (1992). A model of the electrophysiological properties of thalamocortical relay neurons. *J Neurophysiol* **68**, 1384-1400.
- Moore JW. (2010). A personal view of the early development of computational neuroscience in the USA. *Front Comput Neurosci* **4**, Article 20.
- Neher E & Sakmann B. (1976). Single-channel currents recorded from membrane of denervated frog muscle fibres. *Nature* **260**, 799-802.
- Neher E & Stevens CF. (1977). Conductance fluctuations and ionic pores in membranes. *Ann Rev Biophys Bioeng* **6**, 345-381.
- Nicholls JG, Martin AR, Fuchs PA, Brown DA, Diamond ME & Weisblat DA. (2012). Ionic Basis of the Resting Potential. In *From Neuron to Brain*, Fifth edn, ed. Nicholls JG, Martin AR, Fuchs PA, Brown DA, Diamond ME & Weisblat DA, pp. 99-128. Sinauer Associates Inc, Sunderland, MA.
- Noble D. (1962). A modification of the Hodgkin-Huxley equations applicable to Purkinje fibre action and pace-maker potentials. *J Physiol* **160**, 317-352.
- Noble D. (2007). From the Hodgkin-Huxley axon to the virtual heart. *J Physiol* **580**, 15-22.

- Orkand RK, Nicholls JG & Kuffler SW. (1966). Effect of nerve impulses on the membrane potential of glial cells in the central nervous system of amphibia. *J Neurophysiol* **29**, 788-806.
- Patton HD. (1982). Special properties of nerve trunks and tracts. In *Physiology and Biophysics: IV Excitable Tissues and Reflex Control of Muscle*, ed. Ruch T & Patton H, pp. 101-127. W.B. Saunders Company, Philadelphia.
- Piccolino M. (1998). Animal electricity and the birth of electrophysiology: the legacy of Luigi Galvani. *Brain Res Bull* **46**, 381-407.
- Piccolino M & Galvani L. (1997). Luigi Galvani and animal electricity: two centuries after the foundation of electrophysiology. *TINS* **20**, 443-448.
- Powell CL & Brown AM. (2021). A classic experiment revisited: membrane permeability changes during the action potential. *Adv Physiol Educ* **45**, 178-181.
- Purves D, Augustine GJ, Fitzpatrick D, Hall WC, LaMantia A-S & White LE. (2012). Electrical Signals of Nerve Cells. In *Neuroscience*, Fifth edn, ed. Purves D, Augustine GJ, Fitzpatrick D, Hall WC, LaMantia A-S & White LE, pp. 25-56. Sinauer Associates Inc, Sunderland, MA.
- Rall W. (1977). Core conductor theory and cable properties of neurons. In *Handbook of Physiology Section 1: The Nervous System*, ed. Kandel E, pp. 39-99. American Physiological Society, Bethesda, Maryland.
- Raman IM & Ferster DL. (2021). *The Annotated Hodgkin and Huxley: A Reader's Guide*. Princeton University Press.
- Rasband MN & Shrager P. (2000). Ion channel sequestration in central nervous system axons. *J Physiol* **525**, 63-73.
- Rich LR & Brown AM. (2018). Fibre sub-type specific conduction reveals metabolic function in mouse sciatic nerve. *J Physiol* **596**, 1795-1812.
- Ritchie JM. (1995). Physiology of axons. In *The Axon: Structure, Function and Pathophysiology*, ed. Waxman SG, Kocsis JD & Stys PK. Oxford University Press, Oxford.
- Sawyer JER, Hennebry JE, Revill A & Brown AM. (2017). The critical role of logarithmic transformation in Nernstian equilibrium potential calculations. *Adv Physiol Edu* **41**, 231-238.
- Schwindt PC, Spain WJ & Crill WE. (1988a). Influence of anomalous rectifier activation on afterhyperpolarizations of neurons from cat sensorimotor cortex in vitro. *J Neurophysiol* **59**, 468-481.

## A companion guide to the Hodgkin-Huxley papers

Schwindt PC, Spain WJ, Foehring RC, Stafstrom CE, Chubb MC & Crill WE. (1988b). Multiple potassium conductances and their functions in neurons from cat sensorimotor cortex in vitro. *J Neurophysiol* **59**, 424-449.

Seyfarth EA. (2006). Julius Bernstein (1839-1917): pioneer neurobiologist and biophysicist. *Biol Cybern* **94**, 2-8.

Software-1. <http://www.cs.cmu.edu/~dst/HHsim/>

Software-2. <http://www.genesis-sim.org/GENESIS/>

Software-3. <https://neuron.yale.edu/neuron/>

Sotelo-Hitschfeld T, Niemeyer MI, Machler P, Ruminot I, Lerchundi R, Wyss MT, Stobart J, Fernandez-Moncada I, Valdebenito R, Garrido-Gerter P, Contreras-Baeza Y, Schneider BL, Aebischer P, Lengacher S, San Martin A, Le Douce J, Bonvento G, Magistretti PJ, Sepulveda FV, Weber B & Barros LF. (2015). Channel-mediated lactate release by K<sup>+</sup>-stimulated astrocytes. *J Neurosci* **35**, 4168-4178.

Steinbach HB & Spiegelman S. (1943). The sodium and potassium balance in squid nerve axoplasm. *J Cell Comp Physiol* **22**, 187-196.

Sterratt D, Graham B, Gillies A & Willshaw D. (2011). *Principles of Computational Modelling in Neuroscience*. Cambridge University Press, Cambridge, UK.

Strassberg AF & DeFelice LJ. (1993). Limitations of the Hodgkin-Huxley formalism: Effects of single channel kinetics on transmembrane voltage dynamics. *Neural Comput* **5**, 843-855.

Teorell T. (1949). Membrane electrophoresis in relation to bio-electrical polarisation effects. *Acta Physiol Scand* **3**, 205-218.

Ussing HH. (1949). The distinction by means of tracers between active transport and diffusion. *Acta Physiol Scand* **19**, 43-56.

Video-1. <http://www.science.smith.edu/departments/neurosci/courses/bio330/squid.html>

Video-2. [https://www.youtube.com/watch?v=pw6\\_Si5jOpo](https://www.youtube.com/watch?v=pw6_Si5jOpo)

Video-3.

<https://www.youtube.com/watch?v=6SyVPc1F9fl>  
<https://www.youtube.com/watch?v=6SyVPc1F9fl>

Video-4.

<https://www.youtube.com/watch?v=k48jXzFGMc8>  
<https://www.youtube.com/watch?v=k48jXzFGMc8>

Video-5. <http://www.bbc.co.uk/archive/scientists/10607.shtml>

- Wallisch P, Lusignan ML, Benayoun M & Baker TI. (2014). *Matlab for Neuroscientists: An Introduction to Scientific Computing in MATLAB*. Academic Press.
- Watson JD. (1968). *The Double Helix*. Weidenfeld & Nicolson, London.
- Watson JD & Crick FHC. (1953). Molecular structure of nucleic acids: a structure for deoxyribose nucleic acid. *Nature* **171**, 737-738.
- Woodbury JW. (1982). The cell membrane: ion fluxes and the genesis of the resting potential. In *Physiology and Biophysics IV; Excitable tissues and reflex control of muscle*, 20th Edition edn, ed. Ruch T & Patton H. W.B. Saunders Company, London.
- Young JZ. (1936). The giant fibres and epistellar body of cephalopods. *J Cell Sci* **78**, 367-386.
- Young JZ. (1938). The functioning of the giant nerve fibres of the squid. *J Exp Biol* **15**, 170-185.



The  
Physiological  
Society

ISBN: 978-1-9162559-1-3

[f physoc](#)

[@ThePhySoc](#)

[PhySocTV](#)

[@thephysoc](#)

[in the-physiological-society](#)

The Physiological Society is a company limited by guarantee. Registered in England and Wales, No. 323575.  
Registered Office: Hodgkin Huxley House, 30 Farringdon Lane, London EC1R 3AW, UK. Registered Charity No. 211585.  
'The Physiological Society' and The Physiological Society logo are trademarks belonging to The Physiological Society and are registered in the UK and in the EU, respectively.